INSTITUTO DE CIÊNCIAS BÁSICAS DA SAÚDE
PROGRAMA DE PÓS-GRADUAÇÃO EM CIÊNCIAS BIOLÓGICAS:
NEUROCIÊNCIAS

ESTUDO DA MORFOLOGIA NEURONAL E GLIAL NO NÚCLEO AMIGDALIANO MEDIAL HUMANO

Aline Dall'Oglio

Porto Alegre
2012

INSTITUTO DE CIÊNCIAS BÁSICAS DA SAÚDE
PROGRAMA DE PÓS-GRADUAÇÃO EM CIÊNCIAS BIOLÓGICAS: NEUROCIÊNCIAS

ESTUDO DA MORFOLOGIA NEURONAL E GLIAL NO NÚCLEO AMIGDALIANO MEDIAL HUMANO

Aline Dall'Oglio

Orientador: Alberto A. Rasia Filho
Co-orientadora: Matilde Achaval Elena

Tese de doutorado apresentada ao Programa de Pós-Graduação em Neurociência da Universidade Federal do Rio Grande do Sul como requisito parcial para obtenção do título de doutor em Neurociências

Porto Alegre
2012

SUMÁRIO

LISTA DE ABREVIATURAS

AAA - área amigdaliana anterior
AChE - acetilcolinesterase
AHi - área de transição amígdalo-hipocampal
AStr - área de transição amígdaloestriatal
Ba - núcleo amigdaliano basal
BL - núcleo amigdaliano basolateral
BLNG - grupo de núcleos amigdalianos basolaterais
BM - núcleo amigdaliano basomedial
BST - núcleo da estria terminal
Ce - núcleo amigdaliano central
ChAT - colina-acetiltransferase
CKK - colecistocinina
Cl - claustro
CMEA - grupo de núcleos amigdalianos centromediais
Co - núcleo amigdaliano cortical
D MeP - parte posterior dorsal do núcleo amigdaliano medial
ENK - encefalina
Epn - núcleo endopiriforme
GAL - galanina
GFAP - ir - imunorreatividade à proteína ácida fibrilar glial
GFAP - proteína ácida fibrilar glial
ICN - núcleos amigdalianos intercalados
IMG - substância cinzenta intramedular amigdaliana
La - núcleo amigdaliano lateral
Me - núcleo amigdaliano medial
MeA - porção anterior do núcleo amigdaliano medial
MeP - porção posterior do núcleo amigdaliano medial
NADPH-d - dinucleotídeo nicotinamida adenina fosfatodiaforase
NPY - neuropeptídeo Y
NT - neurotensina
opt - trato óptico
PHA - área de transição amigdalopara-hipocampal
PL - núcleo amigdaliano paralaminar
sCLR - grupo de núcleos amigdalianos tipo corticais superficiais
SLEA - amígdala expandida sublenticular
SN - sistema nervoso
SNC - sistema nervoso central
SP - substância P
SS - somatostatina
st - estria terminal
V MeP - parte posterior ventral do núcleo amigdaliano medial
VIP - peptídeo intestinal vasoativo

LISTA DE FIGURAS

RESUMO

O núcleo medial (Me) é parte superficial do complexo amigdaliano e ainda muito pouco se conhece de seus constituintes celulares em seres humanos. Neste estudo desenvolveu-se uma adaptação do método de Golgi do tipo "single-section" para tecido nervoso humano fixado e conservado em formalina por tempo variável. Além disso, descreveu-se a densidade de neurônios e células da glia no Me, sua morfologia geral, incluindo detalhes de espinhos dendríticos e terminações axonais, a imunorreatividade à proteína ácida fibrilar glial (GFAP) e a ultraestrutura sináptica local. Como resultados demonstrou-se que as células da glia são maioria neste núcleo (cerca de 72% do total de células) e que há significativamente mais neurônios no Me do hemisfério esquerdo ($1.53 \text{ X } 10^5$ neurônios/mm^3). Os somas neuronais impregnados pelo método de Golgi demonstraram-se redondos/ovais, fusiformes ou poligonais (diâmetros entre 10-30 µm), os dendritos estenderam-se por distâncias variadas e contiveram espinhos pleomórficos, caracterizando neurônios com menos e mais espinhos dendríticos (densidades de 1,5 até 5,2 espinhos/µm), e os axônios revelaram terminações desde simples até muito complexas. Os neurônios multipolares foram classificados em Tipos 1, 2 ou 3 de acordo com trabalhos prévios, ou ainda em tipos morfológicos ainda não classificados. Observaram-se astrócitos protoplasmáticos com muitos prolongamentos reativos à GFAP, isolados ou em grupos. Esses, no estudo ultra-estrutural, compuseram sinapses "tripartites" e "tetrapartites", considerando-se o quarto elemento o da matriz extracelular situada entre os elementos pré- e pós-sinápticos. As sinapses axodendríticas apresentaram-se tanto assimétricas (com vesículas redondas pequenas e elétron-lúcidas) como simétricas (com vesículas pleomórficas pequenas e claras e, adicionalmente, com vesículas redondas grandes ou pequenas de centro escuro). Terminais axonais estabelecendo múltiplas sinapses assimétricas, classificados como de tipo "glomérulo", também foram observados. A presente tese contribui com dados descritivos e quantitativos inéditos sobre a morfologia das células do Me, o que pode servir de base para o entendimento e novas investigações sobre o funcionamento desse núcleo em situações normais ou patológicas em seres humanos.

ABSTRACT

The medial nucleus (Me) is a superficial component of the amygdaloid complex. Little is currently known about its cellular composition in humans. Here is reported an adaptation of the "single-section" Golgi method for formalin fixed and stored human brain for diversified periods. Furthermore, the density of neurons and glial cells in the Me, their general morphology including dendritic spines and axonal terminals details, the glial fibrillary acidic protein (GFAP) immunoreactivity, and features of local cells under electron microscopy are described. Our results show that Me had an estimated mean neuronal density around 1.53 X 10^5 neurons/mm^3 (higher in the left hemisphere), more glia (72% of all cells) than neurons, and a nonneuronal/neuronal ratio of 2.7. Golgi-impregnated neurons had cell bodies with a round/ovoid, fusiform or polygonal shape (diameters ranging from 10 to 30 μm), dendrites with varying lengths and pleomorphic spines that characterized neurons more or less spiny (density varying from1.5 to 5.2 spines/μm), and ranging from simple to very complexes terminal axons. Neurons appeared as "bitufted" or stellate multipolar cells, or classified in "Types 1 to 3" according to previous immunohistochemical observations, or other still unclassified morphologies. Protoplasmic astrocytes, either isolated or forming small clusters, were observed and showed multiple branches immunoreactive for GFAP, being equally distributed between right and left hemispheres. They were found composing tripartite synapses or, together with an evident extracellular matrix between pre- and post-synaptic elements, tetrapartite ones. Axo-dendritic synapses were both asymmetrical (with various small, round electron-lucent vesicles) and symmetrical (with small pleomorphic vesicles and, occasionally, few intermingled large dense-core vesicles). Terminal axons with a glomerular-like structure were also found forming various asymmetric contacts. The present thesis add novel descriptive and qualitative information about neuronal and glial population of the human Me, which provide a basic contribution to our understanding, and to further research, of the functional implications of the Me in the brain organization both in normal and pathological conditions .

1. INTRODUÇÃO

1.1. A Amígdala Humana

1.1.1. Localização e classificação

A amígdala ou complexo amigdaliano[1] é uma massa ovóide de substância cinzenta subcortical formada por uma coleção de núcleos localizados bilateralmente na parte basilar do telencéfalo, especificamente na porção dorsomedial do lobo temporal. Compõe a parede superior e a ventromedial da extremidade anterior de cada ventrículo lateral, ventral e próxima aos bordos do claustro (Cl), putâmen e globo pálido, e em parte profunda em relação aos giros semilunar, "ambiens" e "uncinato" (Figura 1; Brodal, 1981; Everitt, 1995; Gloor, 1997; de Olmos, 2004). Anteroposteriormente mede em torno de 20 mm de comprimento. Sua largura mediolateral é de aproximadamente 31 mm em sua porção maior, e sua altura dorsoventral máxima é de 29 mm (conforme Mai e col., 2007).

Embora não tenha sido a primeira, a melhor e maior descrição anatômica detalhada da amígdala humana foi publicada por Johnston em 1923 e este trabalho influenciou as investigações posteriores sobre essa estrutura, incluindo as de outros autores como, por exemplo, Brockhaus (1938), Crosby e Humphrey (1941) e de Olmos (1990; 2004).

---

1. Como contribuição adicional, gostaria de se considerar que o melhor termo a ser incluído na Terminologia Anatômica atual seria complexo amigdaliano e não amigdalóide, uma vez que, nos dicionários da língua portuguesa, 'amigdaliano' é algo relativo ou pertencente à amígdala, enquanto 'amigdalóide' é algo semelhante à amígdala (Rasia-Filho e Hilbig, 2005).

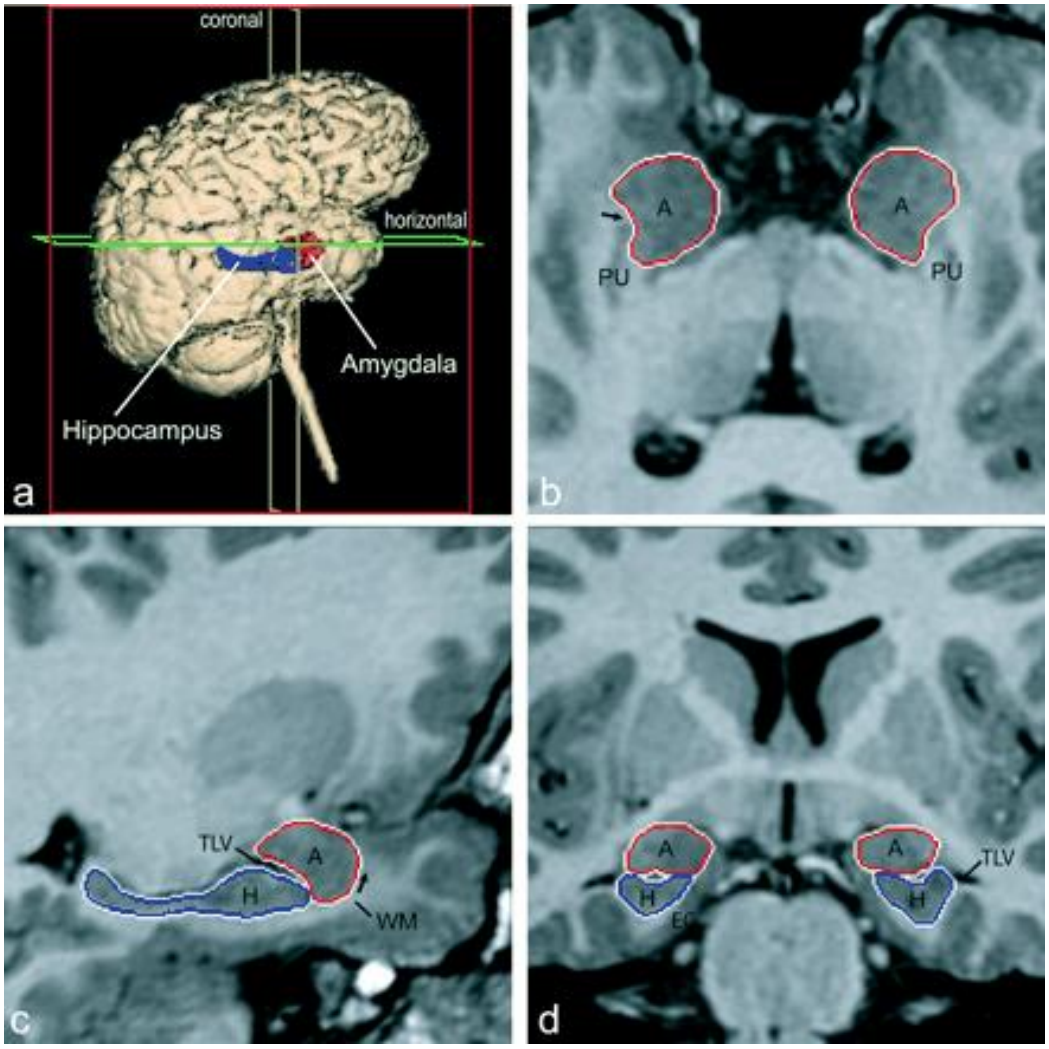

Figura 1. Localização da amígdala (em vermelho; neste caso considerada como uma estrutura única por causa da incapacidade técnica de separação em núcleos) na adjacência do hipocampo (em azul) em secções obtidas por técnica de ressonância magnética. (a) Reconstrução tridimensional do encéfalo com a indicação dos planos de estudo da amígdala nas imagens de ressonância magnética. Planos horizontal (linhas verdes), coronal (linhas brancas) e sagital (linhas vermelhas); (b) secção de ressonância magnética no plano horizontal, (c) secção de ressonância magnética no plano sagital e (d) secção de ressonância magnética no plano coronal. A seta em "b" indica a linha ao longo da substância branca que separa a amígdala do putâmen e a seta em "c" representa a substância branca que forma o bordo ventral da amígdala rostral. A - amígdala; EC - córtex entorrinal; H - hipocampo; PU - putâmen; TLV - corno temporal do ventrículo lateral; WM - substância branca subamigdaliana. Reproduzido e adaptado de Whalen e Phelps (2009).

Evidências morfológicas apontam que a amígdala (especificamente sua subdivisão centromedial) forma uma continuação com o núcleo da estria terminal (BST) e com a "amígdala expandida" sublenticular (SLEA), compondo uma parte da "amígdala expandida" em seres humanos e macacos, do mesmo modo que em

mamíferos não primatas macrosmáticos, como é o caso dos ratos (Martin e col., 1991; Yilmazer-Hanke, 2012). Como nestes, a amígdala humana não parece ser nem uma unidade anatômica, nem funcional (Brodal, 1981; Swanson e Petrovich, 1998; LeDoux e Schiller, 2009). Ela deve ser preferentemente entendida como sendo formada por diferentes núcleos classificados por critérios citoarquitetônicos e fibroarquitetônicos, neuroquímicos, hodológicos e ontogenéticos (Johnston, 1923; Crosby e Humphrey, 1941; Everitt, 1995; Sorvari e col., 1995; Gloor, 1997; Ulfig e col., 2003; de Olmos, 2004, Yilmazer-Hanke, 2012). Porém, há grande dificuldade em se delimitar os bordos precisos desses núcleos e seus subnúcleos e, tendo em vista as frequentes diferenças encontradas na descrição dos diferentes autores, parece ter havido maior consenso a respeito da taxonomia do que na topografia de cada núcleo constituinte (Gloor, 1997).

Uma revisão recente sobre a amígdala humana realizada por Yilmazer-Hanke (2012) sugere que ela deva ser classificada em três regiões principais de acordo com sua organização citoarquitetônica e sua hodologia para o processamento preferencial de informações em circuitos neuronais (Figura 2), como segue: a) grupo nuclear basolateral (BLNG; ou grupo de núcleos de tipo corticais profundos); b) grupo de núcleos tipo corticais superficiais (sCLR) e c) grupo centro-medial (CMEA; sem característica cortical) que inclui os núcleos central (Ce) e medial (Me) e que também pode ser denominado de "amígdala expandida" centromedial, quando da junção com o BST e a SLEA. De Olmos (2004) ainda sugeriu a classificação em um 4º grupo de "núcleos amigdalianos não classificados" que incluíam a área de transição amígdaloestriatal (AStr - suas porções parvicelular e granular), núcleos intercalados (ICN) e substância cinzenta intramedular amigdaliana (IMG), mas Yilmazer-Hanke (2012) discute que há diversas evidências indicando semelhanças dos tipos neuronais encontrados nos ICN e

na IMG com os do Ce (conforme dados de Moga e Gray, 1985a, 1985b; Millhouse, 1986; McDonald e Agustine, 1993; Pitkänen e Amaral, 1994).

Cada um dos três grupos principais é dividido em núcleos (e subnúcleos) conforme segue:

- O BLNG inclui os núcleos lateral (La), basolateral (BL), basomedial (BM) e paralaminar (PL), bem como o núcleo endopiriforme (Epn) que é uma região de transição entre o Cl e o La (Figura 2, em amarelo). É relevante mencionar que nos primatas todos os núcleos deste grupo são maiores que nos insetívoros, o que pode ser correlacionado com o aumento do córtex cerebral e suas conexões com o BLNG (Stephan e Andy, 1977; Stephan e col., 1987);

- O sCLR é dividido em núcleos cortical (Co), área de transição amigdalopara-hipocampal (PHA), e área de transição amígdalo-hipocampal (AHi; Figura 2, em verde);

- Por fim o CMEA é dividido em Ce, Me, ICN e AStr (Figura 2, em azul). O Me, objeto desse estudo, será abordado com maiores detalhes a seguir.

1.1.2. Funções, hodologia e neuroquímica

A amígdala foi considerada como parte do sistema límbico em mamíferos (revisado em Ledoux, 1998) e a sucessão de eventos históricos que culminaram nessa classificação está descrita a seguir: em 1878 Paul Broca chamou a atenção para o fato

de que, na superfície medial do cérebro dos mamíferos, logo abaixo do córtex, existia uma área de substância cinzenta contendo diversos núcleos os quais ele denominou de lobo límbico (do latim *limbus*, aquilo que circunda, bordo). Como já mencionado, Johnston (1923) foi um dos pioneiros a descrever a morfologia de um grupo desses núcleos em mamíferos que, devido a sua aparência lembrar o formato de uma amêndoa, recebeu o nome de "amígdala". A maior parte das descrições incipientes do papel do lobo límbico nas emoções foi desenvolvida apenas em 1937 quando James Papez descreveu seu modelo anatômico da emoção, o que veio a ser conhecido como o clássico circuito de Papez. A amígdala não estava elencada nesse circuito originalmente, mas, basicamente nesta mesma época, Klüver e Bucy relataram os resultados de experimentos de lesão do terço anterior do lobo temporal envolvendo toda a amígdala e estruturas neurais adjacentes, e suas consequências comportamentais marcantes em macacos. E, finalmente em 1952, Paul D. MacLean expandiu essas idéias para incluir estruturas adicionais em um "sistema límbico" mais disperso, as quais se desenvolveram com a emergência dos mamíferos inferiores.

Juntamente com seu conhecido papel no processamento de informações emocionais (LeDoux e Müller, 1997, Davidson e Irwin, 1999, Rasia-Filho e col., 2000; Gazzaniga e col., 2002), incluindo-se a formação de memória com cunho emocional e a avaliação do conteúdo emocional na informação visual e auditiva percebida (Phelps e Anderson, 1997), os núcleos amigdalianos humanos têm se relacionado com a geração de respostas motoras e de ativação dos sistemas simpático e parassimpático necessárias à avaliação e resposta sobre o contexto social do estímulo emocional percebido (Sorvari, 1997; Rasia Filho e Hilbig, 2005; de Olmos 2004).

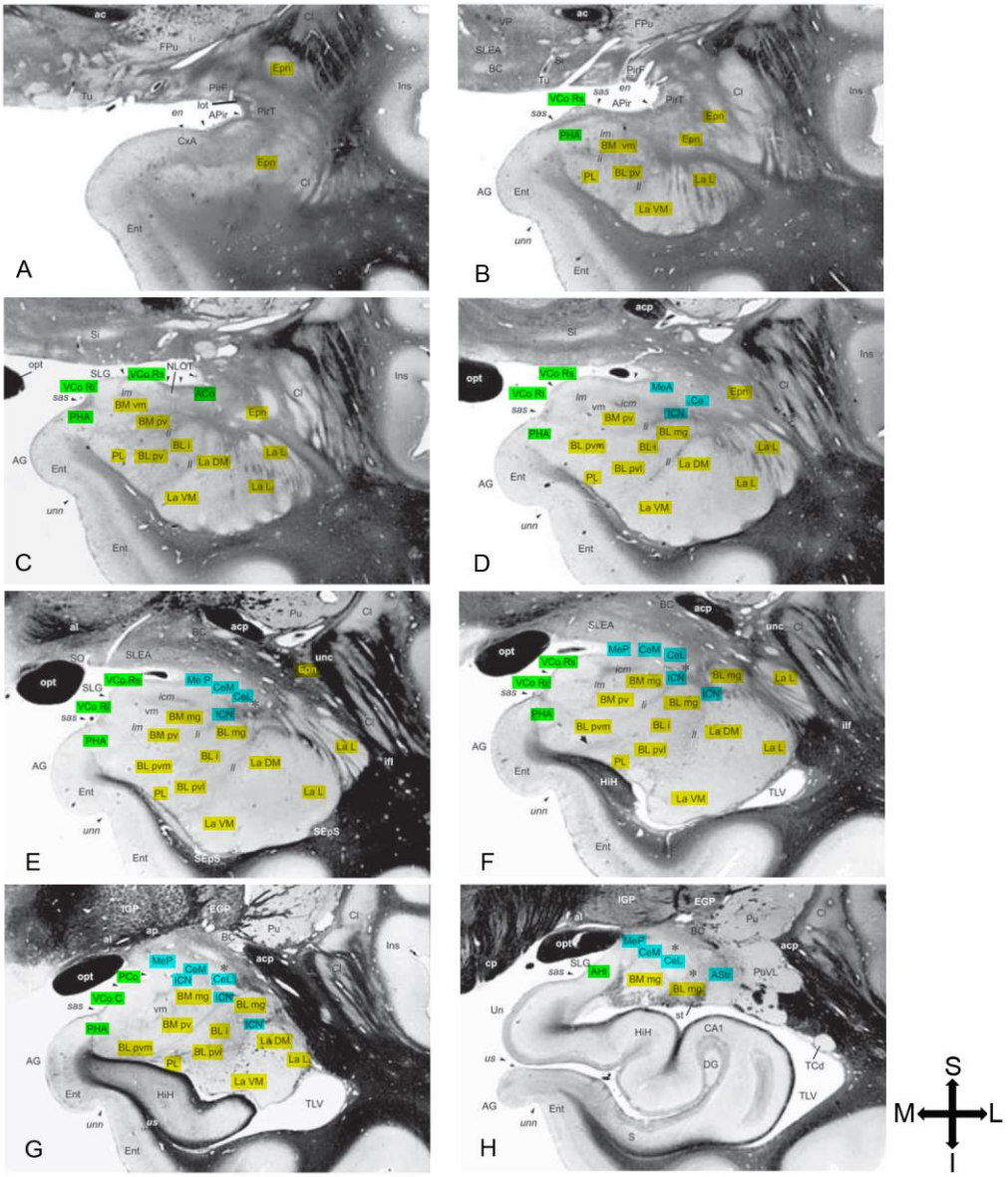

Figura 2. Cortes coronais do encéfalo humano com marcação imuno-histoquímica para mielina e sugerindo a classificação da amígdala em 3 grandes grupos de núcleos: BLNG em amarelo, sCLR em verde e CMEA em azul. A divisão e subdivisão dos grupos em núcleos e subnúcleos também pode ser observada. A figura "A" representa a região mais anterior e "H" a mais posterior. Adaptado de Yilmazer-Hanke (2012), que atribui as imagens ao Atlas do Encéfalo Humano de Mai e col. (2007). ac – comissura anterior; ACo – parte anterior do núcleo amigdaliano cortical; acp – parte posterior da comissura anterior; AG – giro ambiens; AHi – área de transição amígdalo-hipocampal; al – ansa lenticular; ap – ansa penduncular; Apir – área de transição amígdalopiriforme; AStr – área de transição amígdaloestriatal; BC – núcleo basal de Meynert; BL i – parte intermediária do núcleo amigdaliano basolateral; BL mg – parte magnocelular do núcleo amigdaliano basolateral; BL pv – parte parvicelular do núcleo amigdaliano basolateral; BL pvl – parte parvicelular lateral do núcleo amigdaliano basolateral; BL pvm – parte parvicelular medial do núcleo amigdaliano basolateral; BM mg – parte magnocelular do núcleo amigdaliano basomedial; BM pv – parte parvicelular do núcleo amigdaliano basomedial; BM vm – parte ventromedial do núcleo amigdaliano basomedial; CA1 – área CA1 do hipocampo; Ce – núcleo amigdaliano central; CeL – parte lateral do núcleo amigdaliano central; CeM – parte medial do núcleo amigdaliano central; Cl – claustro; cp – pedúnculo cerebral; CxA – área de transição córticoamigdaliana; DG – giro denteado; EGP – globo pálido externo; en – sulco endorrinal; Ent – cortex entorrinal; Epn – núcleo endopiriforme; FPu – fundo do putamen; HiH – cabeça do hipocampo; icm – massa de fibras intermediárias caudomediais; ICN – núcleo intercalado; IGP – globo pálido interno; li – lâmina medular intermediária da amígdala; ilf – fascículo longitudinal inferior; lm – lâmina medular medial da amígdala;

Figura 2, continuação. Ins – ínsula; La L – parte lateral do núcleo amigdaliano lateral; La DM – parte dorsomedial do núcleo amigdaliano lateral; La VM – parte ventromedial do núcleo amigdaliano lateral; ll – lâmina medular lateral da amígdala; lot – trato olfatório lateral; MeA – parte anterior do núcleo amigdaliano medial; MeP – parte posterior do núcleo amigdaliano medial; NLOT – núcleo do trato lateral olfatório; opt – trato óptico; PCo – parte posterior do núcleo amigdaliano cortical; PHA – área de transição amígdalopara-hipocampal; PirF – parte frontal do córtex piriforme; PirT – parte temporal do córtex piriforme; PL – núcleo amigdaliano paralaminar; Pu – putamen; PuVL – parte ventrolateral do putamen; S – subículo; sas – sulco semianular; SEpS – estrato subependimal; Si – substância inominata; SLEA – "amígdala expandida" sublenticular; SLG – giro semilunar; st – estria terminal; SO – núcleo supraóptico; TLV – corno temporal do ventrículo lateral; Tu – tubérculo olfatório; Un – uncus (giro uncinato); unc – fascículo uncinato; unn – entalhe do uncus; us – sulco do uncus; VCo C – parte caudal do núcleo amigdaliano cortical ventral; VCo Ri – parte inferior rostral do núcleo amigdaliano cortical ventral; VCo Rs – parte superior rostral do núcleo amigdaliano cortical ventral. Coordenadas espaciais: S - Superior; I - Inferior; M - Medial; L - Lateral.

Também tem sido demonstrado o envolvimento da amígdala humana em algumas patologias degenerativas do SN, como no caso da doença de Alzheimer (Benzing e col., 1992), na Coréia de Huntington (de Olmos, 2004), na epilepsia do lobo ctemporal (Pitkänen e col., 1998) ou em alguns distúrbios psiquiátricos, como no transtorno bipolar (Garrett e Chang, 2008), em comportamentos agressivo e defensivo geralmente associados à depressão (Trimble e Van Elst, 1999), no transtorno do estresse pós-traumático (Protopopescu e col., 2005; Rasia-Filho e Hilbig, 2005), no autismo (Zirlinger e Anderson, 2003; Schumann e Amaral, 2006; Amaral e col., 2008) e na esquizofrenia (Fudge e Emiliano, 2003).

É denominador comum nessas suas funções (ou disfunções no caso das patologias) a integração e o processamento de informações multimodais originadas de estímulos internos e externos necessários para a modulação de funções cognitivas superiores e de comportamento emocional (Yilmazer-Hanke, 2012). A base anatômica para tais funções é a convergência de impulsos multimodais originados em várias regiões corticais ou subcorticais em direção aos núcleos da amígdala (LeDoux e col., 1990; Amaral e col., 1992; Linke e col., 1999; Aggleton e Saunders, 2000). Neste sentido, a amígdala dos mamíferos, sobretudo a dos primatas, parece conectar-se

reciprocamente e de forma generalizada também com várias outras regiões encefálicas. Há grande quantidade de conexões de e para regiões alocorticais (pré-piriforme e hipocampal), várias regiões mesocorticais e outras isocorticais. Além disso, há conexões extensas e recíprocas dos diversos núcleos amigdalianos com as regiões que circundam o feixe prosencefállico medial, desde o prosencéfalo basal e a área pré-óptica, continuando-se pelo tronco encefálico (Gloor, 1997). Além disso, conecta-se com áreas talâmicas e do estriado (Amaral, 1987, Berry e col., 1995, Gloor, 1997) projetando suas eferências por dois sistemas principais de saída, a estria terminal (st) e a via amígdalofugal ventral (Berry e col., 1995). Já as conexões intrínsecas dos núcleos da amígdala humana parecem ocorrer de um modo aparentemente unidirecional em sua maior parte, onde as fibras têm origem primariamente nos núcleos La e basal (Ba) e terminando-se nos núcleos Ce e Me (Figura 3; Amaral, 1987; Berry e col., 1995; Felten e Józefowicz, 2005).

De acordo com revisão de Gloor (1997), além dos neurotransmissores clássicos excitatórios glutamato e asparatato, ou inibitório como o GABA, estão descritos na amígdala humana (ou de macacos – nesse caso específico será assinalado) presença de terminais colinérgicos (Nitecka e Narkiewicz, 1976; Svendsen e Bird, 1985 e Sims e Williams, 1990); dopaminérgicos (Gaspar e col., 1985); adrenérgicos (Sadikot e Parent, 1990 – macaco) e serotoninérgicos (Sadikot e Parent, 1990 – macaco). Também se descreve a presença da maioria dos peptídeos encontrados no SNC dos mamíferos, tanto nos corpos neuronais como nos terminais axonais, sendo eles: colecistoquinina (CKK; Candy e col., 1985); peptídeo intestinal vasoativo (VIP; Candy e col., 1985); somatostatina (SS; Candy e col., 1985; Bennett-Clarke e Joseph, 1986; Gaspar e col., 1987; e Lesur e col. 1989); neuropeptídeo Y (NPY; Gaspar e col., 1987; e Walter e col.,

1990); neurotensina (NT; Cooper e col., 1981; Sarrieu e col., 1985; Michel e col., 1986; Mai e col., 1987; e Benzing e col., 1992); substância P (SP; Cooper e col., 1981 e Pioro e col., 1990); encefalina (ENK; Candy e col., 1985; Lesur e col., 1989 e Pioro e col., 1990); e, galanina (GAL; Gentleman e col., 1989).

Além disso, há neurônios na amígdala que possuem receptores para hormônios esteróides, particularmente estrógenos (Keefer e Stumpf, 1975 – macaco) e andrógenos (Michael e col., 1990 – macaco).

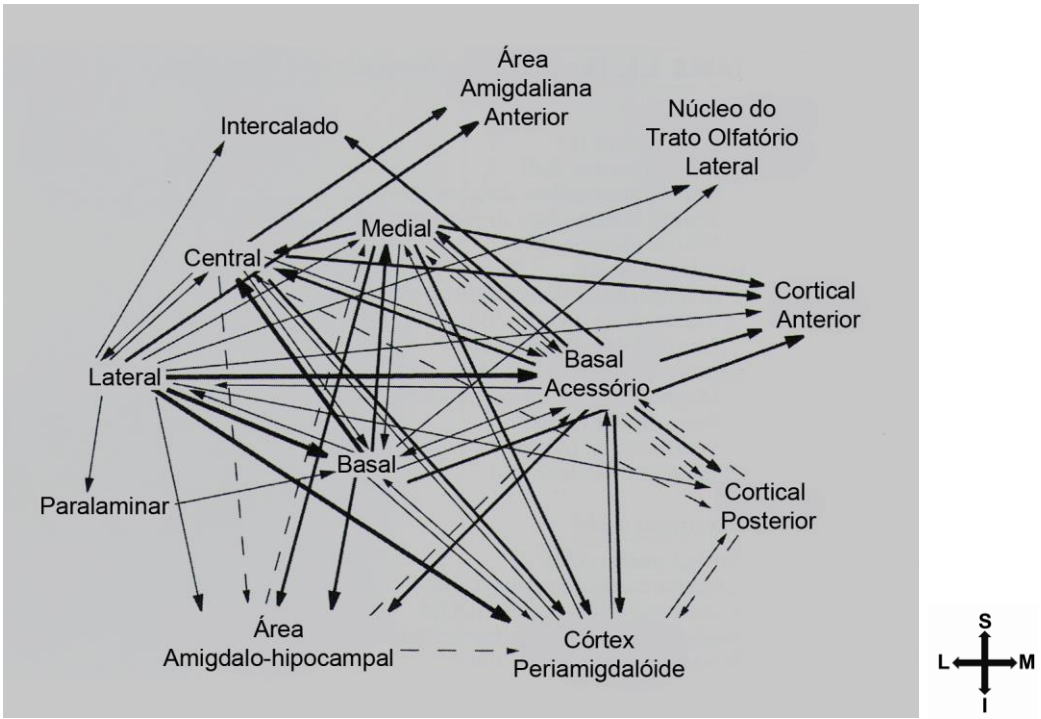

Figura 3. Conexões intra-amigdalianas em primatas. Os núcleos amigdalianos de primatas são fortemente interconectados permitindo um extensivo processamento das informações que chegam à amígdala. As conexões com maior número de axônios são representadas por setas grossas e as com menos axônios, pelas setas finas. Possíveis conexões não confirmadas por limitações técnicas são indicadas pelas setas pontilhadas. Os núcleos estão representados em suas localizações aproximadas e, de um modo geral, as informações aferentes são processadas envolvendo os núcleos amígdalianos de lateral para medial. Imagem modificada de Freese e Amaral (2009). Coordenadas espaciais: S - Superior; I- Inferior; L - Lateral; M- Medial.

Por estudos imuno-histoquímicos, hodológicos e eletrofisiológicos nos diferentes núcleos da amígdala de diferentes espécies de mamíferos (nesse caso não há nada especificamente proposto para humanos), considera-se que o BLNG tenha morfologia e função celulares que se assemelham às do alocórtex, com neurônios principais do tipo piramidal contendo neurotransmissores aminoácidos excitatórios e os interneurônios locais, de tipo não piramidal, preferentemente GABAérgicos ou peptidérgicos (McDonald, 1985; 1989; MacDonald e Pearson, 1989); enquanto que o CMEA se aproximaria de uma característica hipotalâmica, porque a maioria, senão todos os neurônios de projeção dos seus núcleos, contém peptídeos (Uhl e col., 1978a, b; Sakanaka e col., 1981; Higgins e Schwaber, 1983; Moga e Gray., 1995a,b). Segundo Gloor (1997), esta dicotomia não é segura ou característica. Em função disso tudo é que os núcleos amigdalianos "parecem representar uma verdadeira interface entre as partes do sistema nervoso (SN) que primariamente se comunica com o mundo externo e outras que se ocupam de se relacionar com o *milieu intérieur* de Claude Bernard" (Gloor, 1997).

Isso nos dá embasamento para entender porque a principal alteração que ocorre de mamíferos com formas "prototípicas" para primatas e particularmente para humanos, são o aumento do tamanho alométrico do BLNG e o menor aumento alométrico do CMEA ao longo da evolução (Stephan e Andy, 1977; Gloor, 1997, de Olmos, 2004; Yilmazer-Hanke, 2012). Também há uma involução do núcleo do trato olfatório lateral, que virtualmente desaparece nos símios e não é demonstrado nos seres humanos, o que poderia vir a explicar porque o Me parece ser um núcleo em regressão na filogenia de primatas (de Olmos, 2004). Por fim, há uma complexa rotação da amígdala sobre seus eixos anteroposterior e vertical quando comparamos mamíferos prototípicos e primatas,

o que culmina com o posicionamento anatômico como o encontrado na nossa espécie (Gloor, 1997; Whalen e col., 2009; Figura 4).

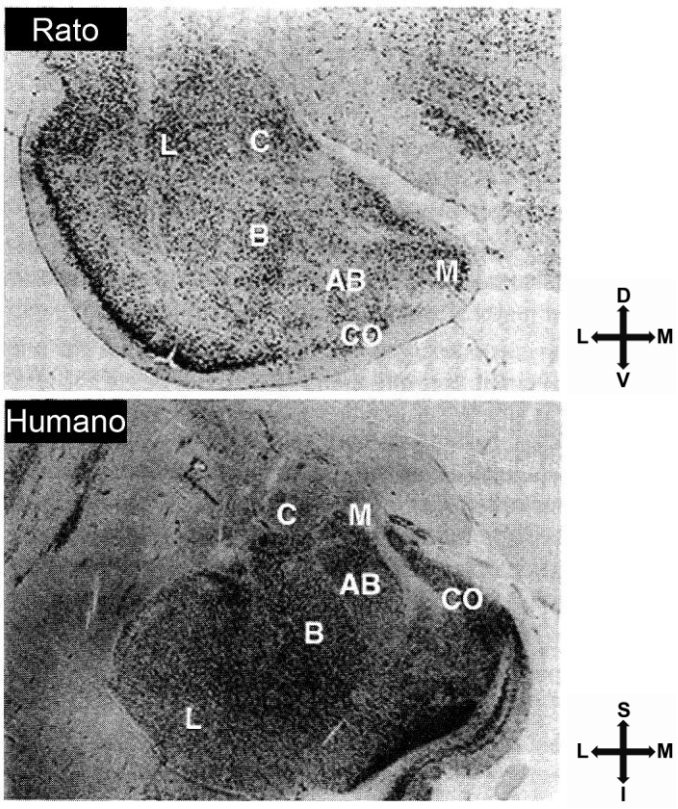

Figura 4. Comparação entre o complexo nuclear amigdaliano do rato e do ser humano. Notar que a amígdala humana sofre uma rotação no sentido anti-horário quando comparada à do rato. Reproduzida e adaptada de Whalen e col., (2009). L - núcleo amigdaliano lateral; C - núcleo amigdaliano central; B - núcleo amigdaliano basal; BA - núcleo amigdaliano basal acessório; M - núcleo amigdaliano medial; CO - núcleo amigdaliano cortical. Coordenadas espaciais: L - Lateral; M - Medial; D - dorsal; V - Ventral; S - Superior; I - Inferior.

1.2. O Núcleo Amigdaliano Medial Humano

1.2.1. Topografia e divisão

O Me é um núcleo de substância cinzenta localizado na porção superficial da amígdala dorsomedial. Possui formato alongado que se estende ao longo da maior parte do eixo anteroposterior da amígdala humana, na adjacência da região mais profunda do sulco endorrinal (Benzing e col., 1992; Gloor, 1997, de Olmos, 2004). Ele forma a parede ventrolateral da fenda entre a amígdala e o trato óptico (opt), uma vez que o opt adentra por este sulco em sentido posterior (Gloor, 1997; de Olmos, 2004; Yilmazer-Hanke, 2012). Em humanos, que possuem um uncus bem desenvolvido, o Me estende-se aproximadamente até os dois terços caudais do complexo amigdaliano (Gloor, 1997; de Olmos, 2004; Yilmazer-Hanke, 2012), embora se mescle com componentes da "amígdala expandida" (Martin e col., 1991).

A parte rostral do Me faz limite com a área amigdaliana anterior (AAA; Brockaus, 1938; Crosby e Humphrey, 1941; Sims e Williams, 1990; de Olmos, 2004). A substância cinzenta da metade anterior do Me se continua ao redor do fundo do sulco endorrinal, na porção ventromedial da substância sublenticular *inominata*, também parte da "amígdala expandida" (Brockhaus, 1938; Alheid e Heimer, 1988; Martin e col., 1991; de Olmos, 1990). Uma vez que o opt se localiza no fundo do sulco endorrinal, o Me ocupa apenas a superfície ventral desse sulco, mas se estende posteriormente até a extremidade posterior da amígdala como um todo. Ao nível onde o Ce se junta ao bordo lateral do Me, o limite entre os dois é mal definido (Gloor, 1997; Figura 5). Mais posteriormente esses dois núcleos são separados por algumas fibras mielinizadas. O bordo ventrolateral do Me em direção ao BM é formado pela porção dorsal da lâmina

medular medial. Já o bordo ventromedial do Me em direção ao Co, e mais posteriormente em direção à AHi, é reconhecido por uma mudança facilmente perceptível no tamanho das células e sua coloração mais intensa (Gloor, 1997; de Olmos, 2004; Figura 5). Mais posteriormente, o Me se mescla com componentes da st que compõe a "amígdala expandida" (Martin e col., 1991), havendo também discrepâncias a respeito de seu término exato.

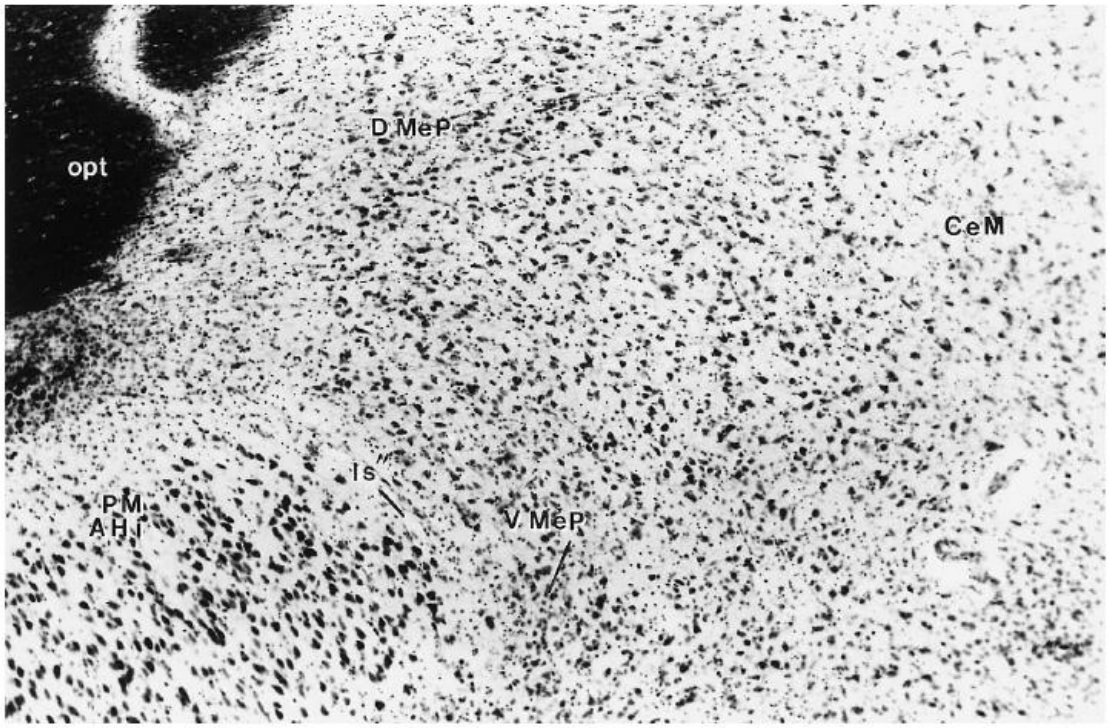

Figura 5. Fotomicrografia de um corte coronal, corado com cresil violeta, mostrando a localização do núcleo amigdaliano medial humano com relação a seus bordos, na altura da sua porção caudal. D MeP - parte posterior dorsal do núcleo amigdaliano medial; V MeP - parte posterior ventral do núcleo amigdaliano medial; CeM - parte medial do núcleo amigdaliano central; PM AHi - parte posteromedial da área de transição amígdalo-hipocampal; opt - trato óptico; ls - lâmina medular superficial. Reproduzido de de Olmos (2004).

Têm sido sugeridas distintas subdivisões para o Me. Ele pode, por exemplo, ser subdividido em uma porção cortical superficial e uma subcortical profunda (Brockhaus,

1938) ou em porção anterior (MeA) e posterior (MeP; Sorvari, 1997; De Olmos, 2004; Mai e col. 2007) sendo que esta última é ainda subdividida por de Olmos (2004) em ventral (V MeP) e dorsal (D MeP; Figura 5).

1.2.2. Componentes celulares

Sorvari e col., (1996a) sugerem a classificação dos neurônios dos núcleos da amígdala humana, incluindo-se o Me, em três tipos morfológicos principais de acordo com estudos de imunorreatividade à calretinina e que são: a) Tipo 1 – neurônios multipolares com soma esféricos (diâmetro aproximado variando entre 10 e 20 μm) de onde surgem 3 a 11 dendritos primários geralmente com espessuras similares e que tipicamente se ramificam em diversos ramos secundários ainda próximos ao corpo celular. Este seria o tipo mais comum no Me humano expressando calretinina (Figura 7, número 1). b) Tipo 2 – neurônios multipolares com somas de aspecto estrelado ou multiangulares e com diâmetro superior a 50 μm de onde surgem ramos dendríticos primários que dão origem a diversos ramos colaterais (Figura 7, número 2). c) Tipo 3 – neurônios multipolares cujos corpos celulares fusiformes dão origem a dendritos em pólos opostos e que podem tanto se ramificar perto do soma, como a longas distâncias deste (Figura 7, número 3).

Em preparações histológicas empregando-se a técnica de Golgi em diversos mamíferos não primatas (como por exemplo, o gato, o rato e o hamster) observam-se neurônios com corpos celulares ovais ou alongados, relativamente pequenos, com dois dendritos primários (neurônios do tipo “bitufted” ou, no termo mais próximo em português, bipenachados; Figura 6, imagem superior) ou com três ou mais dendritos

primários (neurônios do tipo estrelado; Figura 6, imagem inferior), ambos com dendritos longos e pouco ramificados, que se apresentam geralmente com espinhos dendríticos (Hall, 1972; Kamal e Tömböl, 1975; de Olmos e col. 1985; Price, 1987; Rasia-Filho e col., 1999; 2004; Dall'Oglio e col., 2008a,b; Arpini e col., 2010). No Me humano, Benzing e col. (1992) também descreveram a presença de neurônios imunorreativos à neurotensina do tipo "bitufted" (tipo neuronal multipolar erroneamente denominado bipolar por estes e outros autores, pois que caracterizado por dois prolongamentos dendríticos surgindo em pólos opostos do soma, conforme Ramón y Cajal e comentários em Rasia-Filho e col., 1999).

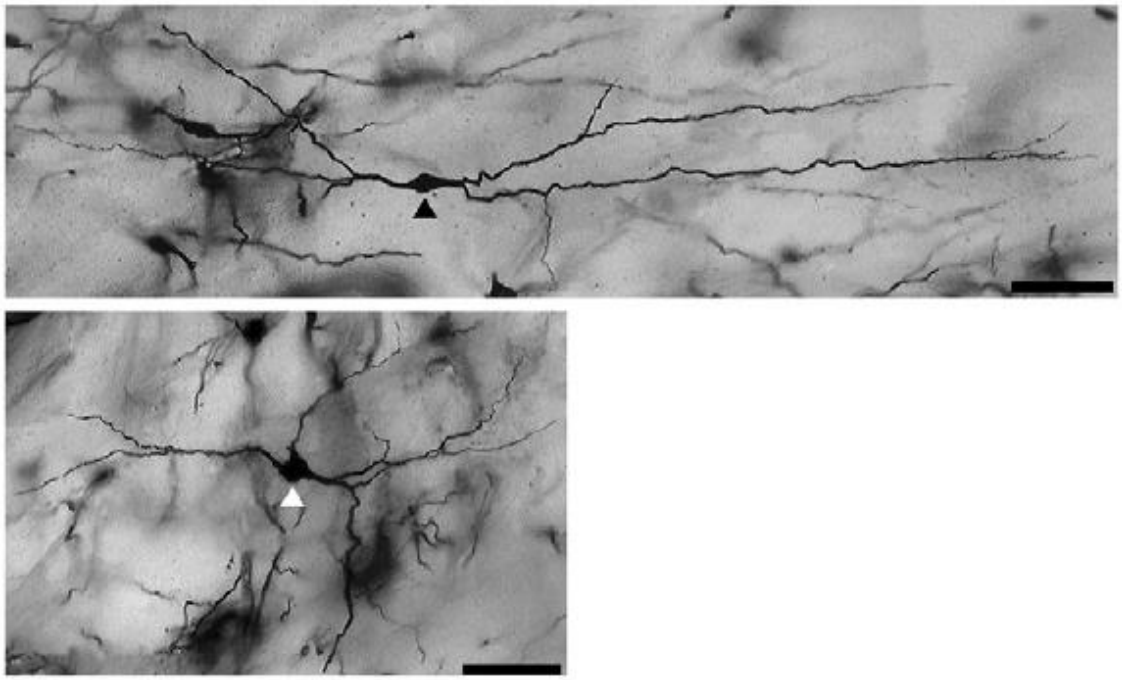

Figura 6. Neurônios de tipo "bitufted" (imagem superior, cabeça de seta preta) e de tipo estrelado (imagem inferior, cabeça de seta branca) com típica arborização dendrítica esparsa na região posterior dorsal do núcleo amigdaliano medial de rato adulto. Impregnação pela técnica de Golgi. Reproduzido de Arpine e col. (2010). Barra de Escala = 50 µm.

Ocorre que não necessariamente os estudos imuno-histoquímicos conseguem revelar todos os tipos neuronais presentes em uma estrutura. Muito provavelmente o que está se observando são uma ou mais subpopulações celulares com uma característica neuroquímica específica. Uma técnica que permitisse uma maior amostragem e a visualização dos neurônios do Me poderia ser muito útil para comparar e acrescentar dados sobre os componentes celulares locais. Além disso, não há nenhum estudo relatando os aspectos morfológicos das células da glia no Me humano até o momento. Um dos objetivos dessa tese foi obter dados para preencher algumas dessas lacunas no conhecimento do encéfalo humano, como será descrito adiante.

1.2.3. Quimioarquitetura do núcleo amigdaliano medial humano

Em uma tentativa de demarcar o Me e descrever quais são os possíveis mediadores químicos da atividade sináptica local, diversos neurotransmissores clássicos e neuropeptídeos ou algumas enzimas envolvidas com a neurotransmissão têm sido estudados e descritos nesse núcleo, em diferentes espécies animais (Martin e col., 1991; Gloor, 1997; de Olmos, 2004; Yilmazer-Hanke, 2012). Isso é relevante na medida em que achados ultraestruturais identificam sinapses com características excitatórias ou inibitórias e abrem perspectivas para futuras correlações entre achados morfológicos básicos e sua correlação funcional.

Alguns desses transmissores químicos e a atividade enzimática serão descritos aqui, mas para revisão mais extensa, vejam-se Gloor (1997), de Olmos (2004) e Yilmazer-Hanke (2012). Vários desses resultados foram observados tanto no neurópilo como nos corpos celulares locais da Me. Todavia, como já se descreveram variações

entre espécies quanto ao padrão de imunomarcação, como é o exemplo dos ramos axonais imunorreativos à somatostatina e que aparecem de abundantes a moderadas no neurópilo de ratos (Johansson e col. 1984), mas que são escassos em macacos (Amaral e col., 1989), optou-se por descrever somente os estudos feitos em seres humanos e em outros primatas (identificados apropriadamente).

O Me aparece com reações pouco intensas para marcadores colinérgicos como a detecção da acetilcolinesterase (AChE) ou da colina-acetiltransferase (ChAT) quando comparado com outros núcleos amigdalianos. A maior parte da marcação parece ocorrer no neurópilo, mas há algumas células AChE positivas também presentes (Parent, 1971 - primatas; Nitecka e Narkiewicz, 1976; Svendsen e Bird, 1985; Sims e Willians, 1990). Por outro lado, os neurônios do Me expressam muitos neuropeptídeos e, em contraste com o BLNG e o sCLR, estes se localizam preferentemente em neurônios de projeção que enviam suas fibras em direção à st ou à via amígdalofugal ventral (Lind e col., 1985, Caffé e col. 1987 e McDonald, 1987). É interessante que essa característica é compartilhada com o Ce, sugerindo haver uma característica em comum para esses componentes da "amígdala expandida" (Gloor, 1997).

Tem-se demonstrado em quantidades de moderada à abundante, especificamente nos pericários do Me, a SS (Amaral e col., 1989 – macacos), o NPY (Water e col., 1990; em não primatas esta se co-localiza com a SS, McDonald, 1989a) e a NT (Michel e col., 1986; Benzing e col., 1990, 1992). Fibras e terminais imunorreativos à SS também são observados no Me em quantidades que variam de abundante para moderado (Amaral e col., 1989 – macacos), bem como fibras imunorreativas à NT que formam um plexo denso nesse núcleo (Mai e col., 1987;

Benzing e col., 1990, 1992). Alguns peptídeos que também se localizam em fibras, mas que não aparecem em quantidade significativa nos somas, têm como exemplo a GAL (Gentleman e col., 1989). Receptores para GAL são encontrados de forma abundante no Me de macacos (Köhler e col., 1989) o que está de acordo com o achado das fibras imunorreativas em humanos.

Em seres humanos, tanto os somas como o neurópilo do Me possuem uma alta atividade para a enzima dinucleotídeo nicotinamida adenina fosfatodiaforase (NADPH-d; Sims e Willians, 1990). No macaco a marcação é mais intensa nos somas, mas há também uma pequena marcação dessa atividade enzimática nas fibras presentes no neurópilo local (Pitkänen e Amaral, 1991).

Um aspecto importante do Me, sem dúvida relacionado ao seu dimorfismo sexual, é que ele representa a estrutura amigdaliana que contém a maior concentração de neurônios que respondem a esteróides gonadais advindos da circulação sanguínea, tanto estrógenos como andrógenos (Keefer e Stumpf, 1975; Pfaff e col., 1976; Bonsall e col., 1986; Michael e col., 1990 – todos em macacos). Além dos esteróides gonadais, o Me contém neurônios com imunomarcação para o hormônio liberador de hormônio luteinizante (Stopa e col., 1991). Algumas células com característica semelhante são também descritas no Me de macacos (Silverman e col., 1982).

1.2.4. Funções e hodologia

Não foi encontrado nenhum estudo demonstrando especificamente o papel funcional do Me em seres humanos até o momento. Isso se deve provavelmente ao fato

de a maior parte dos estudos funcionais serem feitos por técnicas de imageamento ainda insuficientemente específicas para um núcleo com tais dimensões e localização. Outros estudos não específicos baseiam-se em pacientes com lesão ou remoção unilateral ou bilateral da amígdala, as quais abrangem áreas muito maiores do que somente o Me e seu tecido adjacente. Ocorre ainda de o Me ser geralmente estudado como parte dos grupos amigdalianos "centromediais" ou "corticomediais", sem uma separação adequada de seus componentes. Desse modo, pode-se especular sobre sua função baseando-se em achados de mamíferos primatas não humanos e de mamíferos não primatas, como sugerido por de Olmos (2004) ou no que há descrito sobre sua hodologia, quimioarquitetura e morfologia em seres humanos.

Neste sentido, o Me de mamíferos não-primatas, como o rato, tem sido amplamente estudado, chegando-se a grande detalhamento sobre seus subnúcleos. Nesses animais o Me desempenha funções importantes, tais como: interpretação de informações sensoriais interoceptivas e exteroceptivas (Bressler e Baum, 1996; Guillamón e Segovia, 1997; Dielemberg e col., 2001), regulação de comportamentos sociais como o defensivo e o agressivo (Bolhuis e col., 1984; Newman, 1999; 2002), comportamento sexual de machos e de fêmeas e comportamento maternal (Rasia-Filho e col., 1991; Collen e col., 1997; Newman, 1999; 2002; Sheehan e col., 2001) e modulação da memória condicionada e do aprendizado onde componente emocional esteja envolvido (Canteras e col., 1995; Roozendaal e McGaugh, 1996; Rasia-Filho e col., 2000). Por causa disso é que, embora a relevância funcional do contínuo tecidual amígdalosublenticular em primatas ainda esteja por ser descrita e supondo-se que haja algum grau de analogia com outras espécies (Martin e col., 1991), o Me poderia desempenhar um papel importante na modulação de comportamentos típicos de cada

espécie associados com reprodução, alimentação e emoção também em macacos e na nossa espécie (de Olmos, 2004).

O Me é sexualmente dimórfico em diversas espécies e, como revisado especificamente para ratos (Rasia-Filho e col., 2012), a ação dos androgênios na porção posterior dorsal do Me em machos dessa espécie se reflete em uma organização morfológica neuronal que faz com que seus neurônios sejam mais numerosos, tenham maior volume somático, orientação dendrítica espacial com arranjo preferencial, maior densidade de espinhos dendríticos, maior conectividade sináptica e ocorrência de potenciais elétricos pós-sinápticos excitatórios em maior número do que ocorre em fêmeas. Em um único estudo prévio realizado por Murphy (1986) não se detectou diferença no volume do Me entre homens e mulheres, mas isso não invalida a possibilidade de que haja ainda novos conhecimentos a respeito de diferenças mais sutis entre os sexos. Este é um segmento da pesquisa no Me humano que avançou muito pouco e que serviria para ajudar a elucidar se, como em outras espécies, também se observa como função deste núcleo em humanos a modulação do comportamento sexual.

Além disso, o Me pode interagir com o sistema neuroendócrino (Martin e col., 1991; de Olmos, 2004). Nesse sentido, o Me envia projeções a vários núcleos hipotalâmicos em ratos (Petrovich e col., 2001). Também em primatas não humanos os axônios projetam-se em grande parte para a área pré-óptica medial e hipotálamo medial anterior, incluindo-se os núcleos paraventricular e supraóptico (Berry e col, 1995). Isso sugere que a estimulação do Me pode também ser acompanhada pela modulação da secreção do eixo hipotalâmico-hipofisário concomitantemente à modulação de comportamento sociais, embora não se tenha descrições exatas para seres humanos até

agora. Esse é mais um ponto importante que faz evidenciar a necessidade de se conhecer os componentes celulares do Me humano e sua possível aplicação futura para compreensão da função dessa estrutura.

1.3. Breve revisão sobre alguns métodos de estudos morfológicos e morfométricos para células nervosas

Como se tratam de técnicas clássicas procurar-se-á ser sucinto e objetivo nesta descrição. Ela é cabível, no entanto, porque as técnicas utilizadas importam para a presente tese e sua contribuição ao conhecimento. Uma delas, o método de Golgi, foi desenvolvido para poder gerar os resultados descritos para o Me humano a seguir (4.2. Artigo 2 para maiores informações).

1.3.1. Coloração de Nissl

O método de Nissl, desenvolvido no século XIX e que cora parte dos componentes intracelulares de corpos celulares e do início de dendritos proximais, é um método classicamente utilizado no estudo do SN normal (como por exemplo, Ramón y Cajal, 1909; Amaral e Schumann, 2005) ou com alguma patologia (Nobakht e col., 2011; Jiang e col., 2012), sozinho ou conjugado com outros métodos, porque revela os componentes e a distribuição espacial das células de uma determinada região (Figura 5). Tais dados, além de identificar a citoarquitetura de uma área nervosa, também podem ser empregados para contagens celulares, classificação e mensuração dos corpos neuronais, além de algo muito importante, que é a diferenciação entre neurônios e células gliais, de modo que suas populações possam ser estimadas (Figura 7). Porém, de

acordo com Peters e col. (1991), esse método não permite a classificação dos diferentes tipos de células da glia com segurança, o que só pode ser feito pela utilização de métodos mais específicos como imunocitoquímica, ou microscopia eletrônica.

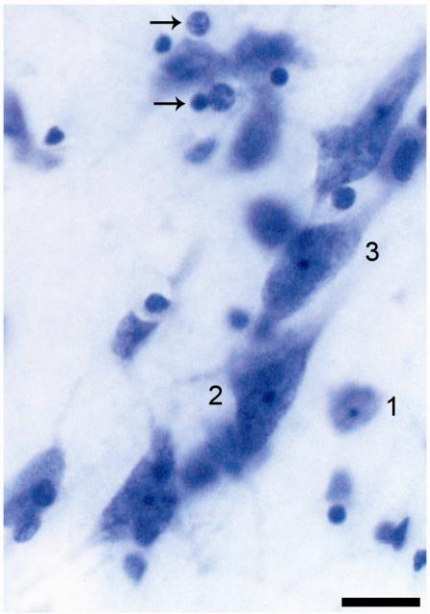

Figura 7. Fotomicrografia demonstrando células do núcleo amigdaliano medial humano reveladas pela coloração de Nissl com tionina. As setas indicam células da glia e os números os tipos neuronais multipolares descritos para o núcleo amigdaliano medial humano por estudos prévios imuno-histoquímicos. Estes neurônios possuem corpos celulares com formato esférico/ovóide/arredondado (1), angular (2), ou fusiforme (3). Barra de Escala = 20 µm.

Na presente tese, esta técnica foi empregada para que se comparasse o agrupamento celular do Me humano das amostras estudadas com as descrições presentes em atlas específico (Mai e col., 2007). Também, conjugada à estereologia (mais informações abaixo), serviu para que se pudesse estimar o número de neurônios e células da glia e sua proporção relativa no Me humano.

1.3.1.1. Estereologia

A Estereologia é um campo interdisciplinar que determina parâmetros quantitativos tridimensionais de materiais ou estruturas anatômicas a partir de secções bidimensionais, e é baseada em princípios fundamentais de geometria (como, por exemplo, o Princípio de Cavalieri) e estatística. (Weibel, 1979, Takase e Nogueira, 2007). Ela fornece técnicas para obtenção de informações quantitativas sobre uma estrutura com três dimensões a partir de secções planares bidimensionais desse material. Além disso, é um método que utiliza amostragem sistemática aleatória para fornecer dados imparciais quantitativos. Possui uma abordagem matemática eficiente com muitas aplicações para a Microscopia e as "Biociências", inclusive a Histologia do SN (Sorvari e col., 1995; Xavier e col., 2005; Schumann e Amaral 2005; 2006).

O "fracionamento e a amostragem sistemática" é um dos vários métodos de emprego da Estereologia e permite determinar o número total de partículas (por exemplo, células no tecido nervoso) em uma estrutura a partir de uma parte conhecida e representativa do volume total, de modo aleatório, porém uniforme. Seu emprego para contagem de neurônios e células da glia tem sido reiterado (para revisão mais extensa vejam-se Gundersein, 1986; Pakkenberg e Gundersen, 1988; Schumann e Amaral 2005; 2006, Takase e Nogueira, 2007).

1.3.2. Método de Golgi

O método de Golgi se baseia na impregnação argêntica de neurônios e células gliais, fazendo com que fiquem com uma cor parda a preta que contrasta com um fundo

mais claro amarelo-alaranjado, e pode prover amostras representativas dos tipos celulares presentes em uma área encefálica. Esta técnica tem sido muito útil no estudo da morfologia celular em diferentes espécies ao longo de décadas (Ramón y Cajal, 1909; Ramón-Molliner, 1962; McDonald, 1992; Woolley e McEwen, 1994; Fairén, 2005; Larriva-Sahd, 2006; Marcuzzo e col., 2007; Dall'Oglio e col., 2008a; 2008b; 2010; Rasia-Filho e col., 2012). Quando gera resultados satisfatórios, somente uma pequena proporção de células nervosas (quiçá 1-10%) presentes no tecido é impregnada pela prata e de uma maneira ainda tida como aleatória. Assim, a técnica de Golgi oferece a vantagem de permitir a visualização de células mais isoladas para estudo e, ao mesmo tempo a desvantagem de que, por seu caráter imprevisível, nunca se saber ao certo quando algum tipo de neurônio ficará visível completamente. Além disso, nem todas as regiões do SN de diferentes espécies impregnam-se igualmente (Ramón y Cajal, 1909; Valverde, 1962; Woolley; McEwen, 1993; Pannese, 1996; Dall'Oglio e col., 2007). Quando ocorre uma visualização adequada, os neurônios podem ter seus componentes (corpo celular, dendritos, espinhos e axônio) passíveis de identificação, classificação e mensuração (Figura 6) e as células gliais (exceto microglia) podem ser igualmente reconhecidas, classificadas e mensuradas (Rasia-Filho e col., 1999; 2004; Dall'Oglio e col., 2007; Arpini e col., 2010).

É notável que várias etapas metodológicas precisem ser seguidas rigorosamente para que resultados satisfatórios possam ser obtidos com essa técnica (Dall'Oglio e col., 2007). O tempo e a qualidade de cada fixação tecidual é um ponto chave nesse processo. E, dados todos os cuidados éticos para obtenção de tecido nervoso humano, seria muito vantajoso que se pudesse ter uma variante da técnica de Golgi que pudesse ser empregada para amostras mantidas em solução fixadora de formalina a 10%, como

corriqueiramente se utiliza em vários laboratórios e departamentos acadêmicos. Isso foi desenvolvido nesta tese, além da sua aplicação para o estudo do Me humano, e compõe os artigos e o capítulo de livro apresentados a seguir.

1.3.2.1. Contagem de espinhos dendríticos

O estudo dos espinhos dendríticos, especializações celulares pós-sinápticas onde ocorrem preferentemente contatos excitatórios, configura-se numa área importante para o entendimento das bases celulares de funcionamento do SN. A determinação do número de espinhos por segmento dendrítico (e, daqui, sua densidade por µm dendrítico) tem servido para estimar a maior ou menor ocorrência de sinapses em uma determinada célula de uma determinada região encefálica (Wooley e McEwen, 1993; Nimchinsky e col., 2002; Rasia-Filho e col., 2004; Hermel e col., 2006; Marcuzzo e col., 2007; de Castilhos e col., 2008).

Os espinhos podem sofrer modificações em sua morfologia e esse processo reflete o rearranjo rápido do citoesqueleto de actina em seu interior, o que pode levar à mudança no tamanho e no número de espinhos (Oertner e Matus, 2005; Tada e Sheng, 2006). Em geral, os espinhos são classificados de acordo com sua morfologia com a seguinte nomenclatura: a) "fino", o qual apresenta pescoço fino e uma cabeça bem definida e que parece ser um tipo mais lábil e capaz de ainda modificar sua forma; b) "espesso", que não apresenta pescoço diferenciado, e se mostra como uma elevação a partir do contorno dendrítico; c) em forma de "cogumelo", que apresenta pescoço mais espesso conectado a uma cabeça de maior tamanho e que parece ser o espinho mais estável em termos de mudanças numéricas e contatos sinápticos duradouros; d)

"ramificado", onde um pescoço pode dar origem a mais de uma cabeça de espinho; e) e outras formas complexas, incluindo algumas com presença de "espínula", uma protrusão que surge do próprio espinho (Figura 8; Peters e Kaiserman-Abramof, 1970; Peters e col., 1991; Hering e Sheng, 2001; González-Burgos, 2004; Brusco e col., 2010). Os filopódios são classificados à parte e têm por característica não apresentar uma cabeça definida, serem finos e compridos e poderem ser uma forma precursora, porém ainda imatura, dos espinhos ainda procurando estabelecer novas sinapses (Nimchinsky e col., 2002).

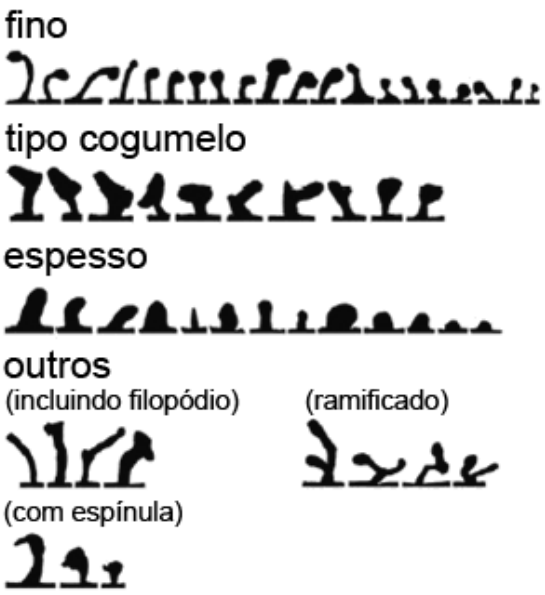

Figura 8. Desenhos representativos de variações da morfologia dos diferentes tipos de espinhos como se observa pelo emprego da técnica de Golgi e à microscopia de luz, surgindo a partir de uma linha de base que representa o tronco dendrítico. Reproduzido com modificações de Brusco e col. (2010).

1.3.3. Imuno-histoquímica para GFAP

A proteína ácida fibrilar glial (GFAP) é constituinte dos filamentos intermediários do citoesqueleto de astrócitos maduros e tem servido para identificar a morfologia e o arranjo astrocitário em diferentes estruturas do SN central (SNC; Gomes e col., 1999; Garcia-Segura e McCarthy, 2004; Kettenmann e Ranson, 2005). Modificações na expressão e fosforilação de GFAP influenciam a forma e a localização espacial dos astrócitos e seus prolongamentos (Gomes e col., 1999). A reação imuno-histoquímica para GFAP (GFAP-ir) contribui para identificar este componente da macróglia com detalhes que permitem inferir sobre a morfologia astrocitária e sua variação em diferentes condições experimentais (Martinez, 2007).

Neste estudo utilizou-se este método para descrever a morfologia dos astrócitos, bem como para complementar os dados obtidos preliminarmente com uso do método de Nissl associado à estereologia. Com isso, a técnica de imuno-histoquímica para a GFAP se configurou em uma abordagem complementar e relevante para o estudo dos astrócitos, dentre os demais componentes gliais, no Me humano.

1.3.4. Microscopia eletrônica de transmissão

A microscopia eletrônica de transmissão é uma ferramenta de pesquisa multidisciplinar com menos de um século de aplicação, dado que o primeiro microscópio eletrônico foi construído por Knoll e Ruska no início da década de 30. O microscópio eletrônico de transmissão foi desenvolvido com o intuito de criar um equipamento com maior resolução (capacidades de distinguir entre dois pontos) e que

permitisse maiores aumentos do que os obtidos com a microscopia de luz. Em preparações histológicas de tecido nervoso próprias (cortes ultrafinos; ver exemplos de protocolos em Hermel e col., 2006 e no item "Atigo 2", que compõe esta tese) podem-se obter aumentos superiores a 50.000X e ultrapassar a resolução de 0,1 nm com um microscópio eletrônico (que utiliza um feixe de elétrons para formar a imagem), enquanto que o microscópio de luz (que utiliza um feixe de fótons ao invés de elétrons) permite aumentos na ordem de 2.000X com limite de resolução em torno de 100nm. Essa diferença se dá porque o comprimento de onda dos elétrons (0,005 nm) é menor que o dos fótons (500 nm), e o comprimento de onda é um fator inversamente proporcional à resolução, ou seja, quanto menor for comprimento de onda, maior será o poder de resolução (Horta Jr. e García, 2007).

A microscopia eletrônica permitiu grande avanço nas Neurociências pelo estudo ultraestrutural detalhado do tecido nervoso, incluindo, por exemplo, detalhes das organelas celulares e dos contatos sinápticos (Peters e col., 1991; Sorvari e col., 1996b; Hermel e col., 2006; Müller e col., 2012), e de suas alterações em estados patológicos (Baloyannis e col., 2006; Scheff e col., 2006). Apesar disso ainda é pouco utilizada no estudo do tecido nervoso humano obtido *post mortem* (exemplos em Sorvari e col., 1996b e Scheff e col., 2006) pelas grandes limitações técnicas impostas pela degeneração rápida do tecido, o que pode explicar porque não foram encontrados dados morfológicos ultraestruturais na literatura sobre o Me humano.

Sendo assim, nesta tese utilizou-se a microscopia eletrônica de transmissão para descrever detalhes ultraestruturais inéditos das células gliais e neurônios do Me humano. Deste último foram estudados, por exemplo, corpos celulares, dendritos,

espinhos e terminais axonais com sinapses bem preservadas (guardadas as alterações inerentes do tempo mínimo de 6h decorrido *post mortem*).

2. JUSTIFICATIVA

Até o momento há dados escassos e incompletos na literatura descrevendo a população neuronal no Me humano. Por exemplo, não se encontram estudos morfológicos detalhando os componentes neuronais como os espinhos dendríticos e os axônios locais, nem as células gliais, e nem tampouco estudos ultra-estruturais envolvendo este núcleo. Descrições morfológicas e dados morfométricos dos componentes celulares do Me servem como base dos conhecimentos anatômicos, histológicos e fisiológicos dessa estrutura. E os resultados obtidos com indivíduos normais, *per se*, são de fundamental relevância para uma melhor elaboração de hipóteses e para a compreensão do papel funcional do Me em circuitos neurais integrados. Além do mais, prestam-se igualmente para comparações com indivíduos em condição patológica, podendo fornecer a base para se entender a fisiopatologia de diversas doenças neurológicas e psiquiátricas. A presente tese descreve uma modificação da técnica de Golgi que permitiu estudar encéfalos mantidos em formol 10% por tempo variável e, associado com outras técnicas em tecido *post mortem* de homens adultos, a primeira descrição detalhada dos componentes celulares do Me com dados de microscopia óptica, estereologia, imuno-histoquímica e microscopia eletrônica.

3. OBJETIVOS

3.1. Geral

Descrever e quantificar aspectos da morfologia neuronal e astrocitária no Me humano que possam servir de base para o entendimento de sua função celular local e, adicionalmente, para correlações futuras com amostras obtidas de indivíduos igualmente saudáveis ou em estados patológicos.

3.2. Específicos

a) Adaptar e desenvolver uma variação na técnica de Golgi que possa ser aplicada em amostras de tecido nervoso humano armazenadas em formalina 10% não tamponada por longos períodos (em nosso caso, variando de 1 mês até 10 anos).

b) Estimar a densidade de neurônios e células gliais no Me de homens adultos *post-mortem* por meio do método de Nissl com tionina e estudo estereológico, e comparar os resultados obtidos nos hemisférios cerebrais direito e esquerdo.

c) Descrever detalhadamente a morfologia neuronal no Me de homens adultos *post-mortem* por meio de técnica de Golgi. Com essa mesma técnica, estimar a densidade de espinhos obtidos em ramos dendritos de até cerca de 200 μm a partir do corpo celular, e descrever a morfologia axonal presente no neurópilo deste núcleo.

d) Estudar a população astrocitária no Me de homens adultos *post-mortem* pela utilização de técnica imuno-histoquímica para a proteína ácida fibrilar glial.

e) Descrever aspectos ultra-estruturais da morfologia neuronal e glial, sobretudo dos sítios sinápticos, no Me de homens adultos *post-mortem* utilizando-se da microscopia eletrônica de transmissão.

4. MATERIAIS E MÉTODOS, RESULTADOS E DISCUSSÃO

4.1. Artigo 1: The "single-section" Golgi method adapted for formalin-fixed human brain and light microscopy. Publicado no "Journal of Neuroscience Methods" em 2010. Página 34.

4.1.1. Capítulo de livro: The adapted "single-section" Golgi method and the DiI fluorescent dye in microscopy for describing neuronal and glial morphology in different species. Publicado no livro "Microscopy: Science, Technology, Applications and Education"; Editora FORMATEX, Espanha, em 2010. Página 39.

4.2. Artigo 2: Cellular components of the human medial amygdaloid nucleus. Submetido para publicação no "Journal of Comparative Neurology" e enviados os acréscimos solicitados pelos revisores. Página 43.

Journal of Neuroscience Methods 189 (2010) 51–55

Contents lists available at ScienceDirect

Journal of Neuroscience Methods

journal homepage: www.elsevier.com/locate/jneumeth

The "single-section" Golgi method adapted for formalin-fixed human brain and light microscopy

Aline Dall'Oglio[a,1], Denise Ferme[b,1], Janaína Brusco[c,d], Jorge E. Moreira[c,d], Alberto A. Rasia-Filho[a,b,e,*]

[a] Program in Neuroscience, Institute of Basic Sciences, Federal University of Rio Grande do Sul, R. Sarmento Leite 500, Porto Alegre RS 90050-110, Brazil
[b] Program in Pathology, Federal University of Health Sciences, R. Sarmento Leite 245, Porto Alegre RS 90050-110, Brazil
[c] Laboratory of Synaptic Structure, Department of Cell/Molecular Biology and Biopathogens, Medical School of Ribeirão Preto, University of São Paulo, Av. Bandeirantes 3900, Ribeirão Preto SP 14049-900, Brazil
[d] Program in Neuroscience & Behavior, Ribeirão Preto School of Medicine, Universidade de São Paulo, Brazil
[e] Department of Basic Sciences/Physiology, Federal University of Health Sciences, R. Sarmento Leite 245, Porto Alegre RS 90050-110, Brazil

ARTICLE INFO

Article history:
Received 26 November 2009
Received in revised form 15 March 2010
Accepted 16 March 2010

Keywords:
Golgi method
Neuronal morphology
Glial cells

ABSTRACT

The Golgi method has been used for over a century to describe the general morphology of neurons in the nervous system of different species. The "single-section" Golgi method of Gabbott and Somogyi (1984) and the modifications made by Izzo et al. (1987) are able to produce consistent results. Here, we describe procedures to show cortical and subcortical neurons of human brains immersed in formalin for months or even years. The tissue was sliced with a vibratome, post-fixed in a combination of paraformaldehyde and picric acid in phosphate buffer, followed by osmium tetroxide and potassium dicromate, "sandwiched" between cover slips, and immersed in silver nitrate. The whole procedure takes between 5 and 11 days to achieve good results. The Golgi method has its characteristic pitfalls but, with this procedure, neurons and glia appear well-impregnated, allowing qualitative and quantitative studies under light microscopy. This contribution adds to the basic techniques for the study of human nervous tissue with the same advantages described for the "single-section" Golgi method in other species; it is easy and fast, requires minimal equipment, and provides consistent results.

1. Introduction

The *colorazione nera* has been used to reveal the general morphology of neurons and glia in various areas of the nervous system of several species (Golgi, 1873; Ramón y Cajal, 1909; Valverde, 1962; Fairén et al., 1977; Scheibel and Scheibel, 1978; McDonald, 1982). For more than a century, phylogenetic and ontogenetic studies have been benefited from the Golgi method, which is a reliable tool to identify different types of neurons, the detailed shape of single cells, and to extract functional hypotheses of brain function from morphology (Ramón y Cajal, 1909; Lorente de Nó, 1934; Valverde, 1962; Szentágothai, 1978; Kisvárday et al., 1990; Larriva-Sahd, 2008; Gómez-Villalobos et al., 2009).

As summarized by Fairén (2005), the Golgi method is based on the metallic impregnation of neurons and glial cells in tissue blocks that had been hardened by potassium dichromate and then treated by silver nitrate. A proper historical and technical review of the diverse Golgi procedures can be found in Alonso (1994) and references therein (see also Nauta and Ebbesson, 1970; Banks, 1999). Following the original description of his "slow method", which used a sequence of potassium or ammonium dichromate and silver nitrate for long time, Golgi proposed that a potassium dichromate and osmium tetroxide mixture could speed up the reaction. This "rapid method" was further developed and masterly applied by Ramón y Cajal. Golgi also tested the use of mercury salts during tissue fixation and for cellular impregnation, which Cox successfully modified later. Other efforts involved the use of different aldehydes as alternative fixative solutions and generated the Golgi–Kopsch, the Golgi–Colonnier, and the Golgi–Rio Hortega procedures, to cite some of them (Alonso, 1994). After a period of oblivion until the second half of the 20th century (Fairén, 2005), Golgi method revived (e.g., Valverde, 1970; Fairén et al., 1977, 1984; Kolb et al., 1981; McDonald, 1982; Feldman, 1984; Millhouse, 1986; Somogyi, 1990; Woolley et al., 1990; Woolley and McEwen, 1994; Jacobs et al., 1997; Dall'Oglio et al., 2008b; Larriva-Sahd, 2008).

All of the procedures in the "family" of Golgi techniques have advantages and restrictions. For example, silver impregnation apparently occurs "at random" and there are no unequivocal explanations about discrepant results of the method. This leads to a number of impregnated neurons but not a homogeneous pattern of cellular staining on each tissue section. To provide useful results, it has been controled the diffusion rate and the pH of the chromation

* Corresponding author at: UFCSPA/Department of Basic Sciences, R. Sarmento Leite 245 (room 308), Porto Alegre 90170-050 RS, Brazil. Tel.: +55 51 91161643; fax: +55 51 33038752.
E-mail addresses: rasiafilho@pq.cnpq.br, aarf@ufcspa.edu.br (A.A. Rasia-Filho).
[1] Both authors contributed equally to this study.

0165-0270/$ – see front matter © 2010 Elsevier B.V. All rights reserved.
doi:10.1016/j.jneumeth.2010.03.018

solution (Ângulo et al., 1996), or the establishment of the best technique according to the lenght of fixation and storage of the tissue (Rosoklija et al., 2003; Melendez-Ferro et al., 2009). It is noteworthy that the fine structure and the specific synaptic interactions of Golgi-stained neurons can be studied by the combination of light and electron microscopy after a de-impregnation procedure (Fairén et al., 1977; Somogyi, 1990; Bolam, 1992; and see also Fairén, 2005).

Freund and Somogyi (1983) developed the "section-Golgi" procedure for thin nervous tissue slices (80–100 μm thick) which allowed histochemical procedures to be carried out prior to silver impregnation. Their contribution made possible to study neurons retrogradely labelled by horseradish peroxidase and, by subsequent gold-toning, specific synaptic contacts in the electron microscope. Soon after, Gabbott and Somogyi (1984) depicted the "single-section" Golgi method that proved to be easy, reliable, and relatively unexpensive. This approach has been successfully applied to clue the neuroendocrine modulation of the number of dendritic spines in different brain areas of male and female rats (Woolley et al., 1990; Woolley and McEwen, 1994; Rasia-Filho et al., 1999, 2004, 2009; Brusco et al., 2008). It consists in sectioning the brain perfused with a paraformaldehyde and picric acid solution, placing the 60–200 μm thick sections in potassium bichromate, and "sandwich" them between cover slips for the impregnation in silver nitrate. Izzo et al. (1987) developed an elegant modification of the "single-section" technique providing another rapid and consistent Golgi tool. In this method, the osmium tetroxide was added to the reaction before the silver nitrate and the brain slices were placed between microscopic slides, which would also allow an easier handling of serial sections (see detailed data in Bolam, 1992). This technique could be combined with immunocytochemistry for neurotransmitters or other substances, as was the case of Golgi-impregnated substance P- and [Met]enkephalin-immunoreactive neurons in the caudate nucleus of cats and ferrets (Izzo et al., 1987).

Other suitable Golgi methods were developed to reveal the neuronal morphology in cortical and subcortical areas of human brains immersed in formalin for long periods of time (Rosoklija et al., 2003; Friedlander et al., 2006; Melendez-Ferro et al., 2009). Here we describe that a combination of the original "single-section" Golgi method (Gabbott and Somogyi, 1984) and the procedure proposed by Izzo et al. (1987) and Bolam (1992) is useful to study the human brain and can be applied to formalin-fixed tissue that has been stored for months or even years. Osmication provided best results. This contribution adds to the basic procedures that made the original "single-section" Golgi method useful for the study of the nervous tissue and providing consistent results.

2. Materials and methods

2.1. Subjects

We studied the brains of 2 males, aged 47 and 68 years old, who died of cardiovascular failure. Part of the temporal lobes was obtained during necropsies from the Institute of Legal Medicine in Rio Grande do Sul, Brazil. No fixative perfusion was done prior to the brain removal. The interval between the death and the necropsies varied from at least 6 h, according to Brazilian laws, to 8 h at the most. Previous clinical and co-morbid data were obtained during an interview directed to the relatives or legal representatives, who also signed an informed consent prior to the inclusion in this study. All the legal and ethical procedures were in accordance with international and local regulatory standards (based on the 1964 Declaration of Helsinki) and ethical committee approvals obtained from the Department of Legal Medicine from the State of Rio Grande do Sul (process number 03/08), the Federal University of Health Sciences of Porto Alegre (process number 541/07), and the Federal University of Rio Grande do Sul (process number 2008009), Brazil.

2.2. Tissue fixation and the impregnation procedure

Small blocks of approximately 5 × 5 × 5 cm away from the anterior pole of the temporal lobe were immediately immersed in unbuffered 10% formalin and kept stored in this same fixative solution for approximately 20 months (fixative solutions were around pH 4.0). Afterwards, small samples were trimmed to ~1.5 cm^3 to contain the temporal cortex (superior temporal gyrus) and the striatum (head of the caudate nucleus; DeArmond et al., 1989). The samples were coronally sectioned in slices 200 μm thick using a vibratome (Leica, Germany), and submitted to the following steps: (1) free-floating sections were post-fixed with 4% paraformaldehyde and 1.5% picric acid in 0.1 M phosphate buffer solution (PBS, pH 7.4) either for 24 h or 72 h in the dark at 4 °C. (2) The sections were quickly rinsed in PBS, transferred to a 0.02% osmium tetroxide solution in PBS for 10–30 min under gentle shaking in the dark; quickly rinsed in PBS for 1–2 min, and (3) immersed in 3% potassium dichromate (Merck, Germany) in deionized water, and kept in the same solution in the dark at 4 °C either for 24 h or 72 h. The sections were quickly rinsed again in distilled water to remove excess of chromation, and "sandwiched" between glass coverslips glued (epoxy glue) in the four corners to allow gradual diffusion of the solution by capillarity. (4) Each "sanwiched" section was gently placed in the impregnation solution of 1.5% silver nitrate (Merck, Germany) in deionized water at room temperature (RT) in the dark either for 24 h or 72 h. After that period, the coverslips were broken, the sections removed, rinsed in distilled water to wash the excess of crystals with the help of a soft paintbrush, and mounted on gelatin-coated slides (gelatin from porcine skin, ~300 g Bloom, Sigma Chemicals Co., USA). The slides were dried at RT (caution was taken to avoid overdrying these brittle) immersed in distilled water (once over 3 min) and dehydrated in ascending series of ethanol as follows: 70% and 80% (3 min each), 95% and 100% (twice, 3 min each), cleared in xylene/ethanol 1:1 and 2:1 (3 min each), xylene 100% (two rinses of 3 and 6 min each), mounted with coverslips and non-acidic synthetic balsam (Soldan, Brazil; or, alternatively, Permount®, USA) avoiding air bubbles, and dried at RT for 24 h.

The required time to finish the procedure would be 5 days if the steps 1, 3, and 4 are done on the minimum time required (24 h), and 11 days using 72 h for each step.

2.3. Image processing

The slides were observed and pictured with a Nikon Eclipse E-600 microscope (400×, Japan) coupled to a Pro-Series High Performance CCD camera (or other of high quality). Stacks of micrographs provided the final image using the Image-Pro Plus 6.0 software (Media Cybernetics, USA). Sharpening, brightness or background contrast was adjusted using the Adobe Photoshop 7.0 software (USA).

3. Results

The protocol as described produced good results. As in other Golgi techniques, our method impregnated a small percentage of neurons and glial cells in the slices of cortex and striatum (Figs. 1 and 2). Sometimes the best stain and contrast was found on the outer limits of the sections. The slices without osmication produced the weakest contrast, and even some peripheral cells of the section were not completely visible (Fig. 1A). In this case the neurons could appear with a fading of the stain or with "cut-off" dendritic branches. As an example, in Fig. 1B, there are pyramidal neurons with apparently short basal dendrites and the apical dendrite with short bifurcated branches (for a deep discussion, see Feldman, 1984). Also, unwanted silver crystals are seen over the

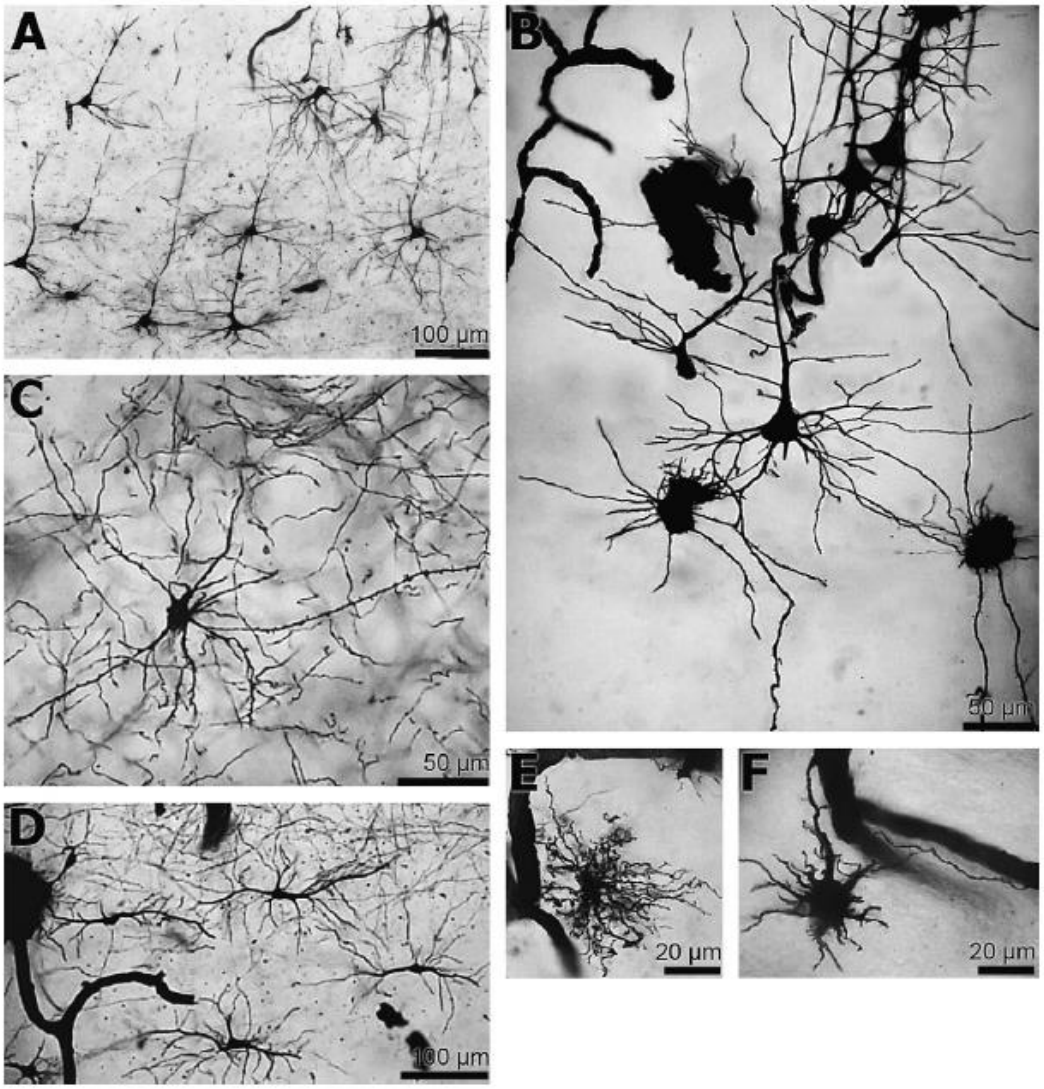

Fig. 1. Golgi-impregnated cells from the human temporal lobe (superior temporal gyrus) and striatum (head of the caudate nucleus). Adaptation of the "single-section" Golgi method in formalin-fixed samples without osmication (A), or after osmication (B–F) and along different impregnating periods (5–11 days). Some neurons appeared incompletely stained (B). A more extensive impregnation reveals the axonal network close to a neuron (C) or the general morphology of a neuronal subpopulation (D). Impregnated astrocytes were found close to blood vessels (E) with characteristic end-feet processes (F).

tissue and impregnated blood vessels. Deceptive results can occur when the formalin solution is renewed before processing the tissue. For example, unbuffered 10% formalin solution with a pH down to 2.5 produced several aspects of irregular impregnation. Nevertheless, this bad result could be partially reversed by maintaining the brain slices in 3% potassium dichromate solution for 7 days. On the other hand, the use of a post-fixative solution with a pH ranging from 7.0 to 11.0 provided nice results as well.

Well-impregnated cells (neurons and glial cells) appear black stained against a minimal soft yellow background with few small particles of precipitation in the neuropil after osmication (Figs. 1C–F and 2). Following this procedure, the quality of stain was similar when visually comparing the results obtained along 5–11 days of chromation/silver nitrate impregnation. Various kinds of neurons could be observed in the same plane of section with radiating dendrites. Profusion of thin axons and their collateral processes were also evident (Fig. 1C and D). In the caudate nucleus, medium-spiny neurons were uniformly impregnated (Fig. 2A and B). They appeared, as in the classical descriptions, with a round cell body and various primary dendrites that branched and tapered along the section. Dendritic spines were visualized even with low magnification. They showed a continuum of different shapes and sizes that could be easily identified, allowing the different classifications by shape as thin, stubby, mushroom-like or wide (Fig. 2C).

Perineuronal glia or glial cells in close apposition to blood vessels also appeared well-impregnated (Figs. 1E,F and 2A). Astrocytes with vascular end-feet processes were found in different grey and white areas (Fig. 1E and F).

4. Discussion

Here, we report the use of the original "single-section" Golgi method (without osmium) and adaptation after Izzo et al. (1987) and Bolam (1992) as another technique to study the morphology of human cells on brain slices. One of the advantages of this method is that it can be applied to formalin-fixed human tissue stored for a long time, as in the routinely fixed anatomical pieces. We developed this technique in brain samples stored for almost 2 years in formalin, but other times can be tested (few months of storage also appeared to provide good results; data not shown). The use of low concentrated osmium tetroxide led to the

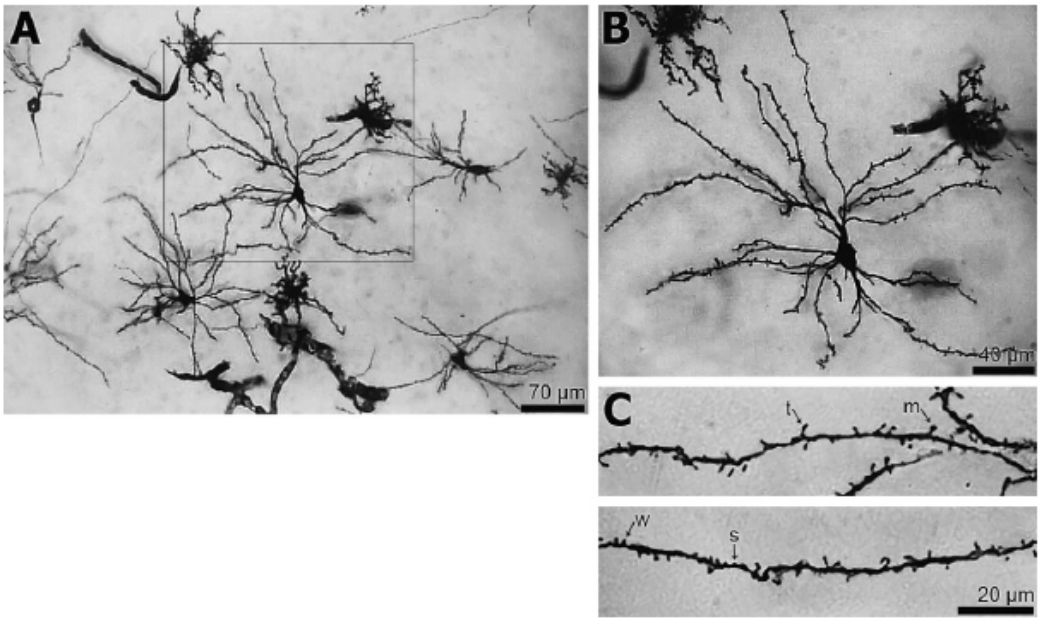

Fig. 2. Neurons from the human caudate nucleus stained with the adapted "single-section" Golgi method for formalin-fixed samples. The inset in A was zoomed up to show details of a cell body, branching dendrites, and spines (B). Pleomorphic dendritic spines (C) classified as thin (t), "mushroom-like" (m), stubby (s) or wide (w).

best results and all the experimental steps could be done in few days.

As from the times of Ramón y Cajal (1909), the application of the Golgi method allows relevant insights on the cytoarchitectonical organization of different brain areas. "Golgi staining requires a significant investment in tissue, time, and materials, and unless great care is taken, it can fail completely" (Rosoklija et al., 2003). This is true under many conditions. The present procedure, which adds to the basics for the study of the human nervous tissue, has the same advantages described for the "single-section" Golgi method in other species. It is relatively easy and fast (5–11 days), requires minimal equipments, and provides good results for human brain tissue fixed in formalin. Qualitative and quantitative studies can be conducted in well-impregnated neurons under light microscopy (see examples in Rasia-Filho et al., 2004; de Castilhos et al., 2006, 2008; Brusco et al., 2008; Dall'Oglio et al., 2008a,b) to be correlated with other neuronal and glial morphological and functional findings (Hermel et al., 2006; Martinez et al., 2006; Cunningham et al., 2007; de Castilhos et al., 2008; Rasia-Filho et al., 2009). Therefore, besides other current techniques and innovations, the Golgi method continues to be a relevant tool to neuroscience.

Common drawbacks using the Golgi method are the absence of a complete neuronal impregnation and variability in the results (Scheibel and Scheibel, 1978; Rasia-Filho et al., 1999). In addition, other inherent variables that might affect the final results are the age of the subjects, their past health condition, the long-term use of medications, the degree of cellular *post-mortem* necrosis, and variations in the diffusion rate of the primary fixative. Nevertheless, when comparing the present protocol to other current ones, the Golgi–Cox method on long-term fixed human tissue (10% neutral buffered formalin for up to 15 years) does not produce satisfactory results even when pretreatments (citrate buffer and sodium borohydrate) are used to remove excess of fixation prior to chromation (Melendez-Ferro et al., 2009). Other procedures as the rapid Golgi and the Golgi–Kopsch gave nice results with tissues fixed in formalin, that had lost its buffering capacity over time, and that were stored from 15 months up to 55 years (Rosoklija et al., 2003). Here, the sections were obtained without prior embedding in polymerized plastic as described by Moss and Whetsell (2004) and the impregnation process did not require microwave heating for 6–8 h as done by Armstrong and Parker (1986). The present method also allowed the observation of glial cells, which can be compared to the Golgi–Hortega–Lavilla silver impregnation technique for glutaraldehyde–paraformaldehyde prolonged fixed brain tissue (D'amelio, 1983).

Finally, the aim of the present work is to propose a new application of a relevant protocol and to report that Golgi-stain sections obtained from brains stored in unbuffered formalin for long periods of time can still be useful to analyze human brain material. This may instigate the interest to applying the Golgi method to normal conditions or to specific neurological diseases in human materials.

Acknowledgements

The authors thank the relatives of the patients that generously donated the tissue for this study. We are also thankful to Dr. Jackson Bittencourt (University of São Paulo) for a methodological improvement, to Dr. Matilde Achaval (University of Rio Grande do Sul, Brazil) for the use of some equipments and for helpful comments during the preparation of the manuscript, and to the reviewers of the manuscript for their insightful suggestions. Grants from the Fundação de Amparo à Pesquisa do Estado de São Paulo, Brazil (FAPESP 05/56447-7 CinAPCe to J.E.M.), and from the Conselho Nacional de Pesquisa e Desenvolvimento (CNPq). J.E.M. and A.A.R.F. are CNPq researchers.

References

Alonso JR. Los Métodos de Golgi. Salamanca: Ediciones Universidad Salamanca; 1994. pp. 230.
Ãngulo A, Fernández E, Merchán JÁ, Molina M. A reliable method for Golgi staining of retina and brain slices. J Neurosci Methods 1996;66:55–9.
Armstrong E, Parker B. A new Golgi method for adult human brains. J Neurosci Methods 1986;17:247–54.
Banks RW. Cytological staining methods. In: Windhorst U, Johansson H, editors. Modern techniques in neuroscience research. Heidelberg: Springer-Verlag; 1999. p. 1–26.
Bolam JP. Experimental neuroanatomy: a practical approach. New York: Oxford University Press; 1992. pp. 296.
Brusco J, Wittmann R, de Azevedo MS, Lucion AB, Franci CR, Giovenardi M, Rasia-Filho AA. Plasma hormonal profiles and dendritic spine density and morphology

in the hippocampal CA1 stratum radiatum, evidenced by light microscopy, of virgin and postpartum female rats. Neurosci Lett 2008;438:346–50.
Cunningham RL, Claiborne BJ, McGinnis MY. Pubertal exposure to anabolic androgenic steroids increases spine densities on neurons in the limbic system of male rats. Neuroscience 2007;150:609–15.
Dall'Oglio A, Gehlen G, Achaval M, Rasia-Filho AA. Dendritic branching features of posterodorsal medial amygdala neurons of adult male and female rats: further data based on the Golgi method. Neurosci Lett 2008a;430:151–6.
Dall'Oglio A, Gehlen G, Achaval M, Rasia-Filho AA. Dendritic branching features of Golgi-impregnated neurons from the "ventral" medial amygdala subnuclei of adult male and female rats. Neurosci Lett 2008b;439:287–92.
D'amelio FE. The Golgi–Hortega–Lavilla technique, with a useful additional step for application to brain tissue after prolonged fixation. Biotech Histochem 1983;58:79–84.
DeArmond SJ, Fusco MM, Dewey MM. Structure of the human brain, third ed. New York: Oxford University Press; 1989. pp. 208.
de Castilhos J, Forti CD, Achaval M, Rasia-Filho AA. Dendritic spine density of posterodorsal medial amygdala neurons can be affected by gonadectomy and sex steroid manipulations in adult rats: a Golgi study. Brain Res 2008;1240:73–81.
de Castilhos J, Marcuzzo S, Forti CD, Frey RM, Stein D, Achaval M, Rasia-Filho AA. Further studies on the rat posterodorsal medial amygdala: dendritic spine density and effect of 8-OH-DPAT microinjection on male sexual behavior. Brain Res Bull 2006;69:131–9.
Fairén A. Pioneering a golden age of cerebral microcircuits: the births of the combined Golgi-electron microscope methods. Neuroscience 2005;136:607–14.
Fairén A, DeFelipe J, Regidor J. Nonpyramidal cells. General account. In: Peters A, Jones EG, editors. Cerebral cortex. Cellular components of the cerebral cortex. New York: Plenum Press; 1984. p. 201–53.
Fairén A, Peters A, Saldanha J. A new procedure for examining Golgi impregnated neurons by light and electron microscopy. J Neurocytol 1977;6:311–37.
Feldman ML. Morphology of the neocortical pyramidal neuron. In: Peters A, Jones EG, editors. Cerebral cortex. Cellular components of the cerebral cortex. New York: Plenum Press; 1984. p. 123–200.
Freund TF, Somogyi P. The Section–Golgi impregnation procedure. 1. Description of the method and its combination with histochemistry after intracellular ionophoresis or retrograde transport of horseradish peroxidase. Neuroscience 1983;9:463–74.
Friedlander DR, Los JG, Ryugo DK. A modified Golgi staining protocol for use in the human brain stem and cerebellum. J Neurosci Methods 2006;150:90–5.
Gabbott PL, Somogyi J. The 'single' section Golgi–impregnation procedure: methodological description. J Neurosci Methods 1984;11:221–30.
Golgi C. Sulla struttura della sostansa grigia del cervello. Gazzetta Medica Italiana 1873;33:244–6.
Gómez-Villalobos MJ, Gordillo AC, López Jr, Flores G. The utility of the Golgi–Cox method in the morphological characterization of the autonomic innervation in the rat heart. J Neurosci Methods 2009;179:40–4.
Hermel EES, Ilha J, Xavier LL, Rasia-Filho AA, Achaval M. Influence of sex and estrous cycle, but not laterality, on the neuronal somatic volume of the posterodorsal medial amygdala of rats. Neurosci Lett 2006;405:153–8.
Izzo PN, Graybiel AM, Bolam JP. Characterization of substance P- and [Met]enkephalin-immunoreactive neurons in the caudate nucleus of cat and ferret by a single section Golgi procedure. Neuroscience 1987;20:577–87.
Jacobs B, Driscoll L, Schall M. Life-span dendritic and spine changes in areas 10 and 18 of human cortex: a quantitative Golgi study. J Comp Neurol 1997;386:661–80.
Kolb H, Nelson R, Mariani A. Amacrine cells, bipolar cells and ganglion cells of the cat retina: a Golgi study. Vision Res 1981;21:1081–114.
Kisvárday ZF, Gulyas A, Beroukas D, North JB, Chubb IW, Somogyi P. Synapses, axonal and dendritic patterns of GABA-immunoreactive neurons in human cerebral cortex. Brain 1990;113:793–812.
Larriva-Sahd J. The accessory olfactory bulb in the adult rat: a cytological study of its cell types, neuropil, neuronal modules, and interactions with the main olfactory system. J Comp Neurol 2008;510:309–50.
Lorente de Nó R. Studies on the structure of the cerebral cortex. II. Continuation of the study of the ammonic system. J Psychol Neurol 1934;113–77.
Martinez FG, Hermel EE, Xavier LL, Viola GG, Riboldi J, Rasia-Filho AA, Achaval M. Gonadal hormone regulation of glial fibrillary acidic protein immunoreactivity in the medial amygdala subnuclei across the estrous cycle and in castrated and treated female rats. Brain Res 2006;1108:117–26.
McDonald AJ. Cytoarchitecture of the central amygdaloid nucleus of the rat. J Comp Neurol 1982;208:401–18.
Melendez-Ferro M, Perez-Costas E, Roberts RC. A new use for long-term frozen brain tissue: Golgi impregnation. J Neurosci Methods 2009;176:72–7.
Millhouse OE. The intercalated cells of the amygdala. J Comp Neurol 1986;247:246–71.
Moss TL, Whetsell Jr WO. Techniques for thick-section Golgi impregnation of formalin-fixed brain tissue. In: Kohwi Y, editor. Methods in Molecular Biology, vol. 277. Totowa: Humana Press; 2004. p. 277–85.
Nauta WJH, Ebbesson SOE. Contemporary research methods in neuroanatomy. first edition New York: Springer-Verlag; 1970. pp. 386.
Ramón y Cajal S. Histologie du système nerveux de lïHomme et des vertébrés. Paris: Maloine; 1909. pp. 986.
Rasia-Filho AA, Brusco J, Moreira JE. Spine plasticity in the rat medial amygdala. In: Baylog RL, editor. Dendritic spines: biochemistry, modeling and properties. Hauppauge: Nova Science Publishers; 2009. p. 67–90.
Rasia-Filho AA, Fabian C, Rigoti K, Achaval M. Influence of sex, estrous cycle and motherhood in dendritic spine density in the rat medial amygdala revealed by the Golgi method. Neuroscience 2004;126:839–47.
Rasia-Filho AA, Londero RG, Achaval M. Effects of gonadal hormones on the morphology of neurons from the medial amygdaloid nucleus of rats. Brain Res Bull 1999;48:173–83.
Rosoklija G, Mancevski B, Ilievski B, Perera T, Lisanby SH, Coplan JD, Duma A, Serafimova T, Dwork AJ. Optimization of Golgi methods for impregnation of brain tissue from humans and monkeys. J Neurosci Methods 2003;131:1–7.
Scheibel ME, Scheibel AB. The Methods of Golgi. In: Robertson RT, editor. Neuroanatomical research techniques. New York: Academic Press; 1978. p. 89–114.
Somogyi P. Synaptic connections of neurons identified by Golgi impregnation: characterization by immunocytochemical, enzyme histochemical, and degeneration methods. J Electron Microsc Techn 1990;15:332–51.
Szentágothai J. The neuron network of the cerebral cortex: a functional interpretation. Proc R Soc Lond B 1978;201:219–48.
Valverde F. Intrinsic organization of the amygdaloid complex. A Golgi study in the mouse. Trab Inst Cajal Invest Biol 1962;54:291–314.
Valverde F. The Golgi method: a tool for comparative structural analyses. In: Nauta WJH, Ebbesson SOE, editors. Contemporary research methods in neuroanatomy. New York: Springer-Verlag; 1970. p. 11–31.
Woolley CS, Gould E, Frankfurt M, McEwen BS. Naturally occurring fluctuation in dendritic spine density on adult hippocampal pyramidal neurons. J Neurosci 1990;10:4035–9.
Woolley CS, McEwen BS. Estradiol regulates hippocampal dendritic spine density via an N-methyl-D-aspartate receptor-dependent mechanism. J Neurosci 1994;14:7680–7.

Microscopy: Science, Technology, Applications and Education
A. Méndez-Vilas and J. Díaz (Eds.)

The adapted "single-section" Golgi method and the DiI fluorescent dye in microscopy for describing neuronal and glial morphology in different species

Alberto A. Rasia-Filho[1,3], Aline Dall'Oglio[3], Francine Dalpian[1], Liliam Midori Ide[4], Janaína Brusco[5,6], and Jorge E. Moreira[5,6,7]

[1]Department of Basic Sciences/Physiology, Federal University of Health Sciences, R. Sarmento Leite 245, Porto Alegre RS 90050-110, Brazil
[2]Graduate Course in Pathology, Federal University of Health Sciences, R. Sarmento Leite 245, Porto Alegre RS 90050-110, Brazil
[3]Graduate Course in Neuroscience, Institute of Basic Sciences, Federal University of Rio Grande do Sul, R. Sarmento Leite 500, Porto Alegre RS 90050-110, Brazil
[4]Department of Natural Sciences, Federal University of São João del-Rei, Praça Frei Orlando 170, São João del-Rei MG 36307-352, Brazil
[5]Laboratory of Synaptic Structure, Department of Cell/Molecular Biology and Biopathogens, [6]Graduate Courses in Neuroscience & Behavior and in [7]Cell and Molecular Biology, University of São Paulo, Ribeirão Preto School of Medicine, Av. Bandeirantes 3900, Ribeirão Preto SP 14049-900, Brazil

The Golgi method has been used for over a century to reveal the general morphology of neurons and glial cells in various areas of the nervous system in several species. The "single-section" Golgi method can provide consistent results using light microscopy in fishes, rats, cats, and ferrets. In human brains, cells can appear well-impregnated even from tissue stored in formalin for months or years. This technique can be combined with immunocytochemistry for different neurotransmitters or with electron microscopy. Features of the glial cells and the cell body, dendrites, spines, and axons from various kinds of neurons can provide descriptive and quantitative data from various cortical and subcortical brain areas. To advance morphological studies, fine powdered carbocyanine dye DiI can be applied extracellularly on brain slices to reveal the shape of dendritic spines under confocal microscopy and in combination with synaptic labeling. Describing the detailed shape of single neurons and glial cells can allow the elaboration of functional hypotheses of brain function from morphology. The methodological details of these techniques are depicted altogether with comments on their methodological advantages.

Keywords: neuronal morphology; dendritic spines; glial cells; carbocyanine dye; synaptic labeling; confocal microscopy; human brain.

1. The "single-section"Golgi method

The Golgi method is an old procedure still in use to examine the general morphology of neurons and glia in different areas of the nervous system. Since the initial applications, phylogenetic and ontogenetic studies benefited from this reliable tool to identify different types of neurons and to explain functional hypotheses of brain function through morphological studies [e.g., 1-8]. The rationale consists of the metallic impregnation of neurons and glial cells in tissue blocks that had been hardened by potassium dichromate and then treated by silver nitrate [9].

As for other techniques, the Golgi method has advantages and limitations, as discussed elsewhere [10,11]. However, to provide further applications and complementary results, several modifications of the original technique were developed [reviewed in 12]. Among them, one approach made available the study of specific synaptic interactions of Golgi-stained neurons by the combination of light and electron microscopy [13]. Moreover, the Golgi method could be combined with histochemical procedures to examine neurons in specific pathways retrogradely labeled by horseradish peroxidase [14] and with immunocytochemical approaches for different neurotransmitters to identify neurochemically-specific subpopulations of neurons [15,16]. This last approach for nervous tissue slices, named the "single-section" Golgi method, served to demonstrate the neuroendocrine modulation of the dendritic spine density in the hippocampus and in the amygdala of male and female rats [17-20]. As originally reported, the "single-section" Golgi method can be applied to rat, cat, and ferret brains [15,16], to fish brain (L.M.I., unpublished data), and to human brain [21].

Some methodological details will be described here [according to 18,20,22]. The "single-section" Golgi method can be done in rats transcardially perfused with paraformaldehyde and picric acid in phosphate buffer solution (PBS). The brains are sliced using a vibratome (coronal sections 100-200 μm thick), "sanwiched" between coverlips, maintained in a potassium dichromate solution and impregnated in silver nitrate. Sections are rinsed in distilled water, dehydrated in an ascending series of alcohol, cleared with xylene, placed on slides, and mounted under coverslips. Good results in rats can also be obtained after a transcardiac perfusion with saline immediately followed by paraformaldehyde and glutaraldehyde in cold sodium cacodilate buffer solution (CBS). The brain sections are rinsed in PBS, transferred to a

Microscopy: Science, Technology, Applications and Education
A. Méndez-Vilas and J. Díaz (Eds.)

osmium tetroxide solution, immersed in potassium dichromate, "sandwiched" between histological slides, and placed in silver nitrate. After that, the sections are dehydrated, cleared and mounted [16,23].

For a South American teleost fish "piauçu" (*Leporinus macrocephalus,* OSTEICHTHYES, ANASTOMIDAE), deep anesthesia can be obtained with aerated tricaine methanesulfonate solution (MS222) administered inside the mouth and through the gills and followed by a transcardially perfusion with isotonic fish electrolyte solution, glutaraldehyde and paraformaldehyde in CBS. The brain is post-fixed in the same fixative solution, placed in sucrose solution in CBS, sectioned with a vibratome (100-200 µm thick), immersed in osmium tetroxide in PBS, in a solution of potassium dichromate and in silver nitrate, and mounted on histological slides as described before.

For cortical and subcortical areas of human brains immersed in formalin for months or even years, small samples of the area of interest have to be trimmed to approximately 1.5 cm^3 to be sectioned in slices with vibratome (200 µm thick). Free-floating sections have to be post-fixed with paraformaldehyde and picric acid in PBS, transferred to an osmium tetroxide solution in PBS, immersed in potassium dichromate, "sandwiched" between glass coverslips, and placed in the impregnation solution of silver nitrate. Afterwards, the sections are mounted on histological slides [21]. These are simple experimental procedures that provide quick results (Figure 1).

2. Data acquisition using light microscopy

The areas of interest can be observed and pictured with a light microscope (from 25 to 1250X) coupled to a high quality videocamera and to a computer with a software for morphometry. Stacks of micrographs can provide two-dimensional or three-dimensional reconstructed images. To be selected for further analysis, the final image of the neurons have to show the following characteristics: a) be within the boundaries of the aimed area; b) be in the middle of the section thickness to have a more profuse dendritic ramification and to avoid excessive "cut-off" branches; c) be relatively isolated from neighboring impregnated cells to prevent "tangled" dendrites; d) have well-impregnated dendrites with defined borders; e) have the majority of their dendrites tapering towards their ends; and, f) have dendritic spines that can be easily recognized in contrast with the background silver deposits in the neuropil [18,20,24].

Results can allow the classification of neurons and glial cells in different morphological categories [3-5,7,24]. Quantitative data can be obtained from measurements on area and volume of the cell bodies, number of dendritic branches in each arborization level, number of branching points (i.e., total number of dendritic ramifications), radial distribution of dendrites in relation to the distance from the cell body, and the predominant spatial distribution of dendritic branches [24]. Dendritic spines can be counted along different dendritic branches to provide mean density values per dendritic micrometer. The shapes of these spines can allow their classification as thin, stubby, wide or "mushroom"-like, among others [8,19,25]. Axonal emergence, length, spatial arrangement and ramifications can also be determind. Glial cells can be studied mainly in terms of location, vicinity to blood vessels or ventricular walls, shape, ramification aspect, and spatial orientation [e.g., see 21].

For neurons and glial cells, the detailed cellular morphology can be obtained and compared under different natural or experimentally-induced pathological conditions. The complexity of dendritic morphology reflects the number of connections made by a neuron and more elaborated inputs require the development of more complex dendrites [24,26]. Both the identification and the quantification of the dendritic spines provide relevant data for different research fields since the spines are involved with synaptic function, integration and plasticity. For example, the shape and density of spines can show dynamic modifications along the estrous cycle or due to motherhood experience, following learning tasks and stressful stimuli or can evidence abnormalities in the course of genetic syndromes with mental retardation, hypoxic-ischemic brain injuries, and neurodegenerative diseases [8,25].

3. DiI Fluorescence and Confocal Microscopy

The use of the lipophilic carbocyanine dye 1,1'-Dioctadecyl-3,3,Y,3'-tetramethylindocarboeyanine perchlorate (DiI) reveals fine details of dendritic spines under confocal microscopy (Figure 2). DiI shows a photostable fluorescence and can diffuse along cell membranes [27,28]. Nice results can be obtained in rats following light tissue fixation with paraformaldehyde in PBS [27], sectioning the brain with a vibratome (100-200 µm thick), and applying sonicated powdered DiI extracellularly, directly or under a stereo microscope, on the brain slice surface for further confocal microscopy data obtention. The Z-stack acquisition (i.e., the distance between each captured image) can be done with a 0.2 µm step interval, avoiding excessive over and undersaturated pixels. This technique can also be done in association with immunolabeling for synaptic proteins (e.g., synaptophysin; Figure 1). This is relatively simple and allows the identification and study of the three-dimensional morphology of dendritic spines from a sample of neurons, providing reproducible results about spine topographical distribution and shapes [e.g., 8,28]. The co-localization of pre-synaptic proteins provides evidence for those spines that are probably forming active synapses. Multiple contacts can also be occurring upon one spine, which adds information to the synaptic complexity of the studied area.

Making clear the detailed shape of single neurons and glial cells can allow the elaboration of functional hypotheses of brain function from morphology. The present approaches expand our knowledge of the features of nervous cells in

different species. Besides other current techniques and innovations, the Golgi method and light microscopy stay as relevant tools for neuroscience [21]. The use of extracellular DiI, which allows the visualization, classification and counting of neuronal features under confocal microscopy, provides an additional level to understand the neuronal organization in various brain areas.

Acknowledgements: The support by Brazilian Agencies Conselho Nacional de Pesquisa e Desenvolvimento (CNPq) and Fundação de Amparo à Pesquisa do Estado de São Paulo (FAPESP, 03/03953-7 and 05/56447-7) is greatefully acknowledged. AARF and JEM are CNPq researchers.

References

[1] Golgi C. Sulla struttura della sostansa grigia del cervello. *Gazzetta Medica Italiana*. 1873;33:244-246.
[2] Ramón y Cajal S. *Histologie du système nerveux de l'Homme et des vertébrés*. Paris: Maloine; 1909.
[3] Lorente de Nó R. Studies on the structure of the cerebral cortex. II. Continuation of the study of the ammonic system. *Journal of Psychology and Neurology*. 1934;46:113-177.
[4] Szentágothai J. The neuron network of the cerebral cortex: A functional interpretation. *Proceedings of the Royal Society (London, B)*. 1978;201:219-48.
[5] Peters A, Jones EG. *Cerebral Cortex. Cellular Components of the Cerebral Cortex*. New York: Plenum Press; 1984.
[6] Millhouse OE. The intercalated cells of the amygdala. *Journal of Comparative Neurology*. 1986;247:246-271.
[7] Larriva-Sahd J. The accessory olfactory bulb in the adult rat: a cytological study of its cell types, neuropil, neuronal modules, and interactions with the main olfactory system. *Journal of Comparative Neurology*. 2008;510:309-350.
[8] Rasia-Filho AA, Brusco J, Moreira, JE. Spine plasticity in the rat medial amygdala. In: Baylog RL, ed. *Dendritic Spines: Biochemistry, Modeling and Properties*. Hauppauge: Nova Science Publishers; 2009:67-90.
[9] Fairén A. Pioneering a golden age of cerebral microcircuits: the births of the combined Golgi-electron microscope methods. *Neuroscience*. 2005;136:607-614.
[10] Nauta WJH, Ebbesson SOE. *Contemporary Research Methods in Neuroanatomy*. New York: Springer-Verlag; 1970.
[11] Scheibel ME, Scheibel AB. The Methods of Golgi. In: Robertson RT, ed. *Neuroanatomical Research Techniques*. New York: Academic Press; 1978:89-114.
[12] Alonso JR. *Los Métodos de Golgi*. Salamanca: Ediciones Universidad Salamanca; 1994.
[13] Fairén A, Peters A, Saldanha J. A new procedure for examining Golgi impregnated neurons by light and electron microscopy. *Journal of Neurocytology*. 1977;6: 311-337.
[14] Freund TF, Somogyi P. The Section-Golgi impregnation procedure. 1. Description of the method and its combination with histochemistry after intracellular iontophoresis or retrograde transport of horseradish peroxidase. *Neuroscience*. 1983;9:463-474.
[15] Gabbott PL, Somogyi J. The 'single' section Golgi-impregnation procedure: methodological description. *Journal of Neuroscience Methods*. 1984;11:221-230.
[16] Izzo PN, Graybiel AM, Bolam JP. Characterization of substance P- and [Met]enkephalin-immunoreactive neurons in the caudate nucleus of cat and ferret by a single section Golgi procedure. *Neuroscience*. 1987;20: 577-587.
[17] Woolley CS, Gould E, Frankfurt M, McEwen BS. Naturally occurring fluctuation in dendritic spine density on adult hippocampal pyramidal neurons. *Journal of Neuroscience*. 1990;10:4035-4039.
[18] Rasia-Filho AA, Fabian C, Rigoti K, Achaval M. Influence of sex, estrous cycle and motherhood in dendritic spine density in the rat medial amygdala revealed by the Golgi method. *Neuroscience*. 2004;126:839-847.
[19] Brusco J, Wittmann R, de Azevedo MS, Lucion AB, Franci CR, Giovenardi M, Rasia-Filho AA. Plasma hormonal profiles and dendritic spine density and morphology in the hippocampal CA1 stratum radiatum, evidenced by light microscopy, of virgin and postpartum female rats. *Neuroscience Letters*. 2008;438:346-350.
[20] de Castilhos J, Forti CD, Achaval M, Rasia-Filho AA. Dendritic spine density of posterodorsal medial amygdala neurons can be affected by gonadectomy and sex steroid manipulations in adult rats: A Golgi study. *Brain Research*. 2008;1240:73-81.
[21] Dall´Oglio A, Ferme D, Brusco J, Moreira JE, Rasia-Filho AA. The "single-section" Golgi method adapted for formalin-fixed human brain and light microscopy. *Journal of Neuroscience Methods*. 2010;189:51-55.
[22] Dall´Oglio A, Marcuzzo S, de Castilhos J, Rasia-Filho AA. Método de Golgi. In: Bittencourt JC, Elias CF, eds. *Métodos em Neurociências*. São Paulo: Editora Roca; 2007:33-56.
[23] Bolam JP. *Experimental Neuroanatomy: A Practical Approach*. New York: Oxford University Press; 1992.
[24] Dall'Oglio A, Gehlen G, Achaval M, Rasia-Filho AA. Dendritic branching features of posterodorsal medial amygdala neurons of adult male and female rats: Further data based on the Golgi method. *Neuroscience Letters*. 2008;430:151–156.
[25] Nimchinsky EA, Sabatini BL, Svoboda K. Structure and function of dendritic spines. *Annual Review of Physiology*. 2002;64:313-353.
[26] Ramón-Moliner E. An attempt at classifying nerve cells on the basis of their dendritic patterns. *Journal of Comparative Neurology*. 1962;119:211–227.
[27] Kim BG, Dai H-N, McAtee M, Vicini S, Bregman B S. Labeling of dendritic spines with the carbocyanine dye DiI for confocal microscopic imaging in lightly fixed cortical slices. *Journal of Neuroscience Methods*. 2007;**162**:237–243.
[28] Cunningham RL, Claiborne BJ, McGinnis MY. Pubertal exposure to anabolic androgenic steroids increases spine densities on neurons in the limbic system of male rats. *Neuroscience*. 2007;150: 609-615.

Microscopy: Science, Technology, Applications and Education
A. Méndez-Vilas and J. Díaz (Eds.)

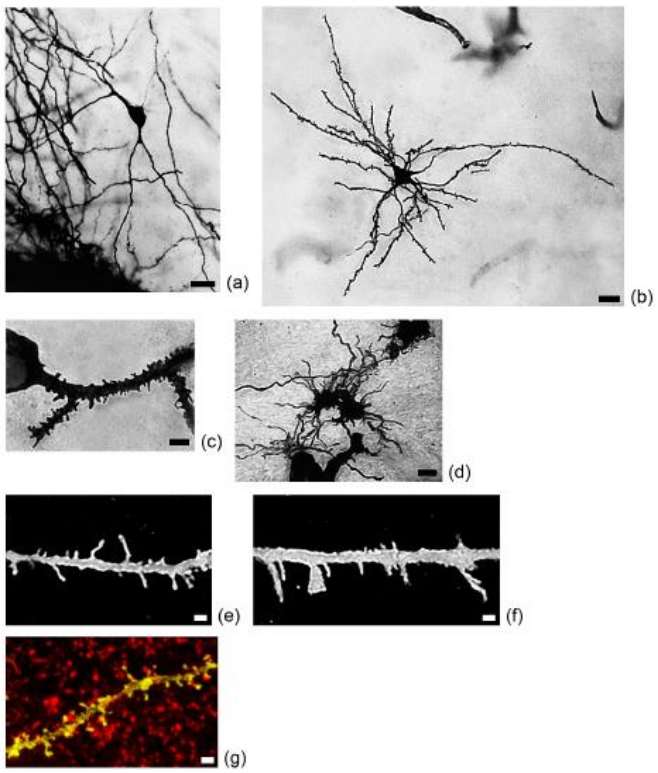

Figure 1 – Examples of reconstructed digitized microscopic image showing Golgi-impregnated neurons from rat (a), human (b), fish (c) or astrocytes from the human brain (d). Note the aspect of the cell bodies (a-c), the different dendritic branches (a,b), pleomorphic dendritic spines (b,c) and glial processes close to a blood vessel (d). A thin axon is emerging from the middle of the cell body (in the upper right) of a multipolar neuron in (a). Dendritic spines were labeled with extracellular sonicated fine powdered DiI in lightly fixed slices (e,f), close to synaptophysin puncta (in red, g). Fluorescent images were three-dimensionally reconstructed with confocal microscopy. Note the details of the different dendritic spines (e-g) and the proximity to the associated labeled presynaptic protein (g). Background and contrast were slightly adjusted using Adobe Photoshop 7.0 software (USA). Scale bar = 20 μm (a,b), 4 μm (c), 10 μm (d),and 2 μm (e-g).

RESEARCH ARTICLE

Cellular Components of the Human Medial Amygdaloid Nucleus

Aline Dall'Oglio,[1] Léder L. Xavier,[2] Arlete Hilbig,[3] Denise Ferme,[4] Jorge E. Moreira,[5] Matilde Achaval,[1,6] and Alberto A. Rasia-Filho[1,4]*

[1]Neuroscience Graduate Program, Federal University of Rio Grande do Sul, Porto Alegre 90170-050-RS, Brazil
[2]Laboratory of Cell and Tissue Biology, Faculty of Biosciences, PUCRS, Porto Alegre 90619-900-RS, Brazil
[3]Department of Clinical Medicine/Neurology, Federal University of Health Sciences of Porto Alegre, Porto Alegre 90170-050-RS, Brazil
[4]Department of Basic Sciences/Physiology, Federal University of Health Sciences of Porto Alegre, Porto Alegre 90170-050-RS, Brazil
[5]Department of Cell, Molecular Biology and Biopathogens/Department of Neuroscience and Behavior, Ribeirão Preto School of Medicine, University of São Paulo, 14049-900-SP, Brazil
[6]Department of Basic Sciences/Histology, Federal University of Rio Grande do Sul, Porto Alegre 90170-050-RS, Brazil

ABSTRACT

The medial nucleus (Me) is a superficial component of the amygdaloid complex. Here we assessed the density and morphology of the neurons and glial cells, the glial fibrillary acidic protein (GFAP) immunoreactivity, and the ultrastructure of the synaptic sites in the human Me. The optical fractionator method was applied. The Me presented an estimated mean neuronal density of 1.53×10^5 neurons/mm^3 (greater in the left hemisphere), more glia (72% of all cells) than neurons, and a nonneuronal:neuronal ratio of 2.7. Golgi-impregnated neurons had round or ovoid, fusiform, angular, and polygonal cell bodies (10–30 μm in diameter). The length of the dendrites varied, and pleomorphic spines were found in sparsely spiny or densely spiny cells (1.5–5.2 spines/dendritic μm). The axons in the Me neuropil were fine or coarsely beaded, and fibers showed simple or notably complex collateral terminations. The protoplasmic astrocytes were either isolated or formed small clusters and showed GFAP-immunoreactive cell bodies and multiple branches. Furthermore, we identified both asymmetrical (with various small, clear, round, electronlucent vesicles and, occasionally, large, dense-core vesicles) and symmetrical (with small, flattened vesicles) axodendritic contacts, also including multisynaptic spines. The astrocytes surround and may compose tripartite or tetrapartite synapses, the latter including the extracellular matrix between the pre- and the postsynaptic elements. Interestingly, the terminal axons exhibited a glomerular-like structure with various asymmetrical contacts. These new morphological data on the cellular population and synaptic complexity of the human Me can contribute to our knowledge of its role in health and pathological conditions. J. Comp. Neurol. 521:589–611, 2013.

INDEXING TERMS: amygdala cytology; extended amygdala; GFAP; Golgi method; stereology; synapses; ultrastructure

The human amygdaloid complex consists of a heterogeneous group of telencephalic subcortical nuclei that rests in the dorsomedial pole of the temporal lobe and is rostral to the hippocampus. It forms the superior and ventromedial wall of the tip of the lateral ventricle and is close to the margins of the claustrum, putamen, and globus pallidus (Brodal, 1981; Everitt, 1995; de Olmos, 2004; Yilmazer-Hanke, 2012). Most functional studies of the human amygdaloid complex describe the region as a whole entity, even though the "amygdala" is not an anatomical unit (Brodal, 1981; Swanson and Petrovich, 1998; LeDoux and Schiller, 2009). The amygdaloid nuclei do not always have clear borders, and some of them expand beyond the limits of the "amygdala" (Brodal, 1981; Martin et al., 1991; de Olmos, 2004).

Grant sponsor: CNPq; Grant number: 481992/2010-3 (to A.A.R.-F.); Grant sponsor: FAPESP and FAEPA; Grant number: 03/03953-7 (to J.E.M.); Grant number: 09/01571-6 (to J.E.M.); Grant number: 11/10753-0 (to J.E.M.).

*CORRESPONDENCE TO: Prof. A. A. Rasia-Filho, UFCSPA, R. Sarmento Leite 245, Porto Alegre 90170-050-RS, Brazil. E-mail: rasiafilho@pq.cnpq.br; aarf@ufcspa.edu.br

Received December 29, 2011; Revised April 22, 2012; Accepted July 10, 2012
DOI 10.1002/cne.23192
Published online July 18, 2012 in Wiley Online Library (wileyonlinelibrary.com)

The nomenclature for the human amygdaloid nuclei and subnuclei is not uniform despite the efforts to identify particular morphological, neurochemical, hodological, and ontogenetic characteristics (Johnston, 1923; Crosby and Humphrey, 1941; Martin et al., 1991; Everitt, 1995; Sorvari et al., 1995; Gloor, 1997; Ulfig et al., 2003; de Olmos, 2004). This also applies to the medial amygdaloid nucleus (Me). According to the most recent studies in mice, the neurons of the Me have multiple telencephalic and extratelencephalic histogenetic origins (García-López et al., 2008; Hirata et al., 2009; Carney et al., 2010; Bupesh et al., 2011). In rats, the Me has four anatomical subdivisions, as described elsewhere (Petrovich et al., 2001; Choi et al., 2005; Dall'Oglio et al., 2008a,b; Rasia-Filho et al., 2012a,b). The Me has been included in the "centromedial" amygdaloid group in different species of monkeys (McDonald and Augustine, 1993; Barton and Aggleton, 2000; Carlo et al., 2010). It has also been classified as being part of the "centromedial" (Yilmazer-Hanke, 2012) and the "corticomedial" amygdaloid group in humans (Brodal, 1981; Saygin et al., 2011). The Me is considered part of the "medial extended amygdala", a corridor of cells in the basal forebrain of rats and primates (Martin et al., 1991; Heimer, 2000; de Olmos, 2004). Different technical reasons have prevented the unanimous, precise localization of the borders and subdivisions of the primate Me (see, e.g., Sims and Williams, 1990; Martin et al., 1991; Sorvari et al., 1995; Gloor, 1997; Carlo et al., 2010; Yilmazer-Hanke, 2012). Currently, little is known about the cellular composition of the human Me (Schumann and Amaral, 2005; Chareyron et al., 2011).

However, based on Nissl-stained coronal sections, the human Me has been located in a superficial position, lateral to the optic tract (opt) and showing an irregular shape at the fundus of the endorhinal sulcus. The Me lies dorsal to most amygdaloid nuclei and the periamygdaloid cortex, and myelinated fibers separate the Me from the central nucleus laterally (Everitt, 1995; Gloor, 1997; de Olmos, 2004). In the monkey (cf. Everitt, 1995; Freese and Amaral, 2009), the Me receives intra-amygdaloid connections mainly from the basal and lateral nuclei. It projects fibers to the accessory basal, anterior cortical, and central nuclei as well as to the periamygdaloid cortex and amygdalohippocampal area. The major extrinsic connections of the Me originate from the brainstem peripeduncular nucleus, the rostral insular cortex and the hypothalamic ventromedial nucleus, the lateral area, and the supramammillary region. The efferent connections reach the medial areas of the bed nucleus of the stria terminalis (BST), the medial preoptic area and anterior medial hypothalamus (including the paraventricular and supraoptic nuclei), the hypothalamic ventromedial, the dorsal and ventral premammillary nuclei, and the midline thalamic nuclei. Indirect connections also allow the Me to modulate the processing of both cortical and subcortical information (McDonald, 1998; Rasia-Filho et al., 2000). These connections highlight the importance of this nucleus in determining the direction of the flow of information toward, within, and outward from the amygdaloid complex.

The number of neurons in the different nuclei of the human amygdaloid complex has been estimated by using a stereological sampling technique (Schumann and Amaral, 2005). In this study, however, the Me was not outlined. Changes in the neuronal density or neuron number of the amygdaloid nuclei appear to be associated with the pathogenesis of various neurological and psychiatric disorders, such as epilepsy, autism, schizophrenia, Parkinson's disease, Huntington's chorea, and Alzheimer's disease (see Sorvari, 1997; Schumann and Amaral, 2005; and references therein). Nevertheless, the separate functions and disorders of each amygdaloid nucleus have not been well established because standard imaging techniques have been unable to differentiate the specific nuclei (Saygin et al., 2011). New discoveries of human Me functions and connectivity will depend on methodological improvements (for critical review see LaBar and Warren, 2009). Currently, new, noninvasive approaches such as probabilistic tractography may contribute to the functional research on the Me (Saygin et al., 2011). The human Me has been associated with olfactory stimuli processing (Zald and Prado, 1997). It is also important for recognizing fearful faces and the positive valence of happy faces (Gamer et al., 2010), which suggests that the Me is vital for modulating emotions and social behaviors.

To provide basic data on the human Me, we investigated the density of neurons and glial cells in the adult human Me by using stereology and characterized the morphology of neurons via the Golgi method. In addition, we assessed the glial fibrillary acidic protein (GFAP) immunoreactivity of local astrocytes and the ultrastructure of local complex synaptic sites.

MATERIALS AND METHODS

Subjects

Postmortem brains were obtained from nine adult males. All ethical and legal procedures of the international regulatory standards (based on the Helsinki Declaration of 1964) were followed. This study was approved by the Brazilian Ethics Committee from the Department of Forensic Medicine ("Instituto Geral de Perícias", City of Porto Alegre, State of Rio Grande do Sul, process number 03/08), the Federal University of Health Sciences of

TABLE 1.
Characteristics of the Human Cases

Age at death (years)	PMI* (hours)	Gender	Cause of death	Type of fixation
56	06:00	Male	Cardiac arrest	Immersion
68	08:30	Male	Acute pulmonary edema	Immersion
52	08:00	Male	Pneumonia	Immersion
75	12:15	Male	Bilateral pneumonia	Immersion
58	11:45	Male	Pulmonary edema	Immersion
83	08:00	Male	Bronchopneumonia	Immersion
67	06:00	Male	Urothelial carcinoma	Immersion
50	06:15	Male	Liver cirrhosis/pneumonia	Immersion
Unknown	06:00	Male	Unknown	Perfusion

*PMI, *post mortem interval*

Porto Alegre (UFCSPA; process number 541/07), the Federal University of Rio Grande do Sul (process number 20080/09), and the Pathology Facility, Clinical Hospital of Ribeirão Preto, University of São Paulo (FMRP-USP process number 01/09). Informed consent was obtained from the next of kin at the morgue for the removal of part of the bilateral temporal lobe during autopsy. Six of the brain blocks were acquired from the Department of Forensic Medicine, two were acquired from the Pathology Facility at FMRP-USP, and one was donated by the Department of Pathology of the UFCSPA (Brazil).

For this study, we selected adult men with no history of neurosurgical interventions or treatment for any neurological or psychiatric disorder. Individuals deceased from a violent cause or infectious neurological disease were excluded from the study. The clinical data and information regarding previous comorbidities were obtained by interviewing the family members or legal representatives that had authorized the brain tissue donation. Each subject received a code to protect the identities. The age, postmortem interval, cause of death, and type of fixation for each subject are presented in Table 1. The sampled tissue from each subject was also analyzed histologically by a neurologist/neuropathologist (A.H.) to confirm the absence of common vascular and neurodegenerative lesions (data not shown).

Tissue processing

Thionin staining and the stereological sampling technique.

The brains were removed from the skull, and the bilateral blocks containing the temporal lobe were immediately immersed in 10% unbuffered formaldehyde solution at room temperature (RT). Best results were obtained after removal of the meninges. From the original tissue blocks, small samples of approximately 1.5 cm^3 were removed from the medial and ventral temporal cortex. The parahippocampal formation, the endorhinal sulcus, and the opt were used as the anatomical references for this step (DeArmond et al., 1989; Mai et al., 2008). The left and right hemispheres were studied separately. The samples were stored in the aforementioned fixative solution for 1–24 months prior to the GFAP immunoreactivity experiments and for 1–42 months prior to the thionin and Golgi processing. The tissue was coronally sectioned along the rostrocaudal axis using a vibratome (1000S; Leica, Wetzlar, Germany). The samples were sectioned in an alternating fashion. One series was sectioned at 50 μm for the thionin technique and GFAP immunohistochemistry. The other series was sectioned at 200 μm for the Golgi method. The ultrastructural analyses required a separate approach, which is described below.

The Me was studied in five cases by using the thionin technique (cases 1–5; Table 1). The serial sections from each tissue block were placed on 7.5- × 5-cm gelatin-coated slides and left to dry at room temperature (RT) for 24 hours. The slides were then immersed in a 4% paraformaldehyde in 0.1 M phosphate buffer solution (PBS; pH 7.4) for 7 days at 4°C protected from light. After drying for 24 hours at RT, the sections were placed in a 70% ethanol solution for 24 hours. Staining involved the following steps. First, the samples were immersed in solutions of increasing concentrations of ethanol and cleared in absolute xylene. Then, they were subjected to decreasing concentrations of ethanol and were washed in distilled water. Next, they were immersed in a solution of 0.25% thionin for 3 minutes, and the excess stain was removed. The samples were then again immersed in solutions of increasing ethanol concentration. They were dipped in a solution of 95% ethanol with 1% acetic acid and absolute xylene. Finally, the slides were mounted with synthetic balsam and coverslipped.

The locations of the Me in both left and right brain hemispheres were identified according to the descriptions and recommendations in the literature (Gloor, 1997; Sorvari, 1997; de Olmos, 2004). Microscopic images of the brain slices were projected onto the schematic drawings of the human brain atlas of Mai et al. (2008). Figure 1 shows low-magnification images of the thionin-stained sections matched with corresponding

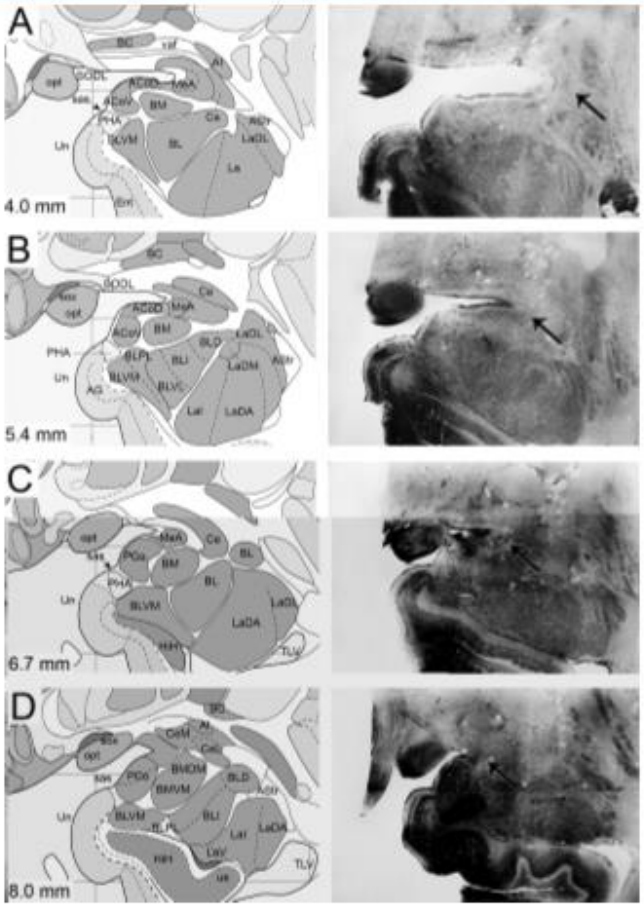

Figure 1. **Left:** A–I: Schematic diagrams of adult human brain coronal sections showing the medial amygdaloid nucleus along its rostrocaudal axis (MeA, MeP, and Me); the surrounding reference structures are also shown. The values in millimeters correspond to the distance posterior to the midpoint of the anterior commissure. Adapted from Mai et al. (2008). **Right:** Matched, thionin-stained coronal brain sections showing the location of the human medial amygdaloid nucleus (arrow). The abbreviations also correspond to the terminology used in the Mai et al. (2008) atlas. ACoD, anterior cortical amygdaloid nucleus, dorsal part; ACoV, anterior cortical amygdaloid nucleus, ventral part; AG, ambiens gyrus; AHi, amygdalohippocampal area; AI, amygdaloid island; AStr, amygdalostriatal transition area; BC, basal nucleus, compact part; BL, basolateral amygdaloid nucleus; BLD, basolateral amygdaloid nucleus, dorsal (magnocellular) part; BLI, basolateral amygdaloid nucleus, intermediate part; BLPL, basolateral amygdaloid nucleus, paralaminar part; BLVL, basolateral amygdaloid nucleus, ventrolateral part; BLVM, basolateral amygdaloid nucleus, ventromedial part; BM, basomedial amygdaloid nucleus; BMCM, basomedial amygdaloid nucleus, centromedial part; BMDL, basomedial amygdaloid nucleus, dorsolateral part; BMDM, basomedial amygdaloid nucleus, dorsomedial part; BMVM, basomedial amygdaloid nucleus, ventromedial part; Ce, central amygdaloid nucleus; CeL, central amygdaloid nucleus, lateral part; CeM, central amygdaloid nucleus, medial part; Ent, entorhinal cortex; ers, endorhinal sulcus; HIH, hippocampal head; La, lateral amygdaloid nucleus; LaDA, lateral amygdaloid nucleus, dorsal anterior part; LaDL, lateral amygdaloid nucleus, dorsolateral part; LaDM, lateral amygdaloid nucleus, dorsomedial part; LaI, lateral amygdaloid nucleus, intermediate part; LaV, lateral amygdaloid nucleus, ventral part; Me, medial amygdaloid nucleus; MeA, medial amygdaloid nucleus, anterior part; MeP, medial amygdaloid nucleus, posterior part; opt, optic tract; PCo, posterior cortical amygdaloid nucleus; PHA, parahippocampal-amygdaloid transition area; sas, semiannular sulcus; SLG, semilunar gyrus; SODL, supraoptic nucleus, dorsolateral part; sox, supraoptic commissure; st, stria terminalis; TLV, temporal horn of lateral ventricle; Un, uncus; us, uncal sulcus; vaf, ventral amygdalofugal pathway; vt; velum terminale. Scale bars = 0.5 cm.

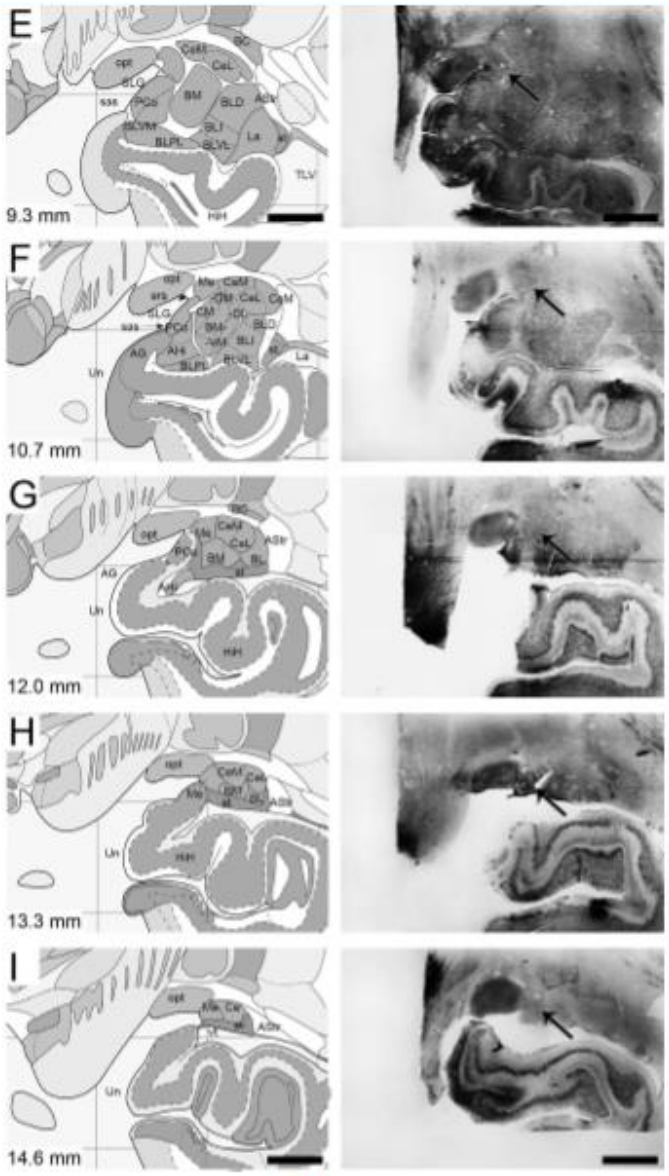

Figure 1. Continued

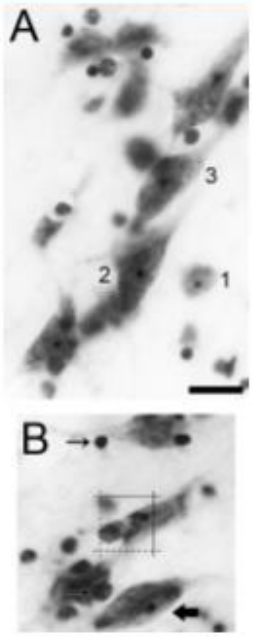

Figure 2. Photomicrographs of thionin-stained cells in the human medial amygdaloid nucleus (Me) at the magnification used for the optical fractionator technique. **A:** Three types of multipolar neurons were expected to be present in the Me, according to previous immunohistochemical studies. These subtypes were expected to have cell bodies with round/ovoid (1), angular (2), or fusiform (3) morphologies. Scale bar = 20 μm. **B:** For the stereological procedure, the area of interest (400 μm^2) and including (dashed lines) and excluding (solid lines) borders (20 μm each) are shown. The neuron with an evident nucleolus is indicated by a thick arrow (in this case, it has a fusiform soma). The astrocytes and oligodendrocytes are depicted by thin arrows (pooled as "glia cells" in this study).

drawings to demonstrate the location of the human Me. These images were applied in our investigation of the human Me.

For the stereological estimation, images were obtained with an Olympus BX61 microscope (Olympus, Tokyo, Olympus Japan) and a ×100 oil immersion objective lens (VPlan S-apo 1.40/0.17). The microscope was motorized for movement in the three spatial axes. It was attached to a high-resolution digital D172 camera and a computer with the Cell^P software (Olympus). The neurons in the Me were identified morphologically by their large, pale nuclei with evident nucleolus and by the dark cytoplasm that contained Nissl bodies. The glial cells were identified according to their relative size and unstained cytoplasm. The nucleolus was used as the counting marker for neurons, and the nucleus was used as the counting marker for glial cells (Fig. 2). For technical reasons, the few cells that were not clearly identifiable were also counted and classified as "undefined cells."

The cell density (the number of neurons, glia, or undefined cells per cubic millimeter of the Me) was estimated by the optical fractionator method (adapted from Schumann and Amaral, 2005, and references therein). All cases were studied along the rostrocaudal axis, beginning at 4.0 mm and going to 14.6 mm posterior to the midpoint of the anterior commissure, according to the atlas of Mai et al. (2008; Fig. 1). One of five serial sections containing the Me was selected proceeding along the rostrocaudal axis. On each coronal section, the Me was identified, and a square counting frame of 20 × 20 μm was overlaid onto the nucleus. The presumed borders of the Me were avoided when data were gathered. No counting obtained from the Me superficial, cell-sparse molecular layer (Martin et al., 1991) was included in the measurements of cell densities. Four counting frames per section and 7 to 11 sections per case/hemisphere were analyzed. The cells were counted at different focal planes in the z axis throughout the brain slice. The cells overlaying the "including" borders of the counting frame were counted in addition to the cells located within the counting frame. The cells overlaying the "excluding" borders of the counting frame were not counted (Fig. 2).

The numerical densities of the neurons, glial, and undefined cells were estimated using the following formula:

$$Nv = (1/[a/f \cdot h]) \cdot (\Sigma Q/\Sigma P),$$

where Nv = estimated numerical density, a/f = area of the counting frame (400 μm^2); h =, dissector height; ΣQ = sum of cells (neurons, glial or undefined cells) counted, and ΣP = sum of analyzed counting frames. The postprocessing thickness of each brain slice was measured, and the section height was used as the dissector height (Costa Ferro et al., 2010). The precise borders of the rostral and the caudal parts of the Me could not be determined. Thus, the Cavalieri method was not used for estimating the Me volume.

The Golgi method.

We employed the "single-section" Golgi technique (Gabbott and Somogyi, 1984; Rasia-Filho et al., 2004; de Castilhos et al., 2008; Arpini et al., 2010), according to the modifications proposed by Izzo et al. (1987) and Bolam (1992), and used the methodology specific for human nervous tissue recently described by Dall'Oglio et al. (2010). We tested different fixative concentrations at various fixation times in different brain areas, including

TABLE 2.
Primary Antibody Used

Antigen	Immunogen	Manufacturer	Dilution used
GFAP	GFAP, 50 kDa from human brain	Dako (Glostrup, Danmark), mouse monoclonal, clone 6F2, MO761	1:600

the hippocampus, striatum, and other amygdaloid nuclei. We found that incomplete impregnations of Me neurons occurred frequently. However, better results were obtained with the following procedure. Brain blocks containing the Me of seven subjects (cases 1–6, 9; Table 1) were subjected to an additional postfixation step with 4% paraformaldehyde and 1.5% picric acid in PBS (0.1 M, pH 7.4) for 5–90 days at RT. Tissue samples were cut using a vibratome to 200 μm thickness, and the sections were maintained in the same postfixation solution for an additional 72 hours at RT. Then, the sections were quickly rinsed in PBS and transferred to a solution of 0.1% osmium tetroxide (Sigma, St. Louis, MO) in PBS. They were immersed for 10–30 minutes under gentle agitation and were protected from light. Next, they were rinsed in PBS, immersed in a 3% potassium dichromate (Merck, Darmstadt, Germany) in deionized water, and maintained in the dark at 4°C for 48 hours. After this step, they were rinsed again in distilled water and were "sandwiched" between coverslips (epoxy glue was placed at the four corners to minimize the flow of the impregnation solution into the tissue). The slides were then placed in a solution of 1.5% silver nitrate (Merck) diluted in deionized water at RT and kept in the dark for 24 hours. Afterward, the coverslips were broken and the sections removed. The sections were washed in distilled water, and a soft brush was used to remove the unavoidable crystals on the slices. They were then placed on gelatin-coated histological slides and dried at RT. After drying, they were immersed in distilled water and dehydrated in an ascending series of ethanol. The sections were cleared in a solution of xylene/absolute ethanol followed by 100% xylene. Finally, they were covered with nonacidic synthetic balsam and coverslips.

To be selected for the study, the well-impregnated neurons were required to 1) have neuronal cell bodies located within the boundaries of the Me, according to the atlas of Mai et al. (2008; Fig. 1); 2) be isolated from neighboring cells, to avoid "tangled" dendrites; 3) have dendrites with defined borders that were tapered distally; and 4) have dendritic spines that were clearly distinguishable from the background (based on Rasia-Filho et al., 2004; de Castilhos et al., 2008). The general morphology of the neurons was studied at ×400 or ×1,000 under optical microscopy (Olympus BX-61 coupled to a CCD DP72 camera). Three-dimensional reconstruction of the neurons was performed in Image Pro Plus 7.0 with 3D Reconstructor software (Media Cybernetics, Silver Spring, MD). Fine adjustments of the background contrast and sharpness were made in Adobe Photoshop CS3.

The dendritic spine density (i.e., the number of spines per unit length of dendritic segment; data obtained from cases 5 and 9) was calculated by dividing the spine number directly counted at ×2,000 (Olympus UPlanSApo ×100 1.4 NA oil immersion objective lens, magnification changer ×1, and ×20 ocular lens) by the dendritic length measured in the three spatial planes using the same image analysis software. Spines were studied along (mean ± SD) 183.9 ± 36.4 μm of the centrifugal dendrites arising from the neuronal cell body. The initial dendritic diameter was 4.9 ± 1.5 μm, and the distal segment diameter was 1.4 ± 0.3 μm. However, the spine number counted in the Golgi-impregnated neurons most likely underrepresents the actual values for entire cells because of technical considerations that have been previously described for rats (Woolley and McEwen, 1994; Rasia-Filho et al., 1999). Finally, the axons were studied to provide descriptive data of their morphology and complexity (cf., Larriva-Sahd, 2008).

GFAP immunohistochemistry.

Samples from four cases were used for GFAP immunohistochemistry (cases 1–4; Table 1), adapting the methods described in previous reports (Xavier et al., 2005; Martinez et al., 2006; de Castilhos et al., 2009). Serial sections (50 μm thick) containing the Me (beginning rostrally, one of five sections) were postfixed with 4% paraformaldehyde in PBS and kept in the dark at 4°C for 7 days. The sections were maintained in fresh PBS at 4°C until processing. The free-floating tissue sections were placed in individual 3-ml tissue culture wells filled with 0.01% Triton X (PBS-Tx; Sigma). They were processed under gentle agitation and rinsed in PBS-TX between the following steps. The sections were 1) immersed in 10% methanol and 3% H_2O_2 for 5 minutes each and 2) blocked for 60 minutes in 1.5% normal goat serum (NGS). 3) Next, they were incubated overnight with the primary antibody (monoclonal anti-human GFAP antiserum; Table 2) in 1.5% NGS in PBS-Tx at 4°C and 4) with the biotinylated anti-rabbit secondary antibody (Sigma) diluted to 1:200 for 40 minutes. 5) The sections were then incubated in the avidin-biotin peroxidase complex (ABC; Dako, Glostrup, Denmark) diluted to 1:100 at RT for 60 minutes. 6) They were then incubated in 0.05% 3,3′-diaminobenzidine (DAB; Sigma) and in 0.01% H_2O_2 in PBS in Petri dishes for 10 minutes to stain the reaction product. The

reaction was terminated by rinsing the sections in cold PBS. 7) Finally, the sections were mounted on gelatin-coated slides, air dried for several hours, dehydrated in ethanol, cleared with xylene, and covered with Entellan (Merck) and coverslips. The images were obtained by optical microscopy (×400) using the aforementioned microscope and 3D reconstruction software. Fine adjustments of the background contrast and sharpness were made in Adobe Photoshop CS3.

Antibody characterization

See Table 2 for the primary antibody used. The anti-human GFAP antibody recognized a single band of 50 kDa m.w. on a Western blot of human brain, and its specificity was demonstrated by immunocytochemistry (manufacturer's data sheet; see also Middeldorp et al., 2009). It stained a pattern of cellular morphology and distribution in the human Me that is identical to that described in previous reports (Middeldorp et al., 2009).

Electron microscopy

Ultrastructural observations were carried out in two subjects (cases 7 and 8; Table 1), following the procedures detailed by Moreira et al. (1998), Hermel et al. (2006a), and Rodrigues et al. (2007). Brain tissue blocks that were 2 × 1 mm and contained the Me (approximately at the level of Fig. 1D; Mai et al., 2008) were used in this study. The blocks were fixed in a solution containing 2% glutaraldehyde and 2% paraformaldehyde in cacodylate buffer (CB; 0.1 N, pH 7.4) for 48 hours under gentle agitation. The samples were then washed in CB and immersed in a 1% osmium tetroxide solution with CB for 90 minutes. Next, they were rinsed in CB followed by sodium acetate buffer rinse (SABS; 0.1 M, pH 5.0) and stained in block with 0.5% uranyl acetate in SABS, protected from light, for 24 hours. The osmium and uranyl acetate steps were performed on ice. On the next day, the samples were washed in SABS and dehydrated using a graded series of ethanol ending with 100% propylene oxide. Next, they were infiltrated in EMbed 812 resin (Electron Microscopy Sciences, Fort Washington, PA) and baked at 75°C for 48 hours to polymerize. The plastic blocks were trimmed and sectioned with a Leica Ultracut UCT ultramicrotome. Ultrathin sections (60–70 nm) were collected on Pyoloform and carbon-coated single-slot grids and contrasted with uranyl acetate and lead citrate. Electron micrographs were obtained with a Zeiss 10 transmission electron microscope at a magnification of ×3,000 and ×20,000.

Approximately 850 electron micrographs were taken from the intact neuropil that had not been disrupted by postmortem autolysis. We focused on the cell bodies of the neurons, dendrites, spines, and axon terminals that have identifiable synapses. The ultrastructural characteristics of the neurons, glial cells, and synapses were classified according to Peters et al. (1991). The synaptic terminals were classified as being asymmetric to the postsynaptic density (PSD) and most likely excitatory, when at least 80% of the total vesicles had a round, electron-lucent appearance (Hermel et al., 2006a). The synapse was classified as being inhibitory, when more than 20% of the electron-lucid vesicles on a synaptic terminal were flattened, and the pre- and postsynaptic membranes of the terminal were symmetrical (Matsuda et al., 2004; Hermel et al., 2006a). The dense-core vesicles (DCVs) were also described.

Statistical analysis

The neuronal and glial densities of the right and left hemispheric Me of each subject were compared using a paired, two-tailed Student's *t*-test in GraphPad Prism 4.0. $P \leq 0.05$ was considered statistically significant.

RESULTS

Thionin and stereological data

The thionin technique produced suitable and homogeneous cellular staining along the rostrocaudal axis of the human Me. In both hemispheres, the neurons that were observed had cell bodies with a well-defined cytoplasm and a round, ovoid, fusiform or angular shape (depending on the number of primary dendritic branches emerging from the soma), large nuclei with pale chromatin, and a thick nucleolus. The thionin stain was the first to reveal the general aspects of the glial cells in the Me that surrounded the neurons. The glial cells had condensed chromatin nuclei and narrow adjacent cytoplasm (Fig. 2).

The cell densities measured in the Me are shown in Figure 3. When pooling the data from both hemispheres, the mean values for the neuronal and glial densities were 1.53×10^5 and 4.06×10^5 cells/mm^3, respectively. That is, the glial cells constituted a greater proportion of the total cells in the Me (about 72% of all cells). A significant difference in the neuronal density was found between the right and the left hemispheric Me (approximately 18% greater in the left than the right; $P < 0.02$).

Golgi-impregnated neurons

Small numbers of neurons and glial cells were individualized in the human Me. There was considerable variability in the number of cells in each brain that were adequately stained by the Golgi method. The Me neurons were small and medium-sized (mean diameter of

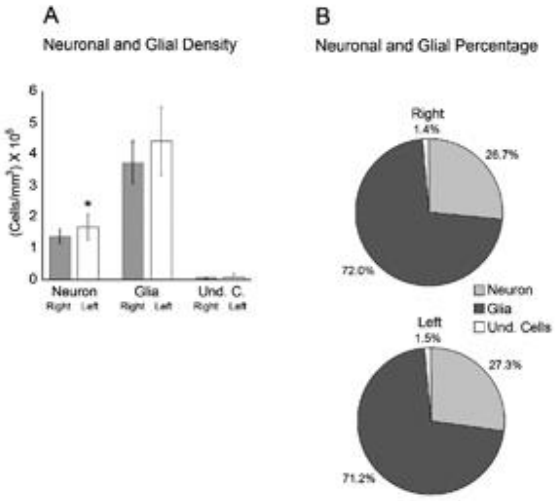

Figure 3. A: Mean (±SD) of the density (cells/mm^3) of neurons, glia, and undefined cells as estimated by the optical fractionator method. The measurements were performed in the human medial amygdaloid nucleus (Me) in the left and right hemispheres. The left Me had 18% more neurons than the right Me (*$P < 0.05$). B: Percentage distributions of the estimated density of neurons, glia, and undefined cells in the right and left hemispheric human Me. Glia were the most commonly observed cells in the Me.

approximately 15 μm) or large (approximately 30 μm; Figs. 4–6). That is, neurons had a fusiform cell body and two (rarely three) primary dendrites arising from its poles that were classified as "bitufted" neurons (Figs. 4B–E, 5B,C, 6C). We did not find characteristic "bipolar" neurons, as classically referred to by Ramón y Cajal, with one dendrite and one axon arising from opposite poles of the cell body (see parallel comments in Rasia-Filho et al., 1999, 2012b). Furthermore, we observed stellate neurons with a round or ovoid cell body that typically had various primary dendrites emerging from their cell body (seven of them in the neuron at the upper left corner of Fig. 4E; see also Fig. 6E) and other neurons with an angular soma giving rise to three primary dendrites (Fig. 4F). Despite the triangular shape of their cell bodies, these cells did not display morphological characteristic of cortical-like pyramidal neurons. These three basic types of neurons resembled presently identified cells visualized by the thionin technique and previously by immunohistochemistry (see Discussion). However, two additional types of Golgi-impregnated multipolar neurons were observed in the Me. One type had a round, pear-shaped cell body and two primary dendrites (Figs. 4B, 5E). The dendrites branched sparingly (Fig. 4B) but were sometimes lengthy (Fig. 5E). The other neuron type had a large, rectangular soma (up to 30 μm in diameter) with multiple primary dendrites (Fig. 6B), the latter being the less frequently cell found in the Me.

The primary dendrites extended in different directions and would typically start to branch near the cell body (Figs. 4–6). The neurons had dendritic branches of varying lengths, with few ramifications within the Me neuropil (compare neurons in Figs. 4, 5). We observed some very long dendrites directed toward the borders of the Me (Fig. 5E; see also Fig. 6C, upper dendrites of the neuron at right). There were various oblique, perpendicular (Fig. 4) and parallel gradually tapering dendrites (Figs. 5, 6) directed to the Me medial surface. The spines that we observed covered the cell bodies and dendrites with different dendritic branching order levels. They were located mainly in the middle or distal branches instead of at the proximal branches. Pleomorphic spines that were a

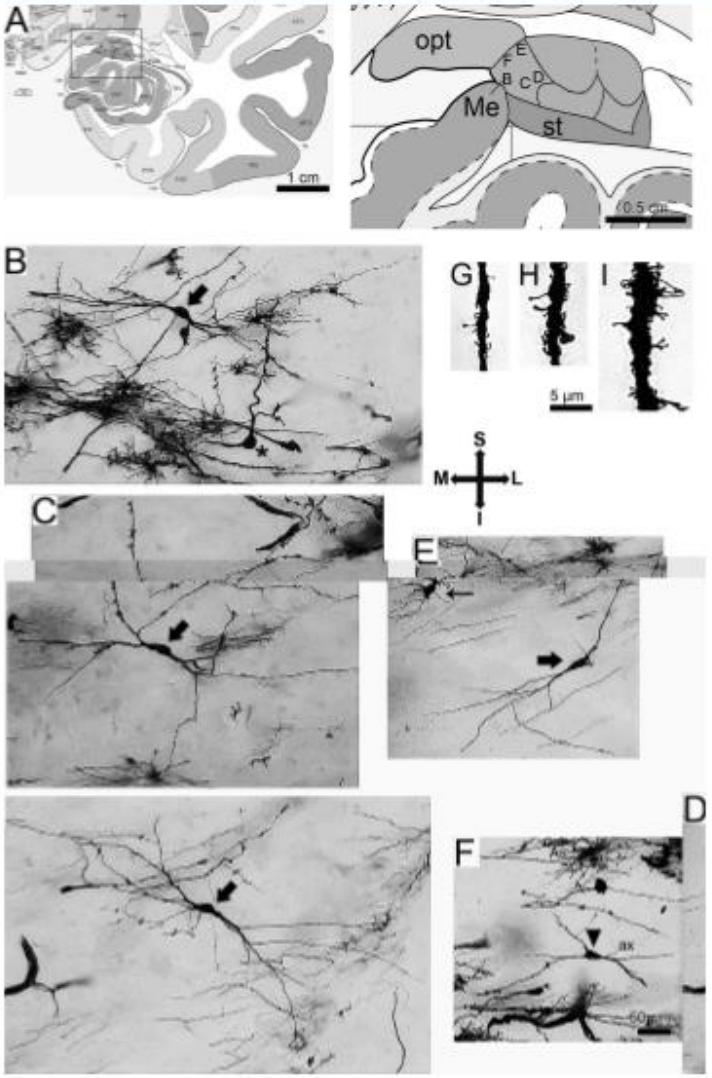

Figure 4. **A:** Schematic diagrams of adult human brain coronal sections showing the location of the medial amygdaloid nucleus (Me; 13.3 mm posterior to the midpoint of the anterior commissure), where the Golgi-impregnated neurons shown in B–F were observed. These letters (from B to F) correspond to the spatial location of the neurons within the Me. opt, optic tract; st, stria terminalis. Other references are consistent with the legend to Figure 1. Adapted from Mai et al. (2008). **B–F:** Reconstructed, digitized microscopic images of representative Golgi-impregnated multipolar neurons from the human Me. According to previous immunohistochemical reports, multipolar neurons have cell bodies with round/ovoid (small arrow), fusiform (large arrow), and angular (arrowhead) morphologies. A new neuronal type characterized by a rounded, pear-shaped cell body and few dendritic branches is shown (indicated by an asterisk). In F, the proximal portion of the axon (ax) coming from a primary dendritic branch is notable. **G–I:** Camera lucida drawings over image reconstruction of Golgi-impregnated dendritic segments to exemplify the spine density found in local neurons. Pleomorphic spines ranged from a low density (G) to a higher one (I). Mean value of dendritic spine density for the sampled population is near that found in H. Fine adjustments of the background contrast and sharpness were made in Adobe Photoshop CS3. The spatial coordinates are: I, inferior; L, lateral; M, medial; S, superior. Scale bars = 1 cm in A, left; 0.5 cm in A, right; 50 μm in F (applies to B–F); 5 μm in G–I.

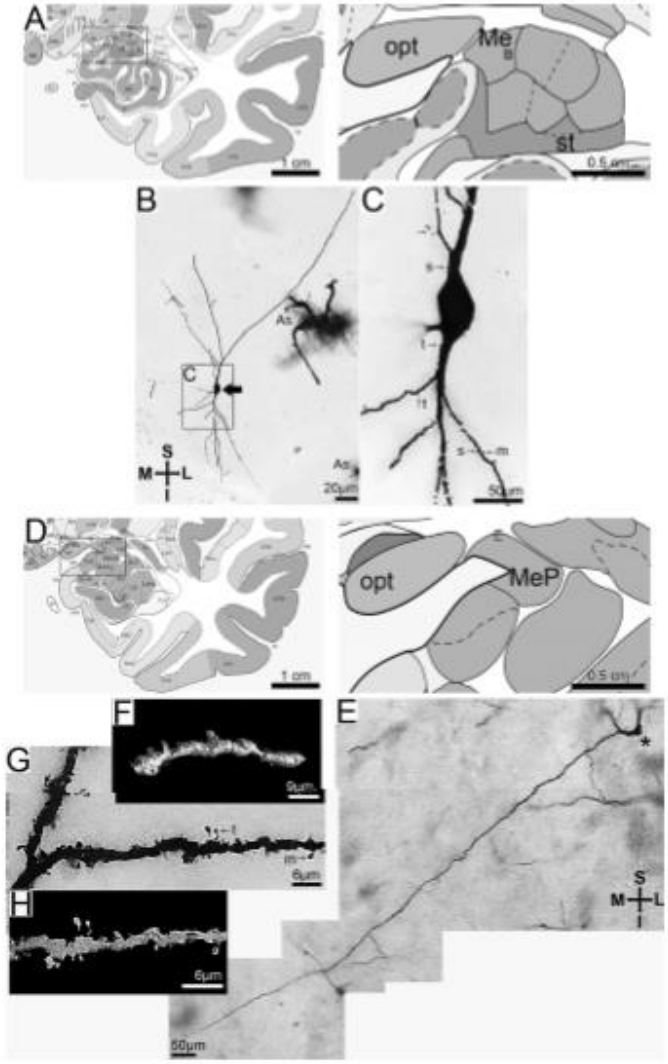

Figure 5. **A,D:** Schematic diagrams of adult human brain coronal sections showing the location of the medial amygdaloid nucleus (Me and MeP; 12 and 8 mm posterior to the midpoint of the anterior commissure in A and D, respectively) from which Golgi-impregnated neurons B and E were observed. These letters (B and E) also correspond to the spatial location of these neurons within the Me and MeP. opt, optic tract; st, stria terminalis. The references are consistent with the legend to Figure 1. Adapted from Mai et al. (2008). **B:** Reconstructed digitized microscopic image of a sparsely spiny fusiform neuron (large arrow). **C:** The area indicated in B was magnified to show the details of the proximal dendrites and spines. Note that, even at this magnification, the spines are isolated or in clusters (small arrow) and have different shapes. The dendritic spines were classified as stubby (s), thin (t), or mushroom-like (m). **E:** Reconstructed, digitized microscopic image of a novel multipolar neuron with a rounded, pear-shaped cell body, two primary dendrites, and few but long dendritic branches. **F–H:** Three-dimensional reconstruction of microscopic images of the dendritic branches and spines from spiny neurons of the human Me. Note the presence of the pleomorphic spines in both sparsely spiny (F) and more densely spiny (G, reconstructed in H) dendritic branches. Fine adjustments of the background contrast and sharpness were made in Adobe Photoshop CS3. The spatial coordinates are: I, inferior; L, lateral; M, medial; S, superior. Scale bars = 1 cm in A,D left; 0.5 cm in A,D right; 20 μm in B; 50 μm in C,E; 9 μm in F; 6 μm in G,H.

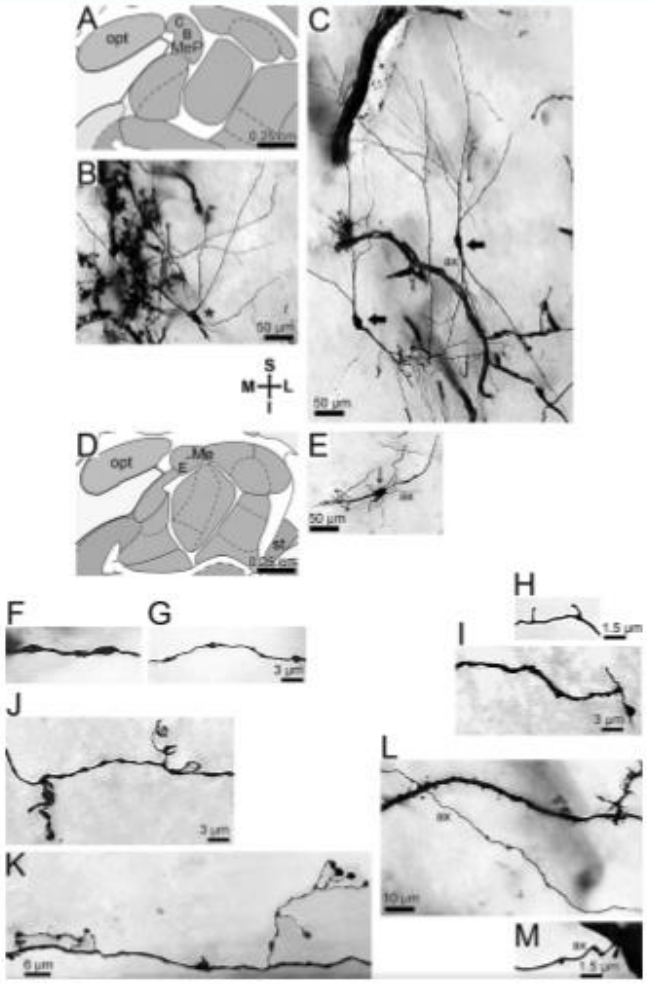

Figure 6. **A,D:** Schematic diagrams of adult human brain coronal sections showing the location of the medial amygdaloid nucleus (MeP and Me; 9.3 and 10.7 mm posterior to the midpoint of the anterior commissure in A and D, respectively) from which Golgi-impregnated neurons B, C, and E were observed. These letters (B,C,E) also correspond to the spatial location of these neurons within the Me and MeP. opt, optic tract; st, stria terminalis. Adapted from Mai et al. (2008). **B:** Reconstructed, digitized microscopic image of another novel multipolar neuron characterized by a large and rectangular cell body and four primary dendrites. **C:** Reconstructed, digitized microscopic image of multipolar fusiform neurons (large arrow) without evident proximal portion of the axon or with a visible axon (ax). The axon originates from the border of the cell body and the primary dendrite. The axon can be followed for a short distance. Although the axon of neuron in C appears to contact the dendrites, their focal microscopic planes were different and cannot be characterized as a recurrent branch. **E:** Reconstructed, digitized microscopic image of a multipolar neuron with a round/ovoid cell body (small arrow), an evident proximal portion of the axon, and a centrifugal axon (ax) coming from the soma. The axon can be traced for a short distance away from the dendrites of the cell from which it originates. In addition, the Me neuropil has a rich axonal network. Reconstructed, digitized microscopic images demonstrate the coarse and finely beaded axons in the Me neuropil (**F** and **G**, respectively), the axonal collateral divisions with single and simple appendages (**H**), and the axons with both simple and bulbous final appendages (**I**). The complex axonal endings show multiple varicosities and branching patterns (**J**) as well as complicated branched and bulbous appearances (**K**). The axons cross perpendicularly to reach the dendrites (**L**) or end in a specific spine (**M**), which most likely forms a synapse. Fine adjustments of the background contrast and sharpness were made in Adobe Photoshop CS3. Very small axons were colored in black to allow better visualization in J,M. The spatial coordinates are: I, inferior; L, lateral; M, medial; S, superior. Scale bars = 0.25 cm in A,D; 50 µm in B,C,E; 3 µm in G (applies to F,G); 1.5 µm in H,M; 3 µm in I,J; 6 µm in K; 10 µm in L.

continuum of different shapes and sizes were found in isolation or in small clusters (Figs. 4G–I, 5C). These spines could be classified according to their shapes as being thin, stubby/wide, or mushroom-like (Fig. 5C,G). Some spines were small and located close to the dendritic shafts, but other spines were considerably larger, with a thin or most commonly mushroom-like shape (Figs. 4G–I, 5G). Golgi-impregnated spines also appeared ramified. They either had a racemose appearance (i.e., branched appendages with multiple bulbous tips) or had a pattern of "coralline excrescence" (i.e., dendritic varicosity extending various thin protrusions; Fiala and Harris, 1999). Spinules emerged from the larger mushroom-like spines (Brusco et al., 2010; data not shown).

In total, 11,000 spines were counted from 21 fusiform neurons, the most commonly observed neurons in the present sample. The density of the sparsely spiny (Fig. 4G, 5C) or more densely spiny (Figs. 4I, 5G) cells ranged from 1.5 to 5.2 spines/dendritic μm, respectively. The mean (±SD) dendritic spine density was 2.9 ± 1.0 spines/dendritic μm (approximate value shown in Fig. 4H).

The thin and most likely unmyelinated axons were observed in the Me neuropil. These axons radiated in all directions, but many axons coursed horizontally in the molecular layer lying adjacent to the opt. We found few axons arising from their neurons with the present Golgi method (Fig. 6C,E). When this occurred, the proximal portion of the axon was observed at cell bodies (Fig. 6C) or at proximal primary dendrites (Fig. 4F). These centrifugal axons could typically be traced for a short distance away from the parent cell. No clear recurrent fibers could be identified in the same focal plane as the cell's dendrites (Fig. 6C,E). The axonal varicosities were present in fine or coarsely beaded fibers (Fig. 6F,G). The axons had simple appendages (Fig. 6H), both simple and bulbous ends (Fig. 6I), or more complex collaterals and branched terminations (Fig. 6J,K). Furthermore, they were found in perpendicular positions in relation to different dendrites (Fig. 6L) and turned to terminate in cell bodies, in dendritic shafts, or on specific spines (Fig. 6M).

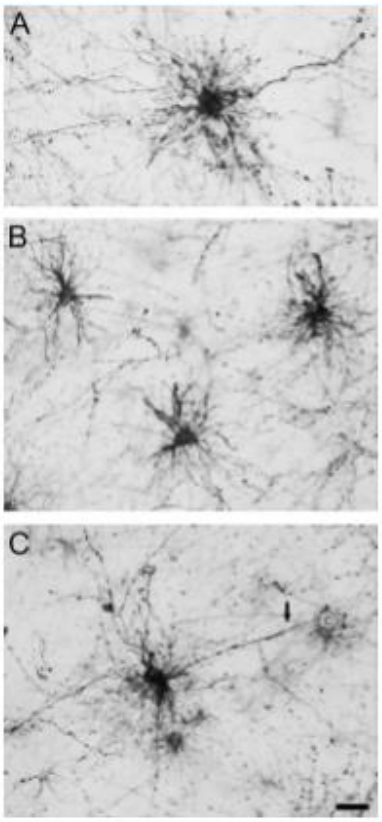

Figure 7. Digitized photomicrographs of the glial fibrillary acidic protein (GFAP)-immunoreactive cells in the human medial amygdaloid nucleus. Note the cell bodies and multiple thick and thin branches with variable lengths of these protoplasmic astrocytes that were found in isolation (A), in clusters (B), and in the proximity of blood vessels (C). c, Capillary. The background contrast and brightness were adjusted in Adobe Photoshop 7.0. Scale bar = 30 μm.

GFAP immunoreactivity

The GFAP immunoreactivity results complemented the identification of the thionin-stained astrocytes. These astrocytes appeared isolated or formed small clusters and extended multiple branches in the Me neuropil (Fig. 7A,B). The staining was light to moderate but allowed us to observe the rod-like, round, and stellate cell bodies. We also observed large primary stem processes. Some of these processes were delicate and thin and stretched in multiple directions (Fig. 7A–C). Others ended adjacent to the blood vessels (Fig. 7C; interesting image also in Fig. 5B, right).

Ultrastructural data

A clear macromolecular damage of the original tissue was caused by the postmortem interval. However, it was possible to visualize neurons and glia cells within the complex Me neuropil (Figs. 8, 9). These cells appeared as

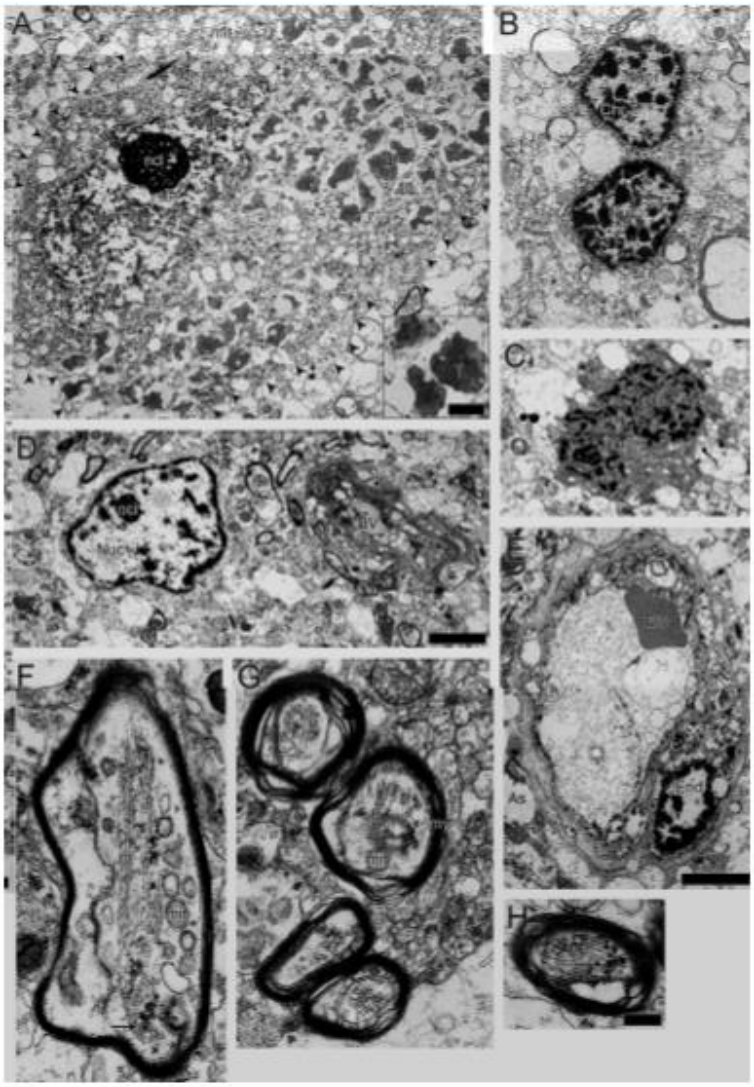

Figure 8. Ultrastructure of the human medial amygdaloid nucleus. The different subcellular components of the neurons and glial cells are indicated in **A–H**. A: Arrowheads indicate the borders of the perikaryon. The **inset** is a higher magnification of the lipofuscin granules (Lf) observed in the cell body of the same neuron. E: Blood vessel with endothelial cell. F–H: Myelinated axons. Arrows point to small, dense-core vesicles (F,H). See text for further details. As, astrocytic process; BV, blood vessel; Chr, chromatin aggregates; End, endothelial cell; Ery, erythrocyte; m, microtubules; my, myelin sheath; ncl, nucleolus; Nuc, nucleus. Scale bars = 3 μm (applies to A–E); 1 μm in inset (A); 0.3 μm in H (applies to F–H).

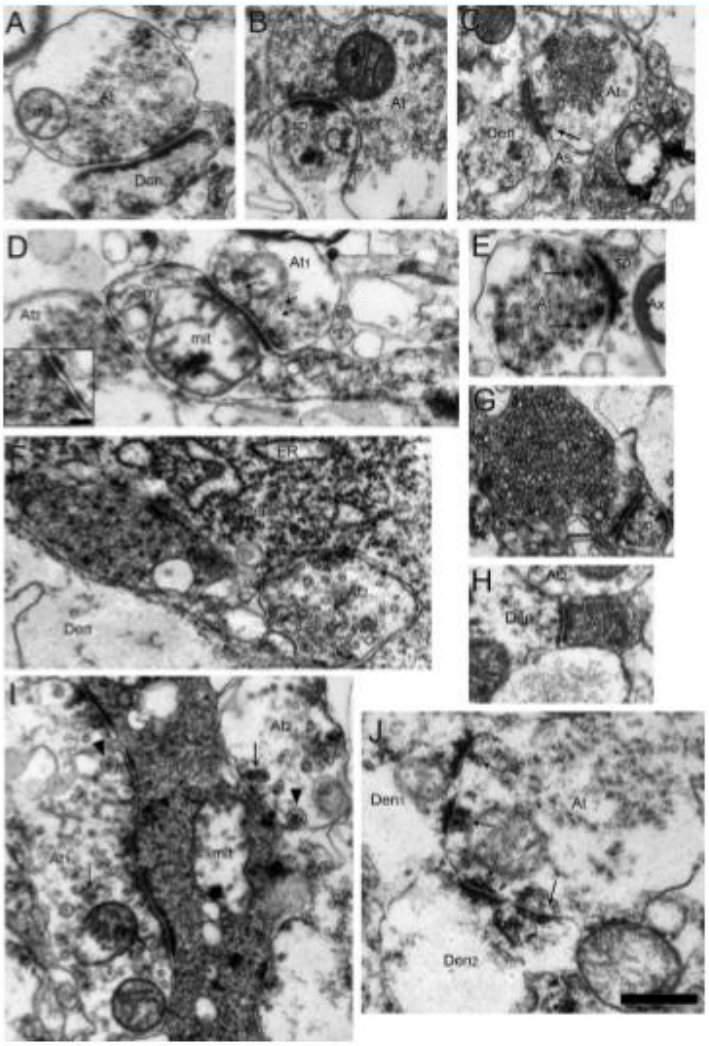

Figure 9. Ultrastructure of the human medial amygdaloid nucleus. **A–J:** Asymmetric (A–C, D in the right, E) and symmetric contacts (D in the left and its insert at higher magnification, G,H) were found on dendrites, cell bodies (F,I), and putative spines (B,D). The presynaptic (arrow in C) and postsynaptic membrane specializations in asymmetric and symmetric synapses (A,B,H) are depicted. A putative multisynaptic spine (D, arrows point to vesicles close to the presynaptic density in both asymmetric and symmetric contacts; inset is a higher magnification of the asymmetric one); the extracellular matrix in the synaptic cleft (A–C, D in the right, G,H), with an example of a tetrapartite synaptic unit (C); and a glomerular-like feature with various synaptic contacts (arrows) in a single terminal (J) are shown. Note also the characteristic aspects of the synaptic vesicles (C,E,G–I). Small (arrows) and large (arrowheads) dense-core vesicles were also observed (I). Unmyelinated axons are marked with asterisks (C). See text for details. As, astrocytic sheath; At, axon terminal; Den, dendrite; ER, granular endoplasmic reticulum; mit, mitochondria; NB, Nissl bodies; Perik, perikaryon; sp, putative dendritic spine. Scale bars = 0.5 μm in J (applies to A–J); 0.1 μm in inset (D).

previously described (see, e.g., Peters et al., 1991; Hermel et al., 2006a) but exhibited various signs of autolysis in the nucleus, organelles, and cytosol. We found in the neurons numerous dense granules of heterochromatin that were dispersed around or attached to the inner nuclear membrane. The nucleoli appeared well preserved and obvious (Fig. 8A,C,D). The neuronal cytosol showed vacuolization and had a uniform distribution of swollen mitochondria and smooth (SER) and rough (RER) endoplasmic reticulum. The RER exhibited enlarged cisternae and free ribosomes or polysomes. We also observed numerous lipofuscin granules with large halos around the dense content (Fig. 8A), which likely was related to the age of the donors. The proximal dendrites contained the same elements as the neuronal perikaryon. Some of the glial cell nuclei showed dense nuclear heterochromatin (Fig. 8B). The cytoplasm of the astrocytes and oligodendrocytes appeared as previously described (see, e.g., Peters et al., 1991), although there were vacuoles and secondary lysosomes in the cytoplasm. For the Me neuropil, we observed few myelinated axons and thin myelin sheaths. The internal part of these axons exhibited numerous microtubules and mitochondria (Fig. 8F–H). Bundles of unmyelinated axons or single axons, blood vessels with endothelial cells and pericytes (with heterochromatin attached to the nuclear membrane), and many transcytotic vesicles were also found (Fig. 8E). The blood vessels were surrounded by several astrocytic processes (e.g., Fig. 8E). We rarely saw terminal arterioles with collagen fibers.

Axosomatic and axodendritic synapses, the latter contacting both dendritic shaft and spines, were also identified in the Me (Fig. 9A–J). Tripartite synapses were common. These structures consisted of pre- and postsynaptic elements and the synaptic site surrounded by astrocytic processes (see, e.g., Fig. 9C). Multiple axosomatic contacts were observed on the surface of the cell body (Fig. 9F,I). Furthermore, there were both symmetrical and asymmetrical axodendritic synapses (Fig. 9A,C,E,G,H,J). These synapses showed notable components of the presynaptic grid (Fig. 9C). The asymmetric type had more dense material at the postsynaptic membrane and, sometimes, perpendicular thin filaments that projected to the adjacent cytoplasm (see, e.g., Fig. 9B,C). Some of these synapses occurred on putative spines with prominent PSDs, filaments resembling actin, smooth endoplasmic reticulum, and mitochondria (Fig. 9B). These putative spines could establish more than one synaptic contact and both asymmetric and symmetric synapses (Fig. 9D). Among these other most commonly observed synaptic arrangements, there was a glomerular-like structure composed of a single terminal axon establishing various asymmetric contacts (Fig. 9J). In contrast, the symmetric type exhibited a thin PSD that was composed of a material similar to the dense substance observed on the inside of the presynaptic membrane (Fig. 9G,H).

The presynaptic terminals of the asymmetric synapses showed clusters of round, small, electron-lucent vesicles (Fig. 9A–D). In the symmetric presynaptic terminals, the vesicles were small, flat, or pleomorphic (Fig. 9H). Occasionally, intermingled large, dense-core vesicles were seen (Fig. 9E). Additionally, we frequently observed an extracellular matrix in the synaptic cleft, a feature that adds one more element to the tripartite synaptic ultrastructure (see, e.g., Fig. 9A,D).

DISCUSSION

Five new results are available indicating that 1) the Me has more glial cells than neurons; 2) different multipolar neurons compose the Me; 3) there are sparsely spiny and densely spiny neurons and an elaborated axonal termination in the local neuropil; 4) astrocytes are GFAP-ir and have multiple branches; and 5) putative excitatory and inhibitory contacts can form complex synaptic units. However, critical evaluation of the methodology applied to studying postmortem human brain tissue is necessary.

Methodological considerations of the stereological study

Some technical limitations could not be avoided in our stereological approach. For example, the shrinkage generated by the brain preservation and histological procedures may affect the interpretations of the neuronal and glial densities. The fractionator and Cavalieri methods are the gold standard for evaluating the total number of cells within brain regions (Schumann and Amaral, 2005). Unfortunately, when studying some neuroanatomical aspects of large structures in human brains, it is not feasible to use approaches that produce little shrinkage such as the inclusion of tissue in durcupan or epoxy resins (Tang and Nyengaard, 1997; Lopez et al, 2005; Hermel et al., 2006a,b).

The slice thickness that we applied as the disector height might also be of concern in this study. "Lost caps" and "split cell" errors could be induced by the irregular slice surfaces produced by the vibratome knife, the fragments of cells that are split by the knife, and the different staining methods and intensities (Willians and Rakic, 1988; Hedreen, 1998). Because of technical limitations, the distance between the top and bottom of each slice (i.e., the slice thickness) was measured with a microcator in our experiments. Thus, the top and bottom planes were defined when only the whole observation field was in focus (Costa-Ferro et al, 2010), resulting in a 2–3-μm guard zone. Given that the counting markers used in our

estimation are very small (nucleolus in neurons and the nucleus in glial cells), we assume that the guard zone was sufficient to reduce the lost caps and split cell errors.

Other precautions were also taken to reduce the estimation error and to improve accuracy. We used immersion oil to ensure that the measured optical height slice was the true height by avoiding the errors associated with Snell's law of refraction (Williams and Rakic, 1988). Additionally, we applied small counting boxes, so that fewer than five cells were counted in each box. This method reduced the human error involved in the estimation (Williams and Rakic, 1988). There are inherent difficulties involved in estimating morphological parameters (Howard and Reed, 2005) in such regions as the human Me. Our results are not completely bias free, mainly because of tissue shrinkage (Coggeshall and Lekan, 1996). Nevertheless, a valid estimate of the percentage of neurons and glial cells in the human Me can be achieved, and the relative values measured in this study can serve as references for this brain area, considering age and cause of death of the subjects.

Methodological limitations for the delineation of the Me

The Cavalieri method to estimate nuclear volume requires a clear delineation of the anatomical boundaries of the region of interest. The precise delineation of the human Me and its subnuclei, however, is still under debate (see, e.g., Martin et al., 1991; Gloor, 1997; de Olmos, 2004; Mai et al., 2008; Yilmazer-Hanke, 2012). Indeed, the morphological differences between the various nuclei and their subdivisions are often subtle (Gloor, 1997). Although atlases are important for studies such as the present one, their usage can neglect the individual variation in nuclear anatomy (Zald and Pardo, 1997; Saygin et al., 2011). Thus, it is not surprising that nuclear borders continue to be refined on the basis of cytoarchitecture, fiber architecture, connections, and chemoarchitecture, but the criteria for delineating the neural structures can differ for individual investigators (Kruger et al., 1995). The human Me is less vividly stained by cholinergic markers and more intensely by NADPH-diaphorase compared with other amygdaloid nuclei (Gloor, 1997; for a more extensive list see Yilmazer-Hanke, 2012). However, the Me has several names and subdivisions from earlier works (cf. Sorvari et al., 1995). For example, it has been named the "supraamygdaleum superficiale" and the "subregio perisupraamygdalea" (Brockhaus, 1938) or was split into anterior and posterior divisions, the latter further separated into dorsal and ventral parts (de Olmos, 2004). Other parcellations for both the human and the monkey Me were suggested based on coronal, Nissl-stained sections by Martin et al. (1991). In their study, the Me, continuous with the part of the sublenticular division of the BST in the posteroventral sublenticular "substantia innominata," was divided into three parts: 1) superficial Me made up of a few neurons; 2) medial Me made up of densely packed neurons; and 3) lateral Me, a loosely arranged cellular group that encapsulates the medial division at rostral levels and, at caudal levels, occupies a lateral position.

According to the atlas of Mai et al. (2008), the Me is composed of an anterior structure (MeA, 4.0–6.7 mm posterior to the midpoint of the anterior commissure), a posterior structure (MeP, 8.0–9.3 mm), and the remaining large component named Me (10.7–14.6 mm). It is debatable whether the Me at the level of A and perhaps B in Figure 1 may be part of the anterior cortical amygdaloid nucleus or this region may be a part of the poorly defined anterior amygdaloid area (see relevant comments and images in Yilmazer-Hanke, 2012). The same occurs for the ultimate lateral borders of the Me, which are close to the central nucleus in B and C. At the levels H and I, the Me was delineated according to Mai et al. (2008). However, this region appears to be in a continuum with parts of the BST (Martin et al., 1991; Heimer et al., 1999; Heimer, 2000; Petrides et al., 2000). Therefore, we decided to analyze only the neuronal and glial cell densities in the human Me. It is worth mentioning that the estimated mean neuronal density found in the Me is compatible with the corresponding values in the human central amygdaloid nucleus (1.04×10^5 neurons/mm^3; Schumann and Amaral, 2005; Chareyron et al., 2011). In addition, the left Me had a greater measured neuronal density than the right Me. The correlation between this observation and functional hemispheric lateralization in the amygdala is open now for further evaluation. For example, a left-to-right amygdala activation difference occurs in the processing of emotionally loaded, threat-related/fearful faces in humans (Suslow et al., 2006; Gamer et al., 2010). The same result is observed when subjects are asked to rate the perceived aversiveness to olfactory stimuli (Zald and Pardo, 1997).

Neuronal types and GFAP-immunoreactive cells in the human Me

The Golgi results indicate that the human Me is composed of multipolar neurons with round/ovoid, fusiform, or angular cell body shapes. In rats, the Me multipolar neurons have been classified as bitufted (with an ovoid or fusiform soma) or stellate cells (see, e.g., Rasia-Filho et al., 1999, 2012b; Cooke et al., 2007; Marcuzzo et al., 2007; Dall'Oglio et al., 2008a,b; Arpini et al., 2010) after previous descriptions (Valverde, 1962; de Olmos et al.,

1985; McDonald, 1992). The overall morphology of these rat Me cells resembles that of the cells in the present report. The Me is an ancient evolutionary structure that is connected with the olfactory pathways, the hippocampus, and the hypothalamus (Johnston, 1923). However, the primate Me does not seem to receive direct olfactory projections (de Olmos, 2004), and these connections are minimal in humans (Brodal, 1981). Although the basic morphological organization of the amygdala is the same in all mammals, the main phylogenetic change is the increase in the proportional volume of the corticobasolateral group in contrast to the centromedial group in primates, and in humans in particular (Gloor, 1997). From the present random Golgi sample, we did not find neurons with the typical pyramidal structure or local cortical-like organization. Our descriptions of these neurons will have to be compared with those reported by other authors (Sims and Williams, 1990; Gloor, 1997; de Olmos, 2004). More appropriate names for these neurons will have to be coined (cf. Peters and Jones, 1984).

One of the advantages of the present Golgi method is that it can be applied to human tissue fixed and stored in formaldehyde. This method allows us to study neurons and glial cells in brains that have been kept in simple and routine fixative solutions (Dall'Oglio et al., 2010). Here, we have assigned previously used names to the Me neurons based on their morphological description from immunohistochemical studies (Sorvari et al., 1996a,b). In doing so, we are attempting to maintain common nomenclature between studies and to allow comparison with previous results. The Golgi impregnation also revealed the presence of multipolar neurons with spherical somas (approximately 10–20 μm in diameter), three to 11 dendrites of approximately equal thickness, and primary dendrites that typically branch into several secondary dendrites near the soma. These neurons were classified as "type 1 calretinin-immunoreactive cells," which are the most common type of neuron in the Me according to Sorvari et al. (1996a). A similar neuron is depicted in Figure 4 (neuron in the upper left of Fig. 4E). Some Golgi-impregnated neurons also resembled "type 2" neurons. These neurons are characterized by an angular cell body and primary dendrites that give rise to several thinner side branches, especially in the intermediate division of the basal amygdaloid nucleus (Sorvari et al., 1996a; comparable to the neuron shown in Fig. 4F). Most impregnated neurons, however, resembled the description of "type 3" cells. These neurons were characterized by primary dendrites that originated from the opposite poles of the spindle-shaped soma. These dendrites remained unbranched for some distance or, occasionally, bifurcated near the cell body (Sorvari et al., 1996a; compare Fig. 4C and D; see also Fig. 6C). These "type 3" neurons were aspiny or sparsely spiny and were observed in the amygdaloid lateral, basal, and accessory basal nuclei and the amygdalohippocampal area (Sorvari et al., 1996a). Fusiform neurons that resemble "type 3" neurons were the most commonly observed subtype in the human Me with the present Golgi procedure, although we found sparsely spiny or more densely spiny neurons (Figs. 4G–I, 5C,G).

We could not reliably identify interneurons on the basis of overall morphology of local neurons in the Me. Electrophysiological recordings and other neuroanatomical techniques will be needed to characterize the interneurons and projecting neurons (see Huttmann et al., 2006; Lanciego and Wounterlood, 2011). However, these cell types are likely subsamples of neurons in the Me associated with specific functional phenotypes. The human Me has three types of calbindin-D28k-immunoreactive neurons, also numbered 1–3. These neurons resemble the aforementioned calretinin-immunoreactive cells (Sorvari et al., 1996b) and might represent different populations of inhibitory neurons (Sorvari et al., 1995, 1996a; Carney et al., 2010). Additionally, the Golgi staining revealed two novel neuron types, which may represent neurons with other neurochemical characteristics and functions. In addition, the morphological differences between the neurons and the glia cells in each lamina (layers 1–3, as previously reported by Sorvari et al., 1995, 1996b) and columnar cellular organization (de Olmos, 2004) of the Me remain to be studied. The "single-section" Golgi method allows histochemical procedures to be carried out prior to silver impregnation in rat brain sections (Freund and Somogyi, 1983), which might be helpful in this regard. Lipofuscin pigment patterns have also been described in other amygdaloid nuclei (Braak and Braak, 1983; Urban and Yilmazer-Hanke, 1999). The analysis of these patterns may also contribute to the identification of different neuronal cell types in the human Me. Furthermore, the common morphological features of the human Me neurons and of other components of the "medial extended amygdala" can also be compared in the future (Martin et al., 1991; de Olmos, 2004).

The Golgi-based findings reported here will be important for investigations of the synaptic organization in the human Me. This field would benefit from further investigation of the identification and quantification of spine subtypes and whether they are formed and shaped by network activity (Kasai et al., 2003; Hayashi and Majewska, 2005; Bourne and Harris, 2007; Arellano et al., 2007; Segal, 2010). Moreover, both simple and complex ramifications along the axon length are present. The varicose aspect of the beaded axons that we observed is consistent with the description of the neurotensin immunoreactivity in the human Me (Benzing et al., 1992). Some of these fibers may form en passage synapses with more

than one element in the Me neuropil. In contrast, the single terminal boutons may contact one specific end target. The axonal protrusions varied from a single fine, prolonged shape to having ramified or bulbous ends (e.g., Fig. 6H–K). These observations suggest that these axons have complex synaptic relationships, as revealed at the ultrastructural level.

We additionally assessed the presence and complexity of glial cells in the human Me by the GFAP immunoreactivity in these cells. More glia than neurons were counted in the adult human Me. Comparatively, the nonneuronal:neuronal ratio in the Me (approximately 2.7) was greater than that of human cortical gray matter (approximately 1.4) but less than that of cortical white matter (15.4; Azevedo et al., 2009). The GFAP-immunoreactive astrocytes appear to be protoplasmic cells within the gray matter that composes the Me (Emsley and Macklis, 2006; Sofroniew and Vinters, 2010). These astrocytes exhibited a widespread and complex ramification pattern in the human Me neuropil. It was proposed earlier that region-specific astroglial heterogeneity, including the local glial density and morphology, may define the discrete cytoarchitecture of the adult mammalian brain (Emsley and Macklis, 2006). The astrocytic ramification patterns should be correlated with the ultrastructural findings. For example, the astrocytic contribution to the synapses may influence transmission in functional arrangements as tripartite or tetrapartite (including the extracellular matrix between the pre- and the postsynaptic elements) synaptic units in the human Me (Araque et al., 1999; Halassa and Haydon, 2010; Dityatev and Rusakov, 2011).

Ultrastructural data

Under the electron microscope, most contacts in the human Me appeared to be excitatory. In addition to the other aforementioned relevant findings, the identification of multisynaptic spines and the glomerular-like synaptic organization are novel. The former was identified by the presence of vesicle accumulation in close proximity to the presynaptic density (Sätzler et al., 2002; Ribeiro et al., 2005) in both asymmetrical and symmetrical contacts. GABA labeling has been described in the presynaptic terminal of symmetric spine synapses in the Me (Cooke and Woolley, 2005; Brusco et al., 2012), and the function of these inhibitory contacts in spines has been hypothetized for rats (Marcuzzo et al., 2007). The latter was recognized based on the description provided by Peters et al. (1991). That is, a bulbous axonal ending filled with many synaptic vesicles that was surrounded by various dendrites. In our case, the axons formed asymmetric synapses. Although they were not commonly observed in local synapses, both specializations offer insight into the strength and complexity of the synaptic transmission and processing in the Me (see parallel comments in Peters el al., 1991; Popov and Stewart, 2009). That is, a multisynaptic spine can compute both excitatory and inhibitory inputs, according to the specific activity pattern of afferent neural circuitries. A glomerular-like axon terminal may simultaneously affect various neurons to diverge information in a network. It will be interesting to identify the origin of the excitatory and inhibitory synapses coming to the human Me. The putative candidates include the insula and cortex-like amygdaloid nuclei for excitatory inputs and the amygdaloid intercalated nuclei for inhibitory inputs (Yilmazer-Hanke, 2012). Moreover, many putative chemical transmitters can modulate the synaptic transmission in the human Me (see Martin et al., 1991; de Olmos, 2004; Gloor, 1997; Yilmazer-Hanke, 2012).

Three-dimensional electron microscopic reconstruction would provide a complete visualization of the Me synaptic organization and plasticity. Nonetheless, there are tremendous difficulties in obtaining and reconstructing 150–400 serial thin sections from a postmortem brain using the methodological approach reported here. Experiments may also require the carbocyanine fluorescent dye DiI in lightly fixed tissue and confocal microscopy (Rasia-Filho et al., 2010; Brusco et al., 2010). Extracellular DiI staining requires intact cellular membranes. In our experience, even several hours (more than 6 hours of postmortem interval) of autolysis can considerably damage the Me. In other studies, postmortem intervals varied between 4 and 48 hours (Sorvari et al., 1996a,b) and between 16 and 30 hours (Schumann and Amaral, 2005). There are currently technical difficulties with obtaining live surgical specimens of the Me, such as during neurosurgical procedures for removing epileptogenic or tumor tissue in the temporal lobe. Other surgical approaches may improve upon the current techniques by avoiding the ischemic/excitotoxic insults that inevitably occur in postmortem tissue. These approaches would preserve dendritic spine morphology, for instance. This observation may guide studies elucidating the structure–function relationships among the spines, synaptic strength, and synaptic plasticity.

CONCLUSIONS

Our report complements previous immunohistochemical studies and provides novel morphological data on the cellular population and synaptic organization of the Me. The neuronal subpopulations as well as their histogenetic origins, connections, and functions have been studied previously in the Me subnuclei of rats and mice (Petrovich et al., 2001; Choi et al., 2005; Carney et al., 2010; Bupesch et al., 2011; Rasia-Filho et al., 2012a,b). However, the features that we describe in the neuropil of the

human Me suggest a higher level of complexity than in the other species studied to date, which may reflect more elaborate sensory and emotional processing and adaptation to species-specific social behaviors. The present basic data are also useful in directing future studies of the human Me under normal conditions and in neurological/psychiatric diseases.

ACKNOWLEDGMENT

The authors thank the relatives of the donors for tissue samples for this descriptive study. We acknowledge the relevant comments and suggestions provided by the reviewers that helped to improve the manuscript. Finally, we acknowledge Ms. Janaína Brusco, Mr. Erico Cadore, and Dr. Helena T. Hubert Silva for their contributions to the experiments. L.L.X., M.A.E., J.E.M., and A.A.R.-F. are CNPq researchers.

CONFLICT OF INTEREST STATEMENT

All authors state that there is no known or potential conflict of interest, including any financial, personal or other relationships with other people or organizations that could inappropriately influence, or be perceived to influence, this work.

ROLE OF AUTHORS

All authors contributed significantly to the elaboration of the paper and/or to the research that led to preparation of the manuscript. Also, all authors had full access to all the data in the study and take responsibility for the integrity of the data and the accuracy of the data analysis. Study concept and design: A.A.R.-F. Acquisition of data: A.D.'O., D.F., L.L.X., A.H., A.A.R.-F. Analysis and interpretation of data: A.D.'O., L.L.X., A.H., J.E.M., M.A., A.A.R.-F. Drafting of the manuscript: L.L.X., J.E.M., A.A.R.-F. Critical revision of the manuscript for important intellectual content: L.L.X., A.H., J.E.M., A.A.R.-F. Statistical analysis: L.L.X., A.A.R.-F. Obtained funding: J.E.M., A.A.R.-F. Study supervision: A.A.R.-F.

LITERATURE CITED

Aggleton JP, Saunders RC. 2000. The amygdala—what's happened in the last decade? In: Aggleton JP, editor. The amygdala, 2nd ed. New York: Oxford University Press. p 1–30.

Araque A, Parpura V, Sanzgiri RP, Haydon PG. 1999. Tripartite synapses: glia, the unacknowledged partner. Trends Neurosci 22:208–215.

Arellano JI, Espinosa A, Fairén A, Yuste R, DeFelipe J. 2007. Non-synaptic dendritic spines in neocortex. Neuroscience 145:464–469.

Arpini M, Menezes IC, Dall'Oglio A, Rasia-Filho AA. 2010. The density of Golgi-impregnated dendritic spines from adult rat posterodorsal medial amygdala neurons displays no evidence of hemispheric or dorsal/ventral differences. Neurosci Lett 469:209–213.

Azevedo FAC, Carvalho LRB, Grinberg LT, Farfel JM, Ferretti REL, Leite REP, Jacob Filho W, Lent R, Herculano-Houzel S. 2009. Equal numbers of neuronal and nonneuronal cells make the human brain na isometrically scaled-up primate brain. J Comp Neurol 513:532–541.

Barton RA, Aggleton JP. 2000. Primate evolution and the amygdale. In: Aggleton JP, editor. The amygdala, 2nd ed. New York: Oxford University Press. p 479–508.

Benzing WC, Mufson EJ, Jennes L, Stopa EG, Armstrong DM. 1992. Distribution of neurotensin immunoreactivity within the human amygdaloid complex: a comparison with acetylcholinesterase- and Nissl-stained tissue sections. J Comp Neurol 317:283–297.

Bolam JP. 1992. Experimental neuroanatomy: a practical approach. New York: Oxford University Press.

Bourne JN, Harris KM. 2007. Do thin spines learn to be mushroom spines that remember? Curr Opin Neurobiol 17: 381–386.

Braak H, Braak E. 1983. Neuronal types in the basolateral amygdaloid nuclei of man. Brain Res Bull 11:349–365.

Brockhaus H. 1938. Zur normalen und pathologischen Anatomie des Mandelkerngebiets. J Psychol Neurol 49:1–136.

Brodal A. 1981. Neurological anatomy. New York: Oxford University Press.

Brusco J, Dall'Oglio A, Rocha LB, Rossi MA, Moreira JE, Rasia-Filho AA. 2010. Descriptive findings on the morphology of dendritic spines in the rat medial amygdala. Neurosci Lett 483:152–156.

Brusco J, Ikeda ET, Merlo S, Gital DG, Papõ-Larson ML, Petralia RS, Kachar B, Rasia-Filho AA, Moreira JE. 2012. Ultrastructure and gene expression of the posterodorsal medial amygdala of rats. Abstract, 6th Annual Canadian Neuroscience Meeting, Vancouver, Canada.

Bupesh M, Legaz I, Abellán A, Medina L. 2011. Multiple telencephalic and extratelencephalic embryonic domains contribute neurons to the medial extended amygdala. J Comp Neurol 519:1505–1525.

Carlo CN, Stefanacci L, Semendeferi K, Stevens CF. 2010. Comparative analysis of the neuron numbers and volumes of the amygdaloid complex in old and new world primates. J Comp Neurol 518:1176–1198.

Carney RSE, Mangin J-M, Hayes L, Mansfield K, Sousa VH, Fishell G, Machold RP, Ahn S, Gallo V, Corbin JG. 2010. *Sonic hedgehog* expressing and responding cells generate neuronal diversity in the medial amygdala. Neural Dev 5: 14.

Chareyron LJ, Lavenex PB, Amaral DG, Lavenex P. 2011. Stereological analysis of the rat and monkey amygdala. J Comp Neurol 519:3218–3239.

Choi GB, Dong H-W, Murphy AJ, Valenzuela DM, Yancopoulos GD, Swanson LW, Anderson DJ. 2005. Lhx6 delineates a pathway mediating innate reproductive behaviors from the amygdala to the hypothalamus. Neuron 46:647–660.

Coggeshall RE, Lekan HE. 1996. Methods for determining numbers of cells and synapses: a case for more uniform standards of review. J Comp Neurol 364:6–15.

Cooke BM, Woolley CS. 2005. Sexually dimorphic synaptic organization of the medial amygdala. J Neurosci 25: 10759–10767.

Cooke BM, Stokas, Woolley CS. 2007. Morphological sex differences and laterality in the prepubertal medial amygdala. J Comp Neurol 501:904–915.

Costa-Ferro ZSM, Vitola AS, Pedroso MF, Cunha FB, Xavier LL, Machado DC, Soares MBP, Ribeiro-dos-Santos R, da Costa JC. 2010. Prevention of seizures and reorganization of hippocampal functions by transplantation of bone marrow cells in the acute phase of experimental epilepsy. Seizure 19:84–92.

Crosby EC, Humphrey T. 1941. Studies of the vertebrate telencephalon: II. The nuclear pattern of the anterior olfactory nucleus tuberculum olfactorium and the amygdaloid complex in adult man. J Comp Neurol 47:309–352.

Dall'Oglio A, Gehlen G, Achaval M, Rasia-Filho AA. 2008a. Dendritic branching features of posterodorsal medial amygdala neurons of adult male and female rats: further data based on the Golgi method. Neurosci Lett 430:151–156.

Dall'Oglio A, Gehlen G, Achaval M, Rasia-Filho AA. 2008b. Dendritic branching features of Golgi-impregnated neurons from the "ventral" medial amygdala subnuclei of adult male and female rats. Neurosci Lett 439:287–292.

Dall'Oglio A, Ferme D, Brusco J, Moreira JE, Rasia-Filho AA. 2010. The "single-section" Golgi method adapted for formalin-fixed human brain and light microscopy. J Neurosci Methods 189:51–55.

de Castilhos J, Forti CD, Achaval M, Rasia-Filho AA. 2008. Dendritic spine density of posterodorsal medial amygdala neurons can be affected by gonadectomy and sex steroid manipulations in adult rats: a Golgi study. Brain Res 1240: 73–81.

de Castilhos J, Rigon P, Xavier LL, Rasia-Filho A, Achaval M. 2009. Sex differences in NADPH-diaphorase activity in the rat posterodorsal medial amygdala. Brain Res 1305: 31–39.

de Olmos JS. 2004. Amygdala. In: Paxinos G, Mai J, editors. The human nervous system, 2nd ed. San Diego: Elsevier. p 739–868.

de Olmos JS, Alheid GF, Beltramino CA. 1985. Amygdala. In: Paxinos G, editor. The rat central nervous system. Sydney: Academic Press. p 223–334.

DeArmond SJ, Fusco MM, Dewey MM. 1989. Structure of the human brain. New York: Oxford University Press.

Dityatev A, Rusakov DA. 2011. Molecular signs of plasticity at the tetrapartite synapse. Curr Opin Neurobiol 21:353–359.

Emsley JG, Mackils JD. 2006. Astroglial heterogeneity closely reflects the neuronal-defined anatomy of the adult murine CNS. Neuron Glia Biol 2:175–186.

Everitt B. 1995. Limbic lobe and olfactory pathways. In: Berry MM, Bannister LH, Standring SM, editors. Gray's anatomy. London: Churchill Livingstone. p 1115–1141.

Fiala JC, Harris KM. 1999. Dendrite structure. In: Stuart G, Spruston N, Häusser M, editors. Dendrites. Oxford: Oxford University Press. p 1–34.

Freese JL, Amaral DG. 2009. Neuroanatomy of the primate amygdala. In: Whalen PJ, Phelps EA, editors. The human amygdala. New York: The Guilford Press. p 3–42.

Freund TF, Somogyi P. 1983. The section-Golgi impregnation procedure. 1. Description of the method and its combination with histochemistry after intracellular ionophoresis or retrograde transport of horseradish peroxidase. Neuroscience 9:463–474.

Gabbott PL, Somogyi J. 1984. The "single" section Golgi-impregnation procedure: methodologicaldescription. J Neurosci Methods 11:221–230.

Gamer M, Zurowski B, Büchel C. 2010. Different amygdala subregions mediate valence-related and attentional effects of oxytocin in humans. Proc Nat Acad Sci U S A 107: 9400–9405.

García-López M, Abellán A, Legaz I, Rubenstein JLR, Puelles L, Medina L. 2008. Histogenetic compartments of the mouse centromedial and extended amygdala base on gene expression patterns during development. J Comp Neurol 506:46–74.

Gloor P. 1997. The temporal lobe and limbic system. New York: Oxford University Press. p 865.

Halassa MM, Haydon PG. 2010. Integrated brain circuits: astrocytic networks modulate neuronal activity and behavior. Annu Rev Physiol 72:335–355.

Hayashi Y, Majewska AK. 2005. Dendritic spine geometry: functional implication and regulation. Neuron 46:529–532.

Hedreen JC. 1998. Lost caps in histological counting methods. Anat Rec 250:366: 372.

Heimer L. 2000. Basal forebrain in the context of schizophrenia. Brain Re Rev 31:205–235.

Heimer L, de Olmos JS, Alheid GF, Pearson J, Sakamoto N, Shinoda K, Marksteiner J, Switzer RC. 1999. The human basal forebrain, part II. In: Bloom FE, Björklund A, Hökfelt T, editors. Handbook of chemical neuroanatomy: the primate nervous system, vol 15, part 3. Amsterdam: Elsevier. p 57–226.

Hermel EE, Ilha J, Xavier LL, Rasia-Filho AA, Achaval M. 2006a. Influence of sex and estrous cycle, but not laterality, on the neuronal somatic volume of the posterodorsal medial amygdala of rats. Neurosci Lett 405:153–158.

Hermel EE, Faccioni-Heuser MC, Marcuzzo S, Rasia-Filho AA, Achaval M. 2006b. Ultrastructural features of neurons and synaptic contacts in the posterodorsal medial amygdala of adult male rats. J Anat 208:565–575.

Hirata T, Li P, Lanuza GM, Cocas LA, Huntsman MM, Corbin JG. 2009. Identification of distinct telencephalic progenitor pools for neuronal diversity in the amygdala. Nat Neurosci 12:141–149.

Howard V, Reed MG. 2005. Unbiased stereology. In: Three-dimensional measurement in microscopy, 2nd ed. New York: Garland Science/Bios Scientific Publishers. p 277.

Huttmann K, Yilmazer-Hanke D, Seifert G, Schramm J, Pape HC, Steinhauser C. 2006. Molecular and functional properties of neurons in the human lateral amygdala. Mol Cell Neurosci 31:210–217.

Izzo PN, Graybiel AM, Bolam JP. 1987. Characterization of substance P- and [Met]enkephalin-immunoreactive neurons in the caudate nucleus of cat and ferret by a single section Golgi procedure. Neuroscience 20:577–587.

Johnston JB. 1923. Further contributions to the study of the evolution of the forebrain. J Comp Neurol 35:337–481.

Kasai H, Matsuzaki M, Noguchi J, Yasumatsu N, Nakahara H. 2003. Structure–stability–function relationships of dendritic spines. Trends Neurosci 26:360–368.

Kruger L, Saporta S, Swanson LW. 1995. Photographic atlas of the rat brain: the cell and fiber architecture illustrated in three planes with stereotaxic coordinates. New York: Cambridge University Press.

LaBar KS, Warren LH. 2009. Methodological approaches to studying the human amygdala. In: Whalen PJ, Phelps EA, editors. The human amygdala. New York: The Guilford Press. p 155–176.

Lanciego JL, Wouterlood FG. 2011. A half century of experimental neuroanatomical tracing. J Chem Neuroanat 42: 157–183.

Larriva-Sahd J. 2008. The accessory olfactory bulb in the adult rat: a cytological study of its cell types, neuropil, neuronal modules, and interactions with the main olfactory system. J Comp Neurol 510:309–350.

LeDoux JE, Schiller D. 2009. The human amygdala: insights from other animals. In: Whalen PJ, Phelps EA, editors. The human amygdala. New York: The Guilford Press. p 43–60.

Lopez I, Ishiyama G, Tang Y, Frank M, Baloh RW, Ishiyama A. 2005. Estimation of the number of nerve fibers in the human vestibular endorgans using unbiased stereology and immunohistochemistry. J Neurosci Methods 145:37–45.

Mai JK, Paxinos G, Voss T. 2008. Atlas of the human brain, 3rd ed. New York: Academic Press.

Marcuzzo S, Dall'Oglio A, Ribeiro MF, Achaval M, Rasia-Filho AA. 2007. Dendritic spines in the posterodorsal medial amygdala after restraint stress and ageing in rats. Neurosci Lett 424:16–21.

Martin LJ, Powers RE, Dellovade TL, Price DL. 1991. The bed nucleus-amygdala continuum in human and monkey. J Comp Neurol 309:445–485.

Martinez FG, Hermel EE, Xavier LL, Viola GG, Riboldi J, Rasia-Filho AA, Achaval M. 2006. Gonadal hormone regulation of glial fibrillary acidic protein immunoreactivity in the medial amygdala subnuclei across the estrous cycle and in castrated and treated female rats. Brain Res 1108:117–126.

Matsuda S, Kobayashi Y, Ishizuka N. 2004. A quantitative analysis of the laminar distribution of synaptic boutons in field CA3 of the rat hippocampus. Neurosci Res 49:241–251.

McDonald AJ. 1992. Cell types and intrinsic connections of the amygdala. In: Aggleton JP, editor. The amygdala: neurobiological aspects of emotion, memory, and mental dysfunction. NewYork: Wiley-Liss. p 67–96.

McDonald AJ. 1998. Cortical pathways to the mammalian amygdala. Prog Neurobiol 55:257–332.

McDonald AJ, Augustine JR. 1993. Localization of GABA-like immunoreactivity in the monkey amygdala. Neuroscience 52:281–294.

Middeldorp J, van den Berge SA, Aronica E, Speijer D, Hol EM. 2009. Specific human astrocyte subtype revealed by affinity purified GFAP^{+1} antibody; unpurified serum cross-reacts with neurofilament-L in Alzheimer. PLoS ONE 4: e7663. doi:10.1371/journal.pone.0007663.

Moreira JE, Reese TS, Kachar B. 1996. Freeze-substitution as a preparative technique for immunoelectronmicroscopy: evaluation by atomic force microscopy. Microsc Res Techniq 33:251–261.

Peters A, Jones EG. 1984. Classification of cortical neurons. In: Jones EG, Peters A, editors. Cerebral cortex. Functional properties of cortical cells, vol 2. New York: Plenum Press. p 107–121.

Peters A, Palay SL, Webster H. 1991. The fine structure of the nervous system. New York: Oxford University Press.

Petrides M, Paxinos G, Huang X-F, Morris R, Pandya DN. 2000. Delineation of the monkey cortex on the basis of a neurofilament protein (SMI-32). In: Paxinos G, Huang X-F, Toga AW, editors. The rhesus monkey brain in stereotaxic coordinates. San Diego: Academic Press. p 167–190.

Petrovich GD, Canteras NS, Swanson LW. 2001. Combinatorial amygdalar inputs to hippocampal domains and hypothalamic behavior systems. Brain Res Rev 38:247–289.

Popov VI, Stewart MG. 2009. Complexity of contacts between synaptic boutons and dendritic spines in adult rat hippocampus: three-dimensional reconstructions from serial ultrathin sections in vivo. Synapse 63:369–377.

Rasia-Filho AA, Londero RG, Achaval M. 1999. Effects of gonadal hormones on the morphology of neurons from the medial amygdaloid nucleus of rats. Brain Res Bull 48: 173–183.

Rasia-Filho AA, Londero RG, Achaval M. 2000. On some functional activities of the amygdala: an overview. J Psychiatry Neurosci 25:14–23.

Rasia-Filho AA, Fabian C, Rigotti K, Achaval M. 2004. Influence of sex, estrous cycle and motherhood in dendritic spine density in the rat medial amygdala revealed by the Golgi method. Neuroscience 126:839–847.

Rasia-Filho AA, Brusco J, Rocha LB, Moreira JE. 2010. Dendritic spines observed by extracellular DiI dye and immunolabeling under confocal microscopy. Nat Protoc/Protoc Exchange. DOI: 10.1038/nprot.2010.153.

Rasia-Filho AA, Dalpian F, Menezes IC, Brusco J, Moreira JE, Cohen RS. 2012a. Dendritic spines of the medial amygdala: plasticity, density, shape, and subcellular modulation by sex steroids. Histol Histopathol 27:985–1011.

Rasia-Filho AA, Hass D, de Oliveira AP, de Castilhos J, Frey R, Stein D, Lazzari VM, Back F, Pires GN, Pavesi E, Winkelmann-Duarte EC, Glovenardi M. 2012. Morphological and functional features of the sex steroid-responsive posterodorsal medial amygdala of adult rats. Mini-Rev Med Chem 12:1090–1106.

Ribeiro SJ, Ciscato JG Jr, de Oliveira R, de Oliveira RC, D'Angelo-Dias R, Carvalho AD, Felippotti TT, Rebougas ECC, Castellan-Baldan L, Hoffmann A, Corrêa SAL, Moreira JE, Coimbra NC. 2005. Functional and ultrastructural neuroanatomy of interactive intratectal/tectonigral mesencephalic opioid inhibitory links and nigrotectal GABAergic pathways: involvement of GABA$_A$ and μ_1-opioid receptors in the modulation of panic-like reactions elicited by electrical stimulation of the dorsal midbrain. J Chem Neuroanat 30:184–200.

Rodrigues GJ, Restini CB, Lunardi CN, Moreira JE, Lima RG, da Silva RS, Bendhack LM. 2007. Caveolae dysfunction contributes to impaired relaxation induced by nitric oxide donor in aorta from renal hypertensive rats. J Pharmacol Exp Ther 323:831–837.

Sätzler K, Söhl LF, Bollmann JH, Borst JGJ, Frotscher M, Sakmann B, Lübke JHR. 2002. Three-dimensional reconstruction of a calyx of Held and its postsynaptic principal neuron in the medial nucleus of the trapezoid body. J Neurosci 22:10567–10579.

Saygin ZM, Osher DE, Augustinack J, Fischl B, Gabrieli JDE. 2011. Connectivity-based segmentation of human amygdala nuclei using probabilistic tractography. NeuroImage 56:1353–1361.

Schumann CM, Amaral DG. 2005. Stereological estimation of the number of neurons in the human amygdaloid complex. J Comp Neurol 491:320–329.

Segal M. 2010. Dendritic spines, synaptic plasticity and neuronal survival: activity shapes dendritic spines to enhance neuronal viability. Eur J Neurosci 31:2178–2184.

Sims KS, Williams RS. 1990. The human amygdaloid complex: a cytologic and histochemical atlas using Nissl, myelin, acetylcholinesterase and nicotinamide adenine dinucleotide phosphate diaphorase staining. Neuroscience 2:449–472.

Sofroniew MV, Vinters HV. 2010. Astrocytes: biology and pathology. Acta Neuropathol 119:7–35.

Sorvari H. 1997. Neurons containing calcium-binding proteins in the human amygdaloid complex. PhD Thesis. University of Kuopio, Kuopio, Finland.

Sorvari H, Soininen H, Paljärvi L, Karkola K, Pitkänen A. 1995. Distribution of parvalbumin-immunoreactive cells and fibers in the human amygdaloid complex. J Comp Neurol 360: 185–212.

Sorvari H, Soininen H, Pitkänen A. 1996a. Calretinin-immunoreactive cells and fibers in the human amygdaloid complex. J Comp Neurol 369:188–208.

Sorvari H, Soininen H, Pitkänen A. 1996b. Calbindin-D28K-immunoreactive cells and fibres in the human amygdaloid complex. Neuroscience 75:421–443.

Suslow T, Ohrmann P, Bauer J, Rauch AV, Schwindt W, Arolt V, Heindel W, Kugel H. 2006. Amygdala activation during masked presentation of emotional faces predicts conscious detection of threat-related faces. Brain Cogn 61: 243–248.

Swanson L, Petrovich G. 1998. What is the amygdala? Trends Neurosci 21:323–331.

Tang Y, Nyengaard JR. 1997. A stereological method for estimating the total length and size of myelin fibers in human brain white matter. J Neurosci Methods 73:193–200.

Uffig N, Setzer M, Bohl J. 2003. Ontogeny of the human amygdala. Ann N Y Acad Sci 985:22–33.

Urban S, Yilmazer-Hanke DM. 1999. The pigmentarchitectonic divisions and neuronal types of the central nucleus and intercalated masses of the human amygdala. J Brain Res 3:311–319.

Valverde F. 1962. Intrinsic organization of the amygdaloid complex: a Golgi study in the mouse. Trab Inst Cajal Invest Biol 54:291–314.

Williams RW, Rakic P. 1988. Three-dimensional counting: an accurate and direct method to estimate numbers of cells in sectioned material. J Comp Neurol 278:344:352.

Woolley CS, McEwen BS. 1994. Estradiol regulates hippocampal dendritic spine density via an N-methyl-D-aspartate receptor-dependent mechanism. J Neurosci 14:7680–7687.

Xavier LL, Viola GG, Ferraz AC, Da Cunha C, Deonizio JM, Netto CA, Achaval M. 2005. A simple and fast densitometric method for the analysis of tyrosine hydroxylase immunoreactivity in the substantia nigra pars compacta and in the ventral tegmental area. Brain Res Protoc 16: 58–64.

Yilmazer-Hanke DM. 2012. Amygdala. In: Paxinos G, Mai J, editors. The human nervous system, 3rd ed. San Diego: Elsevier. p 759–834.

Zald DH, Pardo JV. 1997. Emotion, olfaction, and the human amygdala: amygdala activation during aversive olfactory stimulation. Proc Natl Acad Sci U S A 94: 4119–4124.

5. DISCUSSÃO

5.1 Método de Golgi

As modificações propostas para o método de Golgi são bastante eficazes para revelar neurônios e células da glia em tecido nervoso humano coletado post-mortem e fixado por períodos prolongados (mais de 1 mês até 10 anos). Porém alguns ajustes da técnica podem vir a ser necessários dependendo da região a ser estudada, como se observou com o Me, o qual revelou melhores resultados quando se prolongou o tempo de pós-fixação para 90 dias. Outras regiões encefálicas como estriado ou córtex não precisaram da mesma intervenção, por exemplo.

5.2 Considerações metodológicas do emprego da estereologia

Não foi possível evitar algumas limitações técnicas capazes de afetar a interpretação das densidades neuronais e gliais nesse estudo, como por exemplo, a retração do tecido causada pela fixação e pelos procedimento histológicos. Isso porque, infelizmente, quando se estuda aspectos neuroanatômicos de estruturas encefálicas humanas grandes não se conseguem aplicar as melhores técnicas nesse sentido, como inclusão em resinas "durcupan" ou "epoxy" (Tang and Nyengaard, 1997; Lopez et al, 2005; Hermel et al., 2006a,b).

Por outro lado utilizou-se o método do fracionador óptico e o princípio de Cavalieri, que são considerados os métodos padrão para se estimar o número de células nos núcleos encefálicos (Shumann e Amaral, 2005).

Em função das limitações técnicas fez-se necessário medir a espessura de cada corte (distância entre base e topo) com "microcator" definidos segundo Costa-Ferro et. al. (2010), que garantiu uma zona de segurança de 2-3 µm. Isso somado ao fato de que os marcadores celulares eleitos para a contagem foram bem pequenos (nucléolos nos neurônios e núcleos nas células gliais) nos permite assumir que a zona de segurança foi suficiente para evitar erros do tipo "Lost Caps" e "Split Cell". Adicionalmente utilizou-se óleo de imersão para evitar erros associados à Lei de Refração de Snell (Williams

and Rakic, 1988). Também se elegeram áreas de contagem pequenas (de até 5 células) para diminuir a probabilidade de erro humano na estimativa (Williamsand Rakic, 1988).

Há muitas dificuldades inerentes na estimativa de parâmetros morfológicos em regiões como o Me humano (Howard and Reed, 2005) e nosso estudo não está livre de vieses, sobretudo com relação à retração do tecido (Coggeshall and Lekan, 1996), mas certamente há descrito aqui uma estimativa válida do percentual de neurônios e células gliais nesse núcleo, e esses valores relativos servem de referência para essa área encefálica, considerando-se a idade, o gênero e a causa da morte dos sujeitos.

5.3 Limitações metodológicas para delineamento do Me

O método de Cavalieri usado para estimar o volume de um determinado núcleo requer um delineamento claro dos bordos anatômicos da região de interesse, mas o delineamento preciso do Me humano e seus subnúcleos permanece sob debate (olhar, por exemplo, Martin et al., 1991; Gloor, 1997; de Olmos, 2004; Mai et al., 2008; Yilmazer-Hanke, 2012). Além disso as diferenças morfológicas entre os vários núcleos e suas subdivisões são muitas vezes sutis (Gloor, 1997). Embora o uso de atlas seja muito importante em estudos como este, seu uso pode negligenciar as variações do tamanho e posição dos núcleos em diferentes indivíduos. (Zald e Prado, 1997; Saygin e col., 2011). Desso modo não surpreende que a delimitação dos núcleos continue a ser investigada com base em estudos de citoarquitetura, distribuição axonal, conexões e quimioarquitetura, mas é importante salientar que os critérios utilizados para delimitar as regiões encefálicas não são um consenso para os diferentes autores (Kruger e col., 1995).

6. CONCLUSÕES

O presente trabalho contribuiu com dados descritivos e quantitativos inéditos sobre os neurônios e células da glia, especialmente os astrócitos, do Me de homens adultos *post mortem*, evidenciando uma organização sináptica complexa nessa estrutura encefálica. Este trabalho pioneiro servirá como referência para trabalhos futuros. Com ele se conseguiu dados relevantes para o embasamento do que existe no Me humano nas condições de estudo atuais.

As células gliais revelaram-se como a maior população no Me humano (em torno de 70% das células) e há significativamente mais neurônios no Me esquerdo (em torno de 18%) do que no mesmo núcleo no hemisfério direito. Aspectos da morfologia neuronal foram estudados a partir da utilização da técnica de Golgi adaptada para as amostras armazenadas por períodos variáveis em formalina 10% não tamponada. Isso confirmou a classificação dos neurônios em tipos revelados por técnica imuno-histoquímica em estudos prévios de outros autores (Tipos 1 à 3; Sorvari e col., 1996a), mas também se identificaram outros neurônios até então não descritos. O estudo da densidade de espinhos dendríticos sugere a existência de subpopulações de neurônios com poucos ou com muitos espinhos, como evidenciado em neurônios com soma de tipo fusiforme (Tipo 3), o que apareceu de forma mais numerosa com a presente técnica de Golgi. Os astrócitos imunorreativos à GFAP apresentaram-se como protoplasmáticos e com múltiplas ramificações no neurópilo do Me. Por fim, para a ultra-estrutura neuronal e glial no Me, complementando os achados com a técnica de Golgi e além dos contatos sinápticos classicamente mais abundantes descritos, observaram-se a existência

de estruturas sinápticas do tipo glomérulo, muito complexas e até então não descritas para este núcleo nem mesmo em outras espécies, além de espinhos multissinápticos.

7. PERSPECTIVAS

Ainda se sabe muito pouco sobre as funções do Me humano, mas pistas nos são dadas por sua origem embriológica, citoarquitetura, quimioarquitetura e hodologia, além de dados de imageamento funcional (ainda pouco específicos para um núcleo de tão pequenas dimensões), ou de estados patológicos que comprometam esta região (neste sentido há ainda menos especificidade) ou de outros dados muito bem estabelecidos para outras espécies, os quais podem, cautelosamente, ser-nos úteis, sobretudo no que se sabe sobre primatas não humanos.

A partir disto, por ser uma área ainda pouco explorada e este ser o primeiro estudo nesta linha realizado no Laboratório de Fisiologia da UFCSPA, em parceria com o Laboratório de Estrutura Sináptica da USP-RP, há muitas perspectivas que se abrem a partir de agora. Espera-se poder somar e aprimorar os dados expostos aqui, por exemplo, utilizando-se uma associação de técnicas imuno-histoquímicas que, esperançosamente, permitam decifrar com mais precisão os bordos do Me para que se possam obter dados absolutos sobre o número de neurônios e células da glia nesse núcleo, o que seria mais adequado que a densidade relativa destas células aqui demonstrada. Também se espera, a partir do protocolo bem estabelecido da técnica de Golgi com adaptações próprias para o Me humano, estudar mais casos e obter dados morfométricos completos (incluindo-se dos espinhos dendríticos e o percentual de ocorrência de cada um dos seus tipos) que sejam representativos tanto de homens como de mulheres neurologicamente normais e, em um segundo momento, a partir de parcerias com instituições que contenham banco de encéfalos em diferentes estados

patológicos, por exemplo, estender as pesquisas a essas populações com diferentes condições para comparações e para gerar hipóteses fisiopatológicas.

8. REFERÊNCIAS BIBLIOGRÁFICAS

Aggleton JP, Saunders RC. 2000. The amygdala – what's happened in the last decade? In: Aggleton JP. (ed.). The Amygdala. Second Edition. Oxford University Press, Oxford, pp. 1-30.

Alheid GF, Heimer L. 1988. New perspectives in basal forebrain organization of special relevance for neuropsychiatric disorders: the striatopallidal, amygdaloid, and corticopetal components of substantia innominata. Neurosci 27:1–39.

Amaral DG, Avendano C, Benoit R.1989. Distribution of somatostatin-like immunoreactivity in the monkey amygdale. J Comp Neurol 284:294–313.

Amaral DG, Price JL, Pitkänen A, Carmichael ST. 1992. Anatomical organization of the primate amygdaloid complex. In: Aggleton JP. (ed). The Amygdala. Neurobiological Aspects of Emotion, Memory and Mental Dysfunction. Wiley- Liss, New York, pp 1–66.

Amaral DG, Schumann CM, Nordahl CW. 2008. Neuroanatomy of autism. Trends Neurosci 31:137–145.

Amaral DG. 1987. Memory: anatomical organization of candidate brain regions. In: Plum F. (ed). Handbook of physiology – the nervous system V, Part 2. American Physiological Society, Washington DC, pp. 211-294.

Arpini M, Menezes IC, Dall'Oglio A, Rasia-Filho AA. 2010. The density of Golgi-impregnated dendritic spines from adult rat posterodorsal medial amygdala neurons displays no evidence of hemispheric or dorsal/ventral differences. Neurosci Lett 469:209-213.

Baloyannis SJ, Costa V, Baloyannis IS. 2006. Morphological alterations of the synapses in the locus coeruleus in Parkinson's disease. J Neurol Sci 248:35 – 41.

Bennett-Clarke CA, Joseph SA. 1986. Immunocytochemical localization of somatostatin in human brain. Peptides 7:877-84.

Benzing WC, Mufson EJ, Jennes L, Armstrong DM. 1990. Reduction of neurotensin immunoreactivity in the amygdala in Alzheimer's disease. Brain Res 537: 298-302.

Benzing WC, Mufson EJ, Jennes L, Stopa EG, Armstrong DM. 1992. Distribution of neurotensin immunoreactivity within the human amygdaloid complex: A comparison with acetylcholinesterase- and Nissl-stained tissue sections. J Comp Neurol 317:283-297.

Berry MM, Standring SM, Bannister LH. 1995. Nervous system. In: Williams PL. (ed). Gray's Anatomy. Churchill Livingstone, New York, pp 901-1398.

Bolhuis JR. 1984. The corticomedial amygdala and learning in an agonistic situation in the rat. Physiology and Behav, 32:575-579.

Bonsall RW, Rees HD, Michael RP. 1986. [^{3}H] Estradiol and its metabolites in the brain, pituitary gland, and reproductive tract of the male rhesus monkey. Neuroendocrinol 43: 98-109.

Bressler SC, Baum MJ. 1996. Sex comparison of neuronal Fos immunoreactivity in the rat vomeronasal projection circuit after chemosensory stimulation. Neurosci 71:1063-1072.

Brockhaus H. 1938. Zur normalen und pathologischen Anatomie des Mandelkerngebiets. J Psychol Neurol 49:1-136.

Brodal A. 1981. Neurological Anatomy. Oxford University Press, New York. 1053 pp.

Brusco J, Dall'Oglio A, Rocha LB, Rossi MA, Moreira JE, Rasia-Filho AA. 2010. Descriptive findings on the morphology of dendritic spines in the rat medial amygdala. Neurosci Lett 483:152-156.

Caffé AR, van Leeuwen FW, Luiten PGM. 1987. Vasopressin cells in the medial amygdale of the rat project to the lateral septum and ventral hippocampus. J Comp Neurol 261: 237-252.

Candy JM, Perry RH, Thompson JE, Johnson M, Oakley AE. 1985. Neuropeptide localisation in the substantia innominata and adjacent regions of the human brain, J Anat 140(Pt 2):309–327.

Canteras NS, Simerly RB, Swanson LW. 1995. Organization of projections from the medial nucleus of the amygdala: A PHAL study in the rat. J Comp Neurol 360:213-245.

Coolen LM, Peters HJPW, Veening JG. 1997. Distribution of Fos immunoreactivity following mating versus anogenital investigationin the male rat brain. Neurosci 77:1151-1161.

Cooper PE, Fernstrom MH, Rorstad OP, Leeman SE, Martin JB. 1981**.** The regional distribution of somatostatin, substance P and neurotensin in human brain. Brain Res 218:219-32.

Crosby EC, Humphrey T. 1941. Studies of the vertebrate telencephalon: II. The nuclear pattern of the anterior olfactory nucleus tuberculum olfactorium and the amygdaloid complex in adult man. J Comp Neurol 47:309-352.

Dall'Oglio A, Ferme D, Brusco J, Moreira JE, Rasia-Filho AA. 2010. The "single-section" Golgi method adapted for formalin-fixed human brain and light microscopy. J Neurosci Meth 189:51-55.

Dall'Oglio A, Gehlen G, Achaval M, Rasia-Filho A.A. 2008b. Dendritic branching features of Golgi-impregnated neurons from the "ventral" medial amygdala subnuclei of adult male and female rats. Neurosci Lett 439:287-292.

Dall'Oglio A, Gehlen G, Achaval M, Rasia-Filho AA. 2008a.Dendritic branching features of posterodorsal medial amygdala neurons of adult male and female rats: further data based on the Golgi method. Neurosci Lett 430:151–156.

Dall'Oglio A, Marcuzzo S, de Castilhos J, Rasia-Filho AA. 2007. Método de Golgi. In: Elias C, Bittencourt J. (eds). Métodos em Neurociências. Roca, São Paulo, pp. 33-56.

Davidson, R J, Irwin W. 1999. The functional neuroanatomy of emotion and affective style. Trends Cogn Sci 3:11-21.

de Castilhos J, Forti CD, Achaval M, Rasia-Filho AA. 2008. Dendritic spine density of posterodorsal medial amygdala neurons can be affected by gonadectomy and sex steroid manipulations in adult rats: a Golgi study. Brain Res 1240:73–81.

de Olmos JS, Alheid GF, Beltramino CA. 1985. Amygdala. In: Paxinos, G. (ed). The Rat Nervous System. Academic Press, Sydney, pp. 223-234.

de Olmos JS. 1990. Amygdala. In: Paxinos G. (ed.) The Human Nervous System. Academic Press, San Diego, pp. 583-710.

de Olmos JS. 2004. Amygdala. In: Paxinos G, Mai J. (eds). The Human Nervous System. Second Edition. Elsevier, San Diego, pp. 739-868.

Dielemberg, RA, Hunt GR, McGregor LS. 2001. When a Rat Smells a Cat: The distribution of FOS immunoreactivity in the rat brain following exposure to a predatory odor. Neurosci 104:1085-1097.

Everitt B. 1995. Limbic lobe and olfactory pathways. In: Berry MMm Bannister LH, Standring SM (eds). Gray's Anatomy. Churchill Livingstone, London, pp. 1115-1141.

Fairén, A. 2005. Pioneering a golden age of cerebral microcircuits: The births of combined Golgi-electron microscope methods. Neurosci 136:607-614.

Felten DL, Józefowicz RF. 2005. Atlas de neurociência humana de Netter. Artmed, Porto Alegre.

Freese JL, Amaral DG. 2009. Neuroanatomy of the primate amygdala. In: Whalen PJ, Phelps EA (eds). The Human Amygdala. The Guilford Press, New York, pp. 3-42.

Fudge JL, Emiliano AB. 2003. The Extended Amygdala and the Dopamine System: Another Piece of the Dopamine Puzzle. J Neuropsychiatry Clin Neurosci 15:306-316.

Garcia-Segura LM, McCarthy MM. 2004. Minireview: role of glia in neuroendocrine function. Endocrinol 145:1082–1086.

Garrett A, Chang K. 2008. The role of the amygdala in bipolar disorder development. Dev Psychopathol 20:1285–1296.

Gaspar P, Berger B, Alvarez C, Vigny A, Henry JP. 1985. Catecholaminergic innervation of the septal area in man: immunocytochemical study using TH and DBH antibodies. J Comp Neurol 241:12-33.

Gaspar P, Berger B, Lesur A, Borsotti JP, Febvret A. 1987. Somatostatin 28 and neuropeptide Y innervation in the septal area and related cortical and subcortical structures of the human brain. Distribution, relationships and evidence for differential coexistence. Neurosc 22:49-73.

Gazzaniga, MS, Ivry RB, Mangun GR. 2002. Neurociências cognitiva: a biologia da mente. 2ª ed, Artmed, Porto Alegre.

Gentleman SM, Falkai P, Bogerts B, Herrero MT, Polak JM, Roberts GW. 1989. Distribution of galanin-like immunoreactivity in the human brain. Brain Res 505: 311-315.

Gloor P. 1997. The Temporal Lobe and Limbic System. Oxford University Press. New York.

Gomes FC, Paulin D, Moura Neto V. 1999. Glial fibrillary acidic protein (GFAP): modulation by growth factors and its implication in astrocyte differentiation. Braz J Med Biol Res 32:619–631.

González-Burgos I, Alejandre-Gómez M, Cervantes M. 2004. Spine-type densities of hippocampal CA1 neurons vary in proestrus and estrus rats. Neurosc Let 379:52-54.

Guillamón A, Segovia S. 1997. Sex Differences in the Vomeronasal System. Brain Res Bull 44:377-382.

Gundersen HJ. 1986. Stereology of arbitrary particles. A review of unbiased number and size estimators and the presentation of some new ones, in memory of William R. Thompson. J Microsc 143:3–45.

Hall, E. 1972. Some aspects of the structural organization of the amygdala. In: Eletheriou BE. (ed). The Neurobiology of the Amygdala. Plenum Press, New York, pp 95-121.

Hering H, Sheng M. 2001. Dendritic spines: structure, dynamics and regulation. Nat Rev Neurosci 2: 880-888.

Hermel EE, Faccioni-Heuser MC, Marcuzzo S, Rasia-Filho AA, Achaval M. 2006. Ultrastructural features of neurons and synaptic contacts in the posterodorsal medial amygdala of adult male rats. J Anat 208:565-575.

Higgins GA, Schwaber JS. 1983. Somatostatinergic projections from the central nucleus of the amygdala to the vagal nuclei. Peptides 4:657-62.

Horta Jr. JAC, García DE. 2007. Microscopia Eletrônica de Transmissão Aplicada à Neurociência. In: Elias C, Bittencourt J. (eds). Métodos em Neurociências. Roca, São Paulo, pp. 81-113.

Jiang Y, Yang Y, Wang S, Ding Y, Guo Y, Zhang MM, Wen SQ, Ding MP. 2012. Ketogenic diet protects against epileptogenesis as well as neuronal loss in amygdaloid-kindling seizures. Neurosci Lett 2:22-6.

Johansson O, Hökfelt T, Elde RP. 1984. Immunohistochemical distribution of somatostatin-like immunoreactivity in the central nervous system of the adult rat. Neurosci 13:265-339.

Johnston JB. 1923. Further contributions to the study of the evolution of the forebrain, J Comp Neurol 35:337–481.

Kamal AM, Tömböl T. 1975. Golgi studies on the amygdaloid nucleiof the cat. J Hirnforschung 16:175-201.

Keefer DA, Stumpf WE. 1975. Atlas of estrogen-concentrating cells in the central nervous system of the squirrel monkey. J Comp Neurol 160:419-41.

Kettenmann H, Ransom BR. 2005. Neuroglia. 2ª ed. Oxford University Press, New York.

Köhler C, Persson A, Melander T, Theodorsson E, Sedvall G, Hökfelt T. 1989. Distribution of galanin-binding sites in the monkey and human telencephalon: preliminary observations. Exp Brain Res 75:375-80.

Larriva-Sahd J. 2006. Histological and cytological study of the bed nuclei of the stria terminalis in adult rat. II. Oval nucleus: extrinsic inputs, cell types, neuropil, and neuronal modules. J. Comp. Neurol 497:772-807.

LeDoux JE, Farb C, Ruggiero DA. 1990. Topographic organization of neurons in the acoustic thalamus that project to the amygdale. J Neurosci 10:1043–1054.

LeDoux JE, Müller J. 1997. Emocional memory and psychopathology. Philos Trans R Soc Lond B Biol Sci 352:1719-1726.

LeDoux JE, Schiller D. 2009. The human amygdala: Insights from other animals. In: Whalen PJ, Phelps EA (eds). The Human Amygdala. The Guilford Press, New Yor, pp. 43-60.

Ledoux JE. 1998. O Cérebro Emocional: os misteriosos alicerces da vida emocional. 2ª ed. Objetiva, Rio de Janeiro.

Lesur A, Gaspar P, Alvarez C, Berger B. 1989. Chemoanatomic compartments in the human bed nucleus of the stria terminalis. Neurosc 32:181–194.

Lind RW, Swanson LW, Ganten D. 1985. Organization of angiotensin II immunoreactive cells and fibers in the rat central nervous system. Neuroendocrinol 40: 2-24.

Linke R, de Lima AD, Schwegler H, Pape HC. 1999. Direct synaptic connections of axons from superior colliculus with identified thalamo-amygdaloid projection neurons in the rat: possible substrates of a subcortical visual pathway to the amygdale. J Comp Neurol 403:158–170.

Mai JK, Paxinos G, Voss T. 2007. Atlas of the Human Brain. Academic Press, New York. 271 pp.

Mai JK, Triepel J, Metz J. 1987**.** Neurotensin in the human brain. Neurosci 22:499-524.

Marcuzzo S, Dall'Oglio A, Ribeiro MF, Achaval M, Rasia Filho AA. 2007. Dendritic spines in the posterodorsal medial amygdala after restraint stress and ageing in rats. Neurosci Lett 424: p.16-21.

Martin, LJ, Powers RE, Dellovade TL, Price DL. 1991. The bed nucleus-amygdala continuum in human and monkey. J Comp Neurol 309:445-485.

Martinez FG, Hermel EE, Xavier LL, Viola GG, Riboldi J, Rasia-Filho AA, Achaval M. 2006. Gonadal hormone regulation of glial fibrillary acidic protein immunoreactivity in the medial amygdala subnuclei across the estrous cycle and in castrated and treated female rats. Brain Res 1108:117-126.

McDonald AJ, Augustine JR. 1993. Localization of GABA-like immunoreactivity in the monkey amygdale. Neurosc 52:281–294.

McDonald AJ, Pearson JC. 1989. Coexistence of GABA and peptide immunoreactivity in non-pyramidal neurons of the basolateral amygdale. Neurosci Lett 100:53–58.

McDonald AJ. 1985. Morphology or peptide-containing neurons in the rat basolateral amygdaloid nucleus. Brain Res 338: 186-191.

McDonald AJ. 1987. Somatostatinergic projections from the amygdale to the bed nucleus of the stria terminalis and medial preoptic-hypothalamic region. Neurosci Lett 75:271-277.

McDonald AJ. 1989. Coexistence of somatostatin with neuropeptide Y, but not with cholecystokinin or vasoactive intestinal peptide, in the neurons of the rat amygdala. Brain Res 500: 37-45.

McDonald AJ. 1992. Cell types and intrinsic connections of the amygdala. In: Aggleton JP. (ed) The Amygdala. Wiley-Liss, New York, pp. 67-92.

Michael RP, Rees HD, Bonsall RW. 1990. Sites in the male primate brain at which testosterone acts as an androgen. Brain Res 502: 11-20.

Michel JP, Sakamoto N, Kopp N, Pearson J. 1986. Neurotensin immunoreactive structures in the human infant striatumm septum, amygdala and cerebral cortex. Brain Res 397: 93-102.

Millhouse OE. 1986. The intercalated cells of the amygdale. J Comp Neurol 247:246–271.

Moga MM, Gray TS. 1985a. Evidence for corticotropin-releasing factor, neurotensin, and somatostatin in the neural pathway from the central nucleus of the amygdala to the parabrachial nucleus. J Comp Neurol 241:275–284.

Moga MM, Gray TS. 1985b. Peptidergic efferents from the intercalated nuclei of the amygdala to the parabrachial nucleus in the rat. Neurosci Lett 61:13–18.

Müller M, Faber-Zuschratter H, Yanagawa Y, Stork O, Schwegler H, Linke R. 2012. Synaptology of ventral CA1 and subiculum projections to the basomedial nucleus of the amygdala in the mouse: relation to GABAergic interneurons. Brain Struct Funct 217:5-17.

Murphy, GMJr. 1986. The human medial amygdaloid nucleus: no evidence for sex differences in volume. Brain Res 365:321-332.
Neurosci 106:341-356.

Newman SW. 1999. The medial extended amygdala in male reproductive behavior. A node in the mammalian social behavior network. Ann N Y Acad Sci 877:242-257.

Newman SW. 2002. Pheromonal signals access the medial extended amygdala: one node in a proposed social behavior network. In: Pfaff DW, Arnold AP, Etgen AM, Fahrbach SE, Rubin RT. (eds) Hormones, Brain and Behavior. Academic Press, San Diego, pp. 17-31.

Nimchinsky EA, Sabatini BL, Svoboda K. 2002. Structure and function of dendritic spines. An Revs Physiol 64:313-353.

Nitecka L, Narkiewicz O.1976. Localization of acetylcholinesterase activity in the amygdaloid body of man. Acta Neurobiol Exp (Wars) 36:333–351.

Nobakht M, Hoseini SM, Mortazavi P, Sohrabi I, Esmailzade B, Rahbar Rooshandel N, Omidzahir S. 2011. Neuropathological changes in brain cortex and hippocampus in a rat model of Alzheimer's disease. Iran Biomed J 15:51-8.

Oertner T, Matus A. 2005. Calcium regulation of actin dynamics in dendritic spines. Cell Calcium 37:477-482.

Pakkenberg B, Gundersen HJ. 1988. Total number of neurons and glial cells in human brain nuclei estimated by the disector and the fractionator. J Microsc 150:1–20.

Pannese E. 1996. The black reaction. Brain Res Bull 41:343-349.

Parent A. 1971. Comparative histochemical study of the amygdaloid complex. J Hirnforsch 13: 89-96.

Peters A, Kaiserman-Abramof IR. 1970. The small pyramidal neuron of the rat cerebral cortex. The perikaryon, dendrites and spines. Am J Anat 127:321-356.

Peters A, Palay SL, Webster H. 1991. The Fine Structure of the Nervous System. Oxford University Press, New York. 514 pp.

Petrovich GD, Canteras NS, Swanson LW. 2001. Combinatorial amygdalar inputs to hippocampal domains and hypothalamic behavior systems. Brain Res Rev **38**:247–289.

Pfaff D, Gerlach T, McEwen B, Ferin M, Carmel P, Zimmerman E. 1976. Autoradiographic localization of hormone-concentrating cells in the brain of the rhesus monkey. J Comp Neurol. 170:279-294.

Phelps EA, Anderson AK. 1997. Emotional memory: What does the amygdala do? Curr Biol, 7:311–314.

Pioro EP, Mai JK, Cuello AC. 1990. Distribution of substance P – and enkephalin-immunoreactive neurons and fibers. In PaxinosG. (ed). The Human Nervous System. Academic Press, San Diego, pp 1051-1094..

Pitkänen A, Amaral DG. 1991. Distribution of reduced nicotinamide adenine dinucleotide phosphate diaphorase (NADPH-d) cells and fibers in the monkey amygdaloid complex. J Comp Neurol 313:326–348.

Pitkänen A, Amaral DG. 1994. The distribution of GABAergic cells, fibers, and terminals in the monkey amygdaloid complex: an immunohistochemical and in situ hybridization study. J Neurosci 14:2200–2224.

Pitkänen A, Tuunanen J, Kälviäinen R, Partanen K, Salmenpera T. 1998. Amygdala damage in experimental and human temporal lobe epilepsy. Epilepsy Res 32: 233–253.

Price C. 1987. The Limbic Reegion II: The Amygdaloid complex. In: Björklund A, Hökfelt T, Swanson LW. (eds). Handbook of Chemical Neuroanatomy. Eslevier, Amsterdan, pp. 279-388.

Protopopescu X, Pan H, Tuescher O, Cloitre M, Goldstein M, Engelien W, Epstein J, Yang Y, Gorman J, LeDoux J, Silbersweig D, Stern E. 2005. Differential Time Courses and Specificity of Amygdala Activity in Posttraumatic Stress Disorder Subjects and Normal Control Subjects. Biol Psychiatry, 57:464-473.

Ramón y Cajal, S. 1995 (traduzido da edição francesa de 1909). Neurons: size and general morphology. In: Swanson N.; Swanson SW (eds) Histology of the Nervous System of Man and Vertebrates. Oxford University Press, New York, pp. 46-57.

Ramón-Moliner E. 1962. An attempt at classifying nerve cells on the basis of their dendritic patterns. J Comp Neurol 119:211-227.

Rasia-Filho AA, Fabian C, Rigoti K, Achaval M. 2004. Influence of sex, estrous cycle and motherhood in dendritic spine density in the rat medial amygdala revealed by the Golgi method. Neuroscience 126:839–847.

Rasia-Filho AA, Haas D, de Oliveira AP, de Castilhos J, Frey R, Stein D, Lazzari V, Back F, Pires GN, Pavesi E, Winkelmann-Duarte EC, Giovenardi M. 2012. Morphological and functional features of the sex steroid-responsive posterodorsal medial amygdala of adult rats. Rev. Chem. Med, no prelo.

Rasia-Filho AA, Hilbig A. 2005. Papel da amígdala e do hipocampo no transtorno do estresse pós-traumático. In: Güintert, BI.; Chinally M. (eds.). Transtornos do estresse pós traumático. Parte I. Casa do Psicólogo, São Paulo, pp 37-53.

Rasia-Filho AA, Londero RG, Achaval M. 1999. Effects of gonadal hormones on the morphology of neurons from the medial amygdaloid nucleus of rats. Brain Res Bull 48:173-183.

Rasia-Filho AA, Londero RG, Achaval M. 2000. On some functional activities of the amygdala: an overview. J Psychiatry Neurosci 25:14-23.

Rasia-Filho AA, Peres TM, Cubilla-Gutierrez FH, Lucion AB. 1991. Effect of estradiol implanted in the corticomedial amygdala on the sexual behavior of castrated male rats. Bra J Med Biol Res 24:1041-1049.

Roozendaal LB, McGaugh JL. 1996. Amygdaloid nuclei lesions differentially affect glucocorticoid-induced memory enhancement in inhibitory avoidance task. Neurobiol Learn Mem 65:1-8.

Sadikot AF, Parent A. 1990. The monoaminergic innervation of the amygdale in the squirrel monkey: an immunohistochemical study, Neurosc 36:431–447.

Sakanaka M, Shiosaka S, Takatsuki K, Inagaki S, Takagi H, Senba E, Kawai Y, Matsuzaki T, Tohyama M. 1981. Experimental immunohistochemical studies on the amygdalofugal peptidergic (substance P and somatostatin) fibers in the stria terminalis of the rat. Brain Res 221:231-42.

Sarrieau A, Javoy-Agid F, Kitabgi P, Dussaillant M, Vial M, Vincent JP, Agid Y, Rostène WH. 1985. Characterization and autoradiographic distribution of neurotensin binding sites in the human brain. Brain Res 348:375-80.

Scheff SW, Price DA, Schmitt FA, Mufson EJ. 2006. Hippocampal synaptic loss in early Alzheimer's disease and mild cognitive impairment. Neurobiol Aging 27:1372–1384.

Schumann CM, Amaral DG. 2005. Stereological estimation of the number of neurons in the human amygdaloid complex. J Comp Neurol 491:320–329.

Schumann CM, Amaral DG. 2006. Stereological Analysis of Amygdala Neuron Number in Autism. J Neurosci 26:7674-7679.

Sheehan TP, Amaral E, Numan MJ, Numan M. 2001. Evidence that the medial amygdala projects to the anterior/ventromedial hypotalamic nuclei to inhibit maternal behavior in rats.

Silverman AJ, Antunes JL, Abrams GM, Nilaver G, Than R, Robinson JA. 1982. The luteinizing hormone-releasing hormone pathways in rhesus (*Macaca mulatta*) and pigtailed (*Macaca nemestrina*) monkeys. New observations on thick unembedded sections. J Comp Neurol 211: 309-317.

Sims KS, Williams RS. 1990. The human amygdaloid complex: a cytologic and histochemical atlas using Nissl, myelin, acetylcholinesterase and nicotinamide adenine dinucleotide phosphate diaphorase staining. Neuroscience 2:449-472.

Sorvari H, Miettinen R, Soininen H, Pitkänen A. 1996b. Parvalbumin-immunoreactive neurons make inhibitory synapses on pyramidal cells in the human amygdala: a light and electron microscopic study. Neurosci Lett 217:93-96.

Sorvari H, Soininen H, Paljärvi L, Karkola K, Pitkänen A. 1995. Distribution of parvalbumin-immunoreactive cells and fibers in the human amygdaloid complex. J Comp Neurol 360:185-212.

Sorvari H, Soininen H, Pitkänen A. 1996a. Calretinin-immunoreactive cells and fibers in the human amydaloid complex. J Comp Neurol 369:188-208.

Sorvari, H. 1997. Neurons containing calcium-binding proteins in the human amygdaloid complex. Ph.D. Thesis. University of Kuopio, Finland.

Stephan H, Andy OJ. 1977. Quantitative comparison of the amygdala in insectivores and primates. Acta Anat 98:130–153.

Stephan H, Frahm HD, Baron G. 1987. Comparison of brain structure volumes in Insectivora and primates. J Hirnforsch 28:571–584.

Stopa EG, Koh ET, Svendsen CN, Rogers WT Schwaber JS, King JC. 1991. Computer-assisted mapping of immunoreactive mammalian gonadotropin-releasing hormone in adult human basal forebrain and amygdala. Endocrinol 128:3199-3207.

Svendsen CN, Bird ED. 1985. Acetylcholinesterase staining of the human amygdale. Neurosci Lett 54: 313-318.

Swanson L, Petrovich G. 1998. What is the amygdala? Trends Neurosci 21:323-331.

Tada T, Sheng M. 2006. Molecular mechanisms of dendritic spine morphogenesis. Curr Opin Neur 16:1-7.

Takase LF, Nogueira MI. 2007. Métodos Quantitativos Estruturais e de Dosagem em Neurociências: Princípios de Estereologia em Quantificação. In: Elias C, Bittencourt J. (eds). Métodos em Neurociências. Roca, São Paulo, pp. 201-205.

Trimble MR, Van Elst LT. 1999. On some clinical implications of the ventral

Uhl GR, Goodman RR, Kuhar MJ, Snyder SH. 1978a. Enkephalin and neurotensin: immunohistochemical localization and identification of an amygdalofugal pathway. Adv Biochem Psychopharmacol 18:71-87.

Uhl GR, Kuhar MJ, Synder SH. 1978b. Enkephalin-containing pathway: amygdaloid efferents in the stria terminalis. Brain Res 149:223-8.

Ulfig N, Setzer M, Bohl J. 2003. Ontogeny of the human amygdala. Ann NY Acad Sci 985:22-33.

Valverde, F. 1962. Intrinsic organization of the amygdaloid complex. A Golgi study in the mouse. Trab Inst Cajal Investig Biol 54:291-314.

Walter A, Mai JK, Jiménez-Härtel W. 1990. Mapping of neuropeptide Y-like immunoreactivity in the human forebrain. Brain Res Bull 24: 297-311.

Weibel, ER. 1979. Stereologial methods. In: Pratical methods for biological morphometry. Academic Press, London, pp. 415.

Whalen PJ, Davis FC, Oler, JA, Kim H, Kim J, Neta, M. 2009. Human Amygdala Responses to Facial Expressions of Emotion. In: Whalen PJ, Phelps EA. (eds). The Human Amygdala. The Guilford Press, New York, pp 265-288.

Whalen PJ, Phelps EA. 2009. The Human Amygdala. The Guilford Press, New York.

Wooley CS, McEwen BS. 1993. Roles of estradiol and progesterone in regulation of hippocampal dendritic spine density during the estrous cycle in the rat. J Comp Neurol 336:293-306.

Woolley CS, McEwen BS. 1994. Estradiol regulates hippocampal dendritic spine density via an N-methyl-D-aspartate receptor-dependent mechanism. J Neurosci 14: 7680-7687.

Xavier LL, Viola GG, Ferraz AC, Da Cunha C, Deonizio JM, Netto CA, Achaval M. 2005. A simple and fast densitometric method for the analysis of tyrosine hydroxylase immunoreactivity in the substantia nigra pars compacta and in the ventral tegmental area. Brain Res Protoc 16:58-64.

Yilmazer-Hanke DM. 2012. Amygdala. In: Paxinos G, Mai J. (eds). The Human Nervous System. Third Edition. Elsevier, San Diego, pp. 759-834.

Zirlinger M, Anderson D. 2003. Molecular dissection of the amygdala and its relevance to autism. Genes, Brain and Behav 2:282-294.

9. ADENDOS

9.1. Autorizações dos Comitês de Ética

9.1.1. Universidade Federal de Ciências da Saúde de Porto Alegre – UFCSPA

MINISTÉRIO DA EDUCAÇÃO
FUNDAÇÃO FACULDADE FEDERAL DE CIÊNCIAS MÉDICAS DE PORTO ALEGRE
COMITÊ DE ÉTICA EM PESQUISA
APROVADO PELA CARTA Nº 880/2004-CONEP/CNS/MS
RUA SARMENTO LEITE, 245 – FONE: (51) 3224.8822
CEP 90050-170 – PORTO ALEGRE – RS - cep@fffcmpa.edu.br

Of. 541/07-CEP

Porto Alegre, 18 de outubro de 2007.

Ilmo. Sr.
Prof. Alberto Antônio Rasia Filho
Nesta Faculdade

Senhor Professor

Informamos que o adendo de seu projeto nº 215/07, intitulado "Morfologia dos Neurônios da Amígdala Medial em Seres Humanos.", foi avaliado pelo Comitê de Ética em Pesquisa, na reunião de 18 de outubro de 2007, sendo o adendo aprovado.

Outrossim, informamos que de acordo com o Art. 4º, letra c, do Regulamento do CEP, V. Sa. deverá nos encaminhar relatórios semestrais do desenvolvimento do projeto.

Adendo:

Atenciosamente,

Katya Vianna Rigatto
Vice-coordenadora do CEP/FFFCMPA

9.1.2. Universidade do Rio Grande do Sul – UFRGS

UFRGS

pro pesq

PRÓ-REITORIA DE PESQUISA

COMITÊ DE ÉTICA EM PESQUISA

CARTA DE APROVAÇÃO AD REFERENDUM

O Comitê de Ética em Pesquisa da Universidade Federal do Rio Grande do Sul analisou o projeto:

Número : 2008009

Título : Estudo da ultra-estrutura neuro-glial e da imunorreatividade à proteína ácida fibrilar glial no núcleo amigdaliano medial de seres humanos

Pesquisador (es) :

NOME	PARTICIPAÇÃO	EMAIL	FONE
ALBERTO ANTONIO RASIA FILHO	PESQ RESPONSÁVEL	rasiafilho@yahoo.com.br	
ALINE DALL OGLIO	PESQUISADOR	alidalloglio@yahoo.com.br	33083146
DENISE GOMES RODRIGUES FERME	PESQUISADOR	dferme@terra.com.br	33085423
JORGE EDUARDO MOREIRA DA SILVA	PESQUISADOR		
MATILDE ACHAVAL ELENA	PESQUISADOR	achaval@ufrgs.br	33083092

O mesmo foi aprovado *ad referendum* do Comitê de Ética em Pesquisa da UFRGS , por estar adequado ética e metodologicamente e de acordo com a Resolução 196/96 e complementares do Conselho Nacional de Saúde.

Porto Alegre, quarta-feira, 28 de janeiro de 2009

ILMA SIMONI BRUM DA SILV
Coordenador do CEP-UFRGS

9.2. Autorização de coleta de amostras pelo Departamento Médico Legal de Porto Alegre - DML-POA

GOVERNO DO ESTADO
RIO GRANDE DO SUL
SECRETARIA DA SEGURANÇA PÚBLICA
INSTITUTO-GERAL DE PERÍCIAS
DEPARTAMENTO MÉDICO-LEGAL

PARECER No. 03/08 DO CONSELHO TÉCNICO-CONSULTIVO

O Conselho Técnico-Consultivo reunido no dia 07/05/2008, com base na normativa no.3 e realizada a análise do:

Projeto protocolo DML: 4763/07, 1046/08 e 1360/08.
Autor:
Prof. Dr. Alberto A. Rasia Flho
Profa. Dra. Matilde Achaval Elena
Dra. Aline Dall'Oglio
Projeto: Estudo da ultra-estrutura neuro-glial e da imunorreatividade à proteína ácida friblilar glial no núcleo amigdaliano medial de seres humanos
Instituição: UFRGS
Participantes: Dra. Aline Dall'Oglio
Data: setembro 2007

Emite parecer, a partir dos esclarecimentos fornecidos, autorizando a realização da pesquisa acima referida sem acompanhamento do DML, estando o pesquisador obrigado a:

1. informar, por escrito, ao perito responsável pelo caso a atividade de pesquisa realizada, conforme modelo anexo;
2. fornecer à Seção de Ensino e Pesquisa relatório, atualizado, da nominata, no. de protocolos do DML e da sua pesquisa dos cadáveres envolvidos, conforme modelo anexo;
3. ratificamos que a pesquisa deverá ser realizada em cadáveres cuja causa da morte seja de etiologia clínica e mediante termo de consentimento da família, o qual deverá ser providenciado pela pesquisadora;
4. quanto ao tempo decorrido entre a morte e a retirada do tecido nervoso deverá ser obtida dos dados presentes na documentação quando da realização da perícia;
5. quanto a *causa mortis*, esta poderá ser obtida quando do preenchimento do atestado de óbito, logo após realizada a necropsia.

Porto Alegre, 07 de maio de 2008.

Dr. Roberto Amaral

Dra. Jussara Bocaccio

Dra. Helena Hubert Silva

Conselho Técnico Consultivo

Ciente:
Dra. Débora Maria Vargas de Lima
Diretora do DML

Seção de Ensino e Pesquisa
Av. Ipiranga, 1807 – CEP 90160-093 – Porto Alegre/RS
Fone: 32882660 – Fone/Fax: 32882654
E-mail: dml-sep@igp.rs.gov.br

9.3. Autorização de coleta de amostras pelo Serviço de Patologia do Hospital das Clínicas de Ribeirão Preto - SERPAT

Ribeirão Preto, 19 de janeiro de 2009.

OF. Nº 01/09
RSC/DAM-8/rpf

Prezada Professora,

Gostaria de apresentar nossa concordância para a obtenção de peças para estudo no projeto de doutorado intitulado "Estudo da ultraestrutura neuroglial e da imunorreatividade à proteína ácida fibrilar glial no núcleo amigdaliano medial de seres humanos" junto ao SERPAT - Serviço de Patologia do Hospital das Clínicas de Ribeirão Preto, desde que o mesmo esteja aprovado neste CEP e que o Dr. Gyl Eanes Barros Silva, médico assistente do nosso Serviço faça parte do projeto e seja inserido na autoria do artigo a ser publicado.

Atenciosamente,

Prof. Dr. Roberto Silva Costa
Coordenador e Supervisor do
- SERPAT -
Serviço de Patologia do

Ilustríssima Senhora
Profª Drª Ilma Brum da Silva
M.D. Coordenadora do Comitê de Ética em Pesquisa da
Universidade Federal do Rio Grande do Sul

9.4. Termo de Consentimento Livre e Esclarecido

TERMO DE CONSENTIMENTO LIVRE E ESCLARECIDO

O projeto de pesquisa intitulado “Estudo da ultra-estrutura neuroglial e da imunorreatividade à proteína ácida fibrilar glial no núcleo amigdaliano medial de seres humanos” tem por objetivo estudar as células da amígdala, uma região localizada nos dois lados da parte anterior do cérebro com cerca de 2 cm, para entender como elas são em nós seres humanos. As células do cérebro, que faz parte do sistema nervoso, são responsáveis por coordenar os comportamentos humanos. Apesar de ainda não se saber tudo sobre a amígdala, já se sabe por estudos realizados em diferentes animais que ela regula atividades como o medo e que pode estar modificada em doenças neurológicas como a Doença de Alzheimer. Como os animais são parecidos, mas não iguais a nós, o único jeito de se saber como a amígdala funciona em humanos é estudando nós mesmos. Por isso este estudo pode ajudar a entender mais sobre como a amígdala de humanos funciona normalmente e poderá contribuir para entender como ela funciona em casos de doenças e, assim, no futuro, poderá servir ainda para ajudar a descobrir como prevenir ou curar algumas doenças.

Para que este estudo possa acontecer é necessária a doação de uma pequena parte do cérebro, de não mais do que 5 cm, bem do lugar onde está a amígdala. Esta pequena parte (amostra) poderá ser retirada pelo médico legista durante a necropsia onde o cérebro é examinado também e, se for assim, não se espera nenhum desconforto ou risco para os familiares ou responsáveis legais da pessoa falecida, já que o procedimento de necropsia a ser realizado é o habitual e está indicado por normas técnicas/acadêmicas e legais e não será modificado para este estudo. Depois disso, essa amostra será levada para um laboratório e as células do cérebro serão coradas com técnicas específicas para que sejam vistas e estudadas em microscópio. Todo esse material ficará guardado no Laboratório de Fisiologia da Universidade Federal de Ciências da Saúde de Porto Alegre, R. Sarmento Leite, 245, Porto Alegre – RS durante cinco anos, mas poderá ficar por mais tempo, desde que seja necessário e que o Comitê de Ética em Pesquisa da UFRGS autorize, segundo Resolução 196/96 – CNS. Caso o familiar ou responsável legal pela pessoa falecida tenha alguma dúvida sobre o que foi informado acima, poderá perguntar a qualquer um dos pesquisadores envolvidos neste estudo. Poderá também não querer participar deste estudo, negando a retirada da amígdala sem que isso implique qualquer tipo de prejuízo no procedimento de necropsia. Também poderá abandonar esta pesquisa no momento em que bem entender, sem que isso acarrete necessidade de justificativas ou qualquer tipo de indenização.

Os autores deste estudo se comprometem a divulgar os resultados obtidos para o avanço do conhecimento científico, mas de maneira a não expor dados pessoais completos que possam identificar as pessoas que contribuíram para esta pesquisa.

Eu, ...(familiar ou responsável), RG nº ....., fui informado dos objetivos da pesquisa acima de maneira clara e detalhada. Recebi informação a respeito de como será retirado parte do tecido cerebral para estudo, como o estudo será feito, e esclareci minhas dúvidas. Sei que em qualquer momento poderei solicitar novas informações e modificar minha decisão se assim eu o desejar. A pesquisadora aluna de doutorado Aline Dall'Oglio e/ou a pesquisadora aluna de mestrado Denise Gomes Rodrigues Ferme certificou-me de que todos os dados desta pesquisa serão confidenciais, o procedimento de necropsia não será modificado em razão desta pesquisa e terei liberdade de retirar meu consentimento de participação na pesquisa, em face destas informações. Caso eu tenha novas perguntas sobre este estudo, posso entrar em contato com o Prof. Alberto A. Rasia Filho (pesquisador responsável), com Aline Dall'Oglio (pesquisadora aluna de doutorado) ou com Denise Gomes Rodrigues Ferme (pesquisadora aluna de mestrado) no endereço R. Sarmento Leite, 245, Porto Alegre – RS, telefone 0 xx 51 33039000 ramal 8752. Para qualquer pergunta sobre os meus direitos como participante deste estudo ou se penso que fui prejudicado pela minha participação, posso chamar o coordenador do Comitê de Ética em Pesquisa da Universidade de Ciências da Saúde de Porto Alegre, Prof. José Geraldo V. Taborda, ou seu substituto, na R. Sarmento Leite, 245, Porto Alegre – RS/ telefone 0 xx 51 3303 8804, bem como a coordenadora do Comitê de Ética em Pesquisa da Universidade Federal do Rio Grande do Sul, Profª. Ilma Brum da Silva, ou seu substituto, na Av. Paulo Gama, 110/ 7° andar, Porto Alegre – RS/ telefone: 0 xx 51 3308 3738.

Declaro que recebi cópia do presente Termo de Consentimento

_____

Assinatura de familiar ou do responsável legal

_____

Nome do familiar e grau de parentesco

Data: ___/___/_____

_____

Assinatura do Pesquisador

_____

Nome do Pesquisador

Data: ___/___/_____

Este formulário foi lido para _____ (nome do familiar ou representante legal) *em* _____/_____/_____ (data) *pelo* _____ (nome do pesquisador) *enquanto eu estava presente.*

_____

Assinatura de testemunha